TENOGENIC DIFFERENTIATION OF HUMAN ADIPOSE DERIVED MSCS ON A NOVEL TENDON SCAFFOLD BY GDF-5 SUPPLEMENTATION

A THESIS SUBMITTED TO
THE GRADUATE SCHOOL OF NATURAL AND APPLIED SCIENCES
OF
MIDDLE EAST TECHNICAL UNIVERSITY

BY

MUSTAFA BAHADIR GÜNER

IN PARTIAL FULFILLMENT OF THE REQUIREMENTS
FOR
THE DEGREE OF MASTER OF SCIENCE
IN
BIOMEDICAL ENGINEERING

SEPTEMBER 2018

Approval of the thesis:

TENOGENIC DIFFERENTIATION OF HUMAN ADIPOSE DERIVED MSCS ON A NOVEL TENDON SCAFFOLD BY GDF-5 SUPPLEMENTATION

submitted by **MUSTAFA BAHADIR GÜNER** in partial fulfillment of the requirements for the degree of **Master of Science in Biomedical Engineering Department, Middle East Technical University** by,

Prof. Dr. Halil Kalıpçılar
Dean, Graduate School of **Natural and Applied Sciences** _____

Assoc. Prof. Dr. Ergin Tönük
Head of Department, **Biomedical Engineering** _____

Prof. Dr. Dilek Keskin
Supervisor, **Engineering Science Dept., METU** _____

MD. Sedat Yılancı
Co-Supervisor, **Liv Hospital** _____

Examining Committee Members:

Prof. Dr. Ayşen Tezcaner (Head of Committee)
Engineering Science Dept., METU _____

Prof. Dr. Dilek Keskin (Supervisor)
Engineering Science Dept., METU _____

Prof. Dr. Sreeparna Banerjee
Biological Science Dept., METU _____

Assoc. Prof. Dr. Can Özen
Biotechnology Dept., METU _____

Assoc. Prof. Dr. Sedat Odabaş
Chemistry Dept., Ankara University _____

Date: 05.09.18

I hereby declare that all information in this document has been obtained and presented in accordance with academic rules and ethical conduct. I also declare that, as required by these rules and conduct, I have fully cited and referenced all material and results that are not original to this work.

Name, Last name : Mustafa Bahadır Güner

Signature :

ABSTRACT

TENOGENIC DIFFERENTIATION OF HUMAN ADIPOSE DERIVED MSCS ON A NOVEL TENDON SCAFFOLD BY GDF-5 SUPPLEMENTATION

Güner, Mustafa Bahadır

MSc., Department of Biomedical Engineering

Supervisor: Prof. Dr. Dilek Keskin

Co-Supervisor: MD. Sedat Yılancı

September 2018, 84 pages

Tendon injuries are a significant part of musculoskeletal wounds. Even though tendon wound healing mechanisms provide regeneration after injuries, reduced function of the tendon usually occurs due to limitations of the native healing mechanism. Tendon tissue engineering (TTE) is proposed to repair the injured tendon by a scaffold integrated with biological factors. Therefore, aim of this thesis was to design 3D scaffold, by combining healthy and wounded extracellular matrix (ECM) structure of the tendon, together with stem cells and growth factor. 3D scaffolds were produced by Wet electrospun unaligned poly-ε-caprolactone (ESPCL) or PCL-Gelatin (ESPCL-Gel) fibers to mimic wounded ECM structure of tendon wrapped by aligned poly-ε-caprolactone fibers (FSPCL) produced by Rotary jet spinning to mimic healthy ECM structure of tendon. ESPCL or ESPCL-GeL fibers within FSPCL fibers not only improved the mechanical properties of 3D scaffolds but also provided better attachment and viability of fibroblasts. Furthermore, cell alignment was observed for all groups. Moreover, ESPCL-GeL in FSPCL scaffold showed higher fibroblast attachment and viability. Consequently, FSPCL/ESPCL-Gel scaffold was considered as the most suitable scaffold for TTE. Then, human

adipose derived mesenchymal stem cells (HADMSCs) on FSPCL/ESPCL-Gel scaffold were induced with different concentration of growth differentiation factor 5 (GDF-5). The results revealed that HADMSCs with 100 ng/ mL of GDF-5 showed better proliferation, tenogenic differentiation, hydroxyproline production. As a conclusion, FSPCL/ESPCL-Gel 3D scaffold integrated with ADMSCs and GDF-5 showed promising results for TTE applications.

Keywords: Tendon tissue engineering, Rotary jet spinning, Growth differentiate factor 5, Adipose derived mesenchymal stem cells

ÖZ

İNSAN YAĞ DOKUSUNDAN AYRILMIŞ MEZENKİMAL KÖK HÜCRELERİN ÖZGÜN HÜCRE İSKELESİNDE TENDON HÜCRESİNE DÖNÜŞÜMÜNÜN GDF-5 DESTEĞİYLE SAĞLANMASI

Güner, Mustafa Bahadır
Yüksek Lisans, Biyomedikal Mühendisliği Bölümü
Tez Yöneticisi: Prof. Dr. Dilek Keskin
Ortak Tez Yôneticisi: Dr. Sedat Yılancı

Eylül 2018, 84 sayfa

Tendon yaralanmaları iskelet kası yaralanmalarının ciddi bir bölümünü oluşturur. Vücut iyileşme mekanizmaları tendon yaralarını düzeltmesine karşın bu mekanizmadaki eksiklikler sebebiyle tendonda işlev kaybına sebep olur. Tendon doku mühendisliği (TTE), hasarlı tendonun biyolojik faktörlerle bütübleşmiş bir hücre taşıyıcısı tarafından onarılması için önerilmiştir. Bu nedenle, bu tezin amacı, kök hücreler ve büyüme faktörü ile birlikte tendonun sağlıklı ve yaralı hücre dışı matriks (ECM) yapısını birleştirerek 3B hücre taşıyıcıları tasarlamaktır. Tendonun sağlıklı ECM yapısını taklit etmek için Rotary jet eğirme tarafından üretilen hizalanmış poli-ε-kaprolakton lifleri (FSPCL) tarafıdan sarılmış tendonun yaralı ECM yapısını taklit etmek için ıslak elektrospun ile hizalanmamış poli-ε-kaprolakton (ESPCL) veya PCL-Jelatin (ESPCL-Gel) lifleri kullanılarak 3B hücre taşıyıcıları üretildi. FSPCL fiberleri içerisindeki ESPCL veya ESPCL-GeL fiberleri, sadece 3D iskelelerin mekanik özelliklerini iyileştirmekle kalmamış, aynı zamanda fibroblastların daha iyi bağlanmasını ve yaşayabilmesini sağlamıştır. Buna ek olarakö tüm gruplarda hücrelerin hizalandığı gözlendi. Sonuç olarak, FSPCL / ESPCL-Gel hücre taşıyıcısı, TTE uygulamaları için en uygun hücre taşıyıcısı olarak değerlendirildi. Sonra, FSPCL / ESPCL-Gel hücre taşıyıcılarındakı insan

adipozundan türetilen mezenkimal kök hücreler (HADMSCs) farklı konsantrasyonlarda büyüme farklılaşma faktörü 5 (GDF-5) ile indüklendi. Sonuçlar, 100 ng / mL GDF-5 ile HADMSC'lerin daha iyi proliferasyon, tenojenik farklılaşma, hidroksiprolin üretimi gösterdiğini ortaya çıkardı. Sonuç olarak, ADMSC'ler ve GDF-5 ile entegre FSPCL / ESPCL-Gel 3D iskele TTE uygulamaları için ümit verici sonuçlar verdi.

Anahtar Kelimeler: Tendon doku mühendisliği, Merkezkaç kuvvetiyle eğirme, Büyüme farklılaşma faktörü 5, Yağ kaynaklı mezankimal kök hücreler

To Teoman, Jale, Kübra

ACKNOWLEDGMENTS

The author wishes to express his deepest gratitude to his supervisor Prof. Dr. Dilek Keskin and co-supervisor MD. Sedat Yılancı, for their guidance, advice, criticism, encouragement and insight throughout the research.

The author also would like to thank Prof. Dr. Ayşen Tezcaner, for her constructive Criticism and advice.

The Author also would like to thank Hilal Üstüner and Ali Deniz Dalgıç for their help.

This study was supported by Middle East Technical University.

Project NO: BAP-03-10-2016-002
Project NO: BAP-07-02-2017-004-041
Project NO: GAP- 310-2018-2669.

TABLE OF CONTENTS

LIST OF TABLES

LIST OF FIGURES

LIST OF ABBREAVIATIONS

BMP-14	Bone Morphogenetic Protein-14
CD	Cluster of Differentiation
CDMP-1	Cartilage Derived Morphogenetic Protein-1
CLSM	A Confocal Laser Scanning Microscopy
COL-I	Collagen Type I
COL-III	Collagen Type III
DMEM	Dulbecco's Modified Eagle Medium
ECM	Extra Cellular Matrix
ES	Electrospinning
ET	Extensor Tendon
FACS	Fluorescence-Activated Cell Sorting
FGF	fibroblast Growth Factor
FS	Force Spinning
FSPCL	Consisted of only Aligned Outer Part
FSPCL/ESPCL	Consisted of Aligned Outer Part and Unaligned PCL Inner Part
FSPCL/ESPCL-Gel 3:1	Consisted of Aligned Outer Part and Unaligned PCL/Gelatin Inner Part
FT	Flexor Tendon
GAG	Glycosaminoglycan
GDF-5	Growth Differentiation Factor-5
HADMSCS	Human Adipose Derived Stem Cells

HFIP	1,1,1,3,3,3-Hexafluoro-2-propanol
HYP	Hydroxyproline
ICC	Immunocytochemistry
IGF-1	Insulin Like Growth factor-1
L929	Mouse Fibroblast Cell Line
MSCs	Mesenchymal Stem Cells
OOP	Orientation Order Parameter
PBS	Phosphate Buffered Saline
PCL	poly-ε-caprolactone
PDGF	Platelet Derived Growth Factor
PGs	Proteoglycans
RJS	Rotary Jet Spinning
RPM	Rotation per Minute
SCs	Stem Cells
SEM	Scanning Electron Microscopy
SVF	Stromal Vascular Fraction
TCP	Tissue Culture Plate
TE	Tissue Engineering
TGF-β	Transforming Growth Factor-β
TNMD	Tenomodulin
TTE	Tendon Tissue Engineering
WES	Wet Electrospinning

CHAPTER 1

INTRODUCTION

1.1. Tendon

Tendon is a fibrous hierarchical connective tissue which is specialized to connect muscle to bone with highly orientated extracellular matrix (Doroski, Brink, & Temenoff, 2007). Tendons have a crucial role in musculoskeletal system in terms of force transmission, load absorption, joint movement, and joint stability (Jozsa, Kannus, Balint, & Reffy, 1991). Therefore, tendon tissues must meet specific requirements depending on location in the body. At the kneecap; for example, tendons should provide knee extension and knee joint stability, or tendon available at shoulder joint must enable arm rotation (Carmeli, Patish, & Coleman, 2003; Ricchetti, Aurora, Iannotti, & Derwin, 2012). Such examples would be multiplied to support the important role of the tendon in daily life routine.

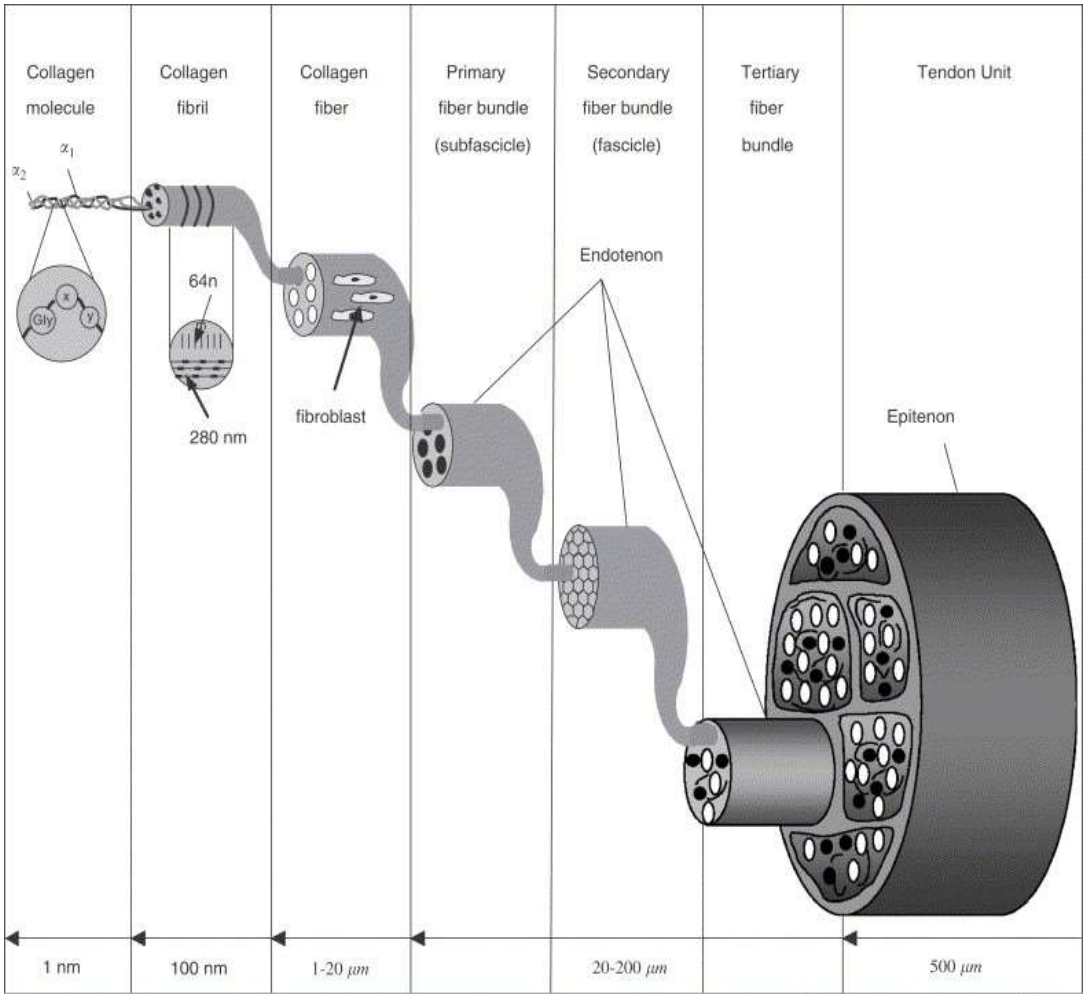

Figure 1. The hierarchical order of tendon tissue (Lui, Rui, Ni, & Chan, 2011).

In general, hierarchical order (Figure 1) of tendon begins with the tropocollagen molecule. Namely, three polypeptide chains each of which is tropocollagen (Figure 2) in triple helix with a diameter around 1 nm form the tropocollagen molecule. These molecules, in the first stage, assemble microfibrils, then turn in to crimped shape collagen fibril in the second stage (Voleti, Buckley, & Soslowsky, 2012). These fibrils are arranged to compose collagen fibers that aggregate fiber bundles. The bundles are wrapped by a loose connective tissue known as the endotenon. Endotenon together with the epitenon, which covers entire tendon, enables tendon to the vascular, lymphatic, and nerve supply (Kannus, 2000). Since tendons experience high mechanical stress, synovial sheets contribute tendon lubrication (Sharma & Maffulli, 2014).

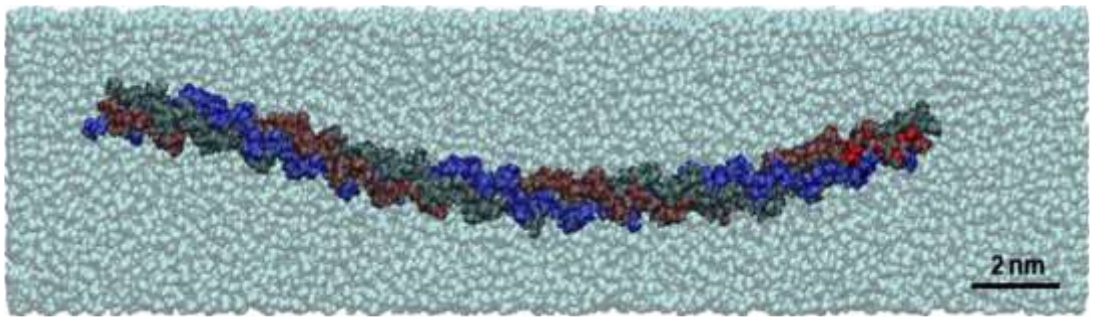

Figure 2. Tropocollagen model in water (Gautieri, Vesentini, Redaelli, & Buehler, 2012).

Tendons are mainly consisting of water (70% of total weight) (Hess, Cappiello, Poole, & Hunter, 1989); however, dry weight of the tendons are mostly made up by collagen type I (COL-I, 80-90%) (Lomas et al., 2015). Human tendons' dry mass, consisted of not only COL-I but also other types of collagens, glycosaminoglycans (GAGs, 0.2%), elastin (1-2%), and proteoglycans (PGs, 1-5%) (Lomas et al., 2015). Specifically, COL-I fiber type matrix accompanied by GAGs, PGs, and water fulfill the mechanical requirements of the tendon tissue under the load (Sharma & Maffulli, 2014). Moreover, physiological processes; such as cell- cell interaction, collagen fibrils aggregation, etc., are also related to GAGs and PGs (Derwin, Soslowsky, Kimura, & Plaas, 2001). Thus, aging and pathophysiology of the tendon tissue are related with other types of collagens (Wenstrup et al., 2011).

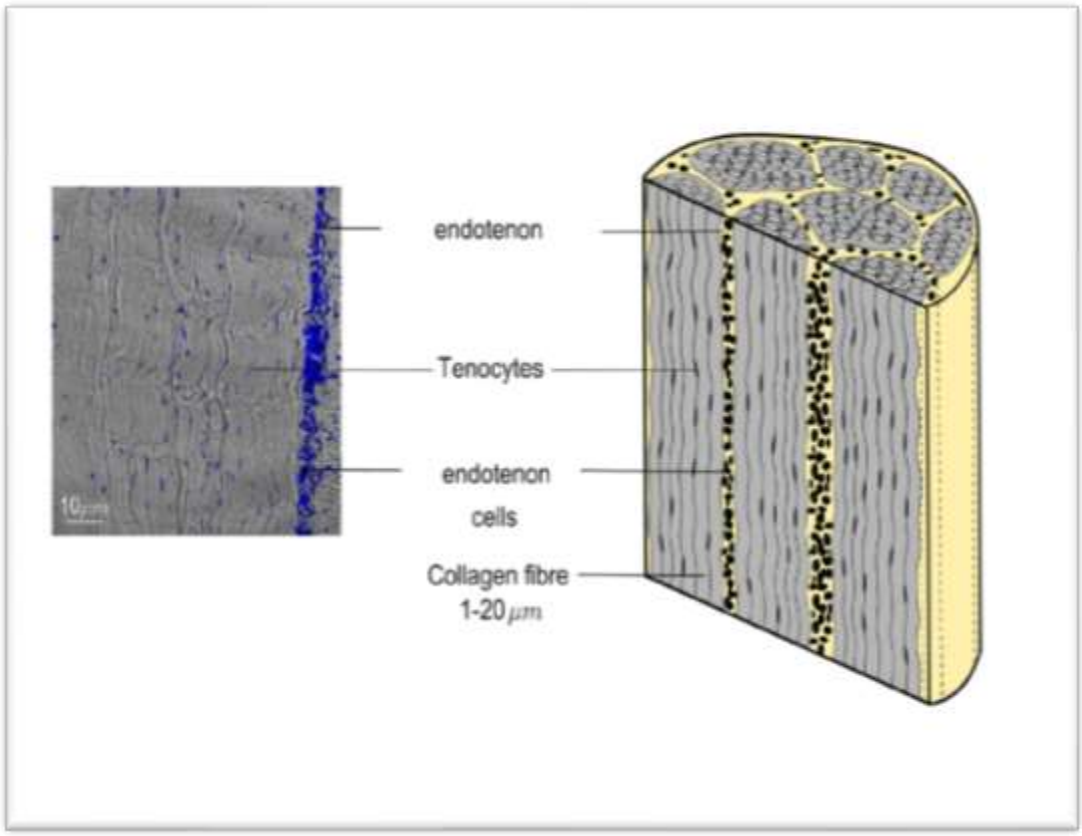

Figure 3. Crimp formation and structure of tendon tissue (Spiesz et al., 2015)

Along with tendon structure, there are two main types of cells; 9-95% of cells in tendon tissue are tenoblasts cells (immature tendon cells) and tenocytes cells (mature tendon cells) (Kannus, 2000). Length and shape of the cells enable to distinguish these two cell types; for instance, while tenoblasts cells are smaller (20-70 μm) than tenocytes (80-300 μm) and have various shapes (round, polygonal, and spindle-star-like) unlike elongated shape of tenocytes ((Chuen et al., 2004; Ippolito, Natali, Postacchini, Accinni, & De Martino, 1980). Besides that, tendon tissue also contains other types of cells; tendon stem cells, chondrocytes, vascular endothelial cells, synovial cells, and smooth muscle cells (Kannus, 2000; Sharma & Maffulli, 2014).

Muscles are connected to bone by tendons and transfer mechanical force to the bone in order to generate joint movement. Myotendinous junction refers to the part where tendon and muscle are attached while osteotendinous or enthesis is the region where bone and tendon connection occur (Kannus, 2000). Depending on tendon location,

tendons shape and size vary from each other. In general, extensor tendons tend to have flattened shape while, flexor tendons tend to have a round or oval shape (Benjamin, Kaiser, & Milz, 2008).

Figure 4. Anatomy of tendons in hand. The flexor tendons (a) and the extensor tendons (b) (Benjamin et al., 2008).

Tendons can maintain structural integrity under great tension force because of its mechanical behaviors; fibroelastic, viscoelastic, and plastic (Haut, 1986; Järvinen, Järvinen, Kannus, Józsa, & Järvinen, 2004). Tendon mechanical characteristics, thus, are influenced by force direction and anatomical location (Voleti et al., 2012). Crimped structure of the collagens which might have different patterns (i.e., planar zig-zag connected structure, helical structure, flattened helices, or spirals) is maintained at rest and serves as a shock absorber when the force is initiated. They

become straightened when the load is applied (Diamant, Keller, Baer, Litt, & Arridge, 1972; Gathercole & Keller, 1978; Jozsa et al., 1991). Stress-strain curve of the tendon can be considered in three regions as toe region, linear region, and failure region (Figure 5) (Roshan James, Kesturu, Balian, & Chhabra, 2008). At toe region, the crimped pattern in the collagen fibers are straightened (Gathercole & Keller, 1978); at the linear region, the collagen fibers have a completely un-crimped pattern (Silver, Christiansen, Snowhill, & Chen, 2001). At last, tissue rupture begins beyond the linear region leading to tendon failure (Rigby, Hirai, Spikes, & Eyring, 1959). Mainly, mechanical properties of tendon tissue are related with the crimp pattern, the thickness, and collagen content (Sharma & Maffulli, 2014). Generally, 0-4% strain range covers toe and linear regions, namely, elastic region of the tendon. Strain exceeding 4% of tendon length causes microscopic, eventually, macroscopic (8-10%) tears.

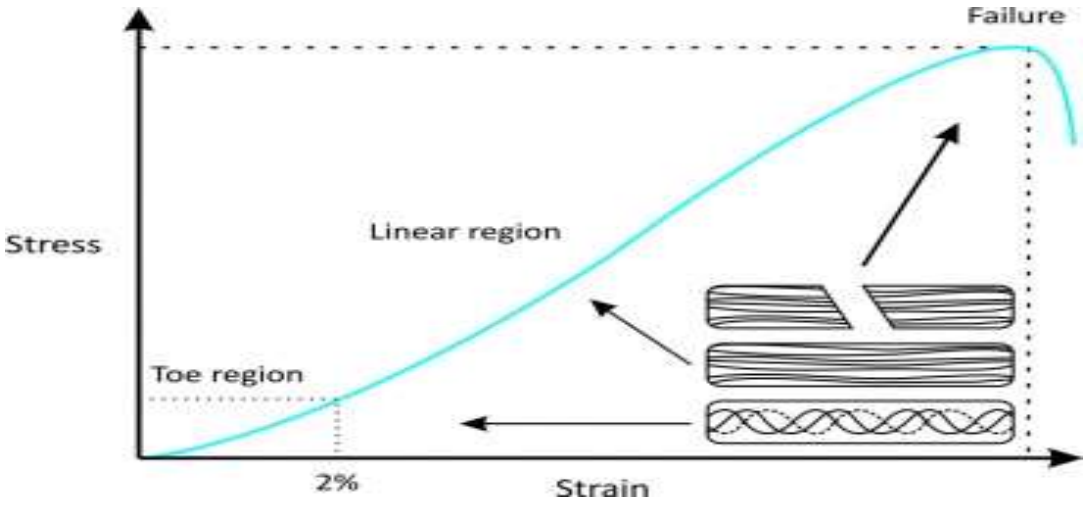

Figure 5. Stress-strain diagram of the tendon (Robi, Jakob, Matevz, & Matjaz, 2013)

1.1.1. Tendon Defects/ Wounds

Tendon tissue injuries are reported as musculoskeletal injuries. Achilles, patellar, and rotator cuff tendon can be classified as most common tendon injuries (Wilson &

Best, 2005). The appearance of the wounded tendon can be easily noticed by its disordered structure and brown color unlike tendon healthy color which is shiny white. Tendon injuries cannot be recognized until full tendon tear, one of the most considerable risks of tendinopathy, occurs (Sharma & Maffulli, 2014). Tendon tissue matrix is degenerated due to intrinsic factors, extrinsic factors, or combination of the both, resulting in the structural and functional deformation of the tendon. Overuse and aging are mostly labeled as intrinsic factors which are in chronic nature, while trauma and rapture are extrinsic factors in acute nature. Eventually, tendon injuries lead loss of function, disability, long-term pain, and a decrease in life quality (Lui et al., 2011; Sharma & Maffulli, 2014).

1.1.2. Tendon Healing

Tendon injuries are particularly problematic due to fibrotic scar tissue formation in tendon healing since the regenerative capacity of tendon tissue is limited. This result in a decrease of mechanical properties of the healed tendon (Lui et al., 2011). Tendon healing process involves three stages which are initiated after acute tendon injuries : inflammatory, repair, and remodeling stages (Figure 6) (Voleti et al., 2012).

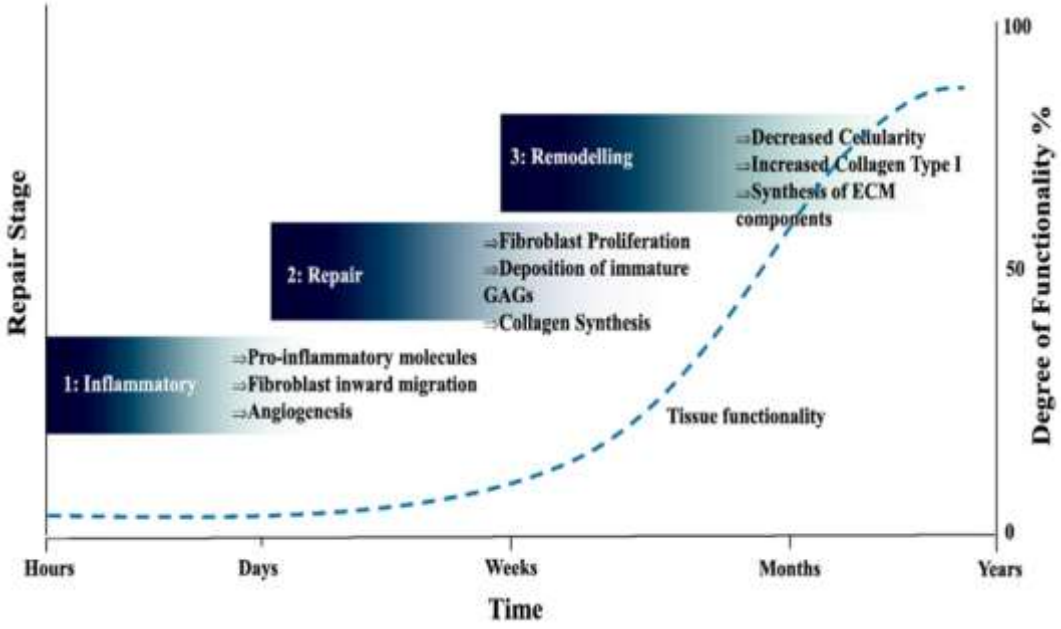

Figure 6. The three phase of tendon healing (Lomas et al., 2015).

The inflammatory phase is the first response of the body to injured tendon side. The phase is immediately initiated after the injury and continued for a few days. Inflammatory cells such as neutrophils, monocytes, and macrophages are stimulated by pro-inflammatory cytokines to remove necrotic cells and tissues (Sharma & Maffulli, 2014).Additional inflammatory cells home to the wound side by the contribution of escalated vascular permeability (Voleti et al., 2012). After that, tendon cells start forming ECM in the wounded side, while the vascular network is synthesized (Gelberman, Vandeberg, Manske, & Akeson, 1985; Voleti et al., 2012).

The repair stage is initiated by cell migration and proliferation, therefore this stage is also known as “proliferative stage” (Voleti et al., 2012). Although the cell proliferation and migration mechanisms after tendon wound require more investigation, it is known that the repair stage initiates soon after the injury and follows up to 30 days. During this stage, collagen type III synthesis increased together with proteoglycans synthesis and water retention leading to a provisional

ECM (Voleti et al., 2012). Formation of collagen type III matrix is completely random and it is reported to increase cell proliferation rate (N. M. Lee et al., 2017).

The remodeling stage is started 6-8 weeks after an injury and required up to 2 years depending on the tendon wound, patient age, and conditions. This phase can be divided into two that are consolidation and maturation. In the consolidation part, synthesis of collagen type III is decreased along with cellularity and matrix production. Cells metabolism, nevertheless, preserved its high activity, in other words collagen type III synthesis is replaced by collagen type I that leads to more fibrous tissue and increasing in mechanical properties of healing tendon (Denitsa Docheva, Müller, Majewski, & Evans, 2015a). Furthermore, alignment of collagen type I is increased in stress direction (Sharma & Maffulli, 2014). Ten weeks after tendon injury, maturation part of the remodeling stage takes place to form more collagen fibril crosslinking and to decrease cells' metabolism and vascularity (Grinstein & Galloway, 2018). On the other hand, neo-tissue turns into scar type tissue instead of healthy tissue; therefore, it cannot gain its native properties (Roshan James et al., 2008).

1.2.Conventional treatments

Conventional therapies for tendon repair can be conservative, surgical operation, or including both. In the conservative approach, physical therapies are applied on the patients accompanied with, more often than not, injection of drugs, like corticosteroids and aprotinin, and nonsteroidal anti-inflammatories (Hampson, Forsynth, El Haj, & Mafulli, 2008). Furthermore, certain procedures which are applied in physiotherapy like low-intensity pulsed ultrasound, and shockwave, are among the most common physical therapies (Lui et al., 2011). Yet, despite effort of conservative treatments in the course of tendon healing- even some tendon tissue repair is achieved-, it is plausible to claim that this approach cannot provide full regeneration of tendon injury, thus leading to the loss of its function, but increasing duration of the treatment and chance of reinjury as well (Hampson et al., 2008).

As mentioned, the conservative approach may not be enough to repair a tendon injury. Tendon damage is beyond the capacity of the conservative treatment when tissue is heavily injured. In that case surgical operation is considered as an option. Surgical operation can be divided into parts; Surgical interventions, surgical suture, transplants, and prostheses (Hampson et al., 2008; Jørgensen, Bak, Ekstrand, & Scavenius, 2001).

Surgical interventions involve the promotion of regeneration through the induction of cells and location and/or removal of present fibrotic tissue (Maffulli, Longo, Loppini, & Denaro, 2010). Considering the site of injury, one of the methods to apply tendon surgery is the endoscopic surgery which is minimally invasive (Mazzocca et al., 2010). Moreover, the suture can be used as a treatment to connect the tendon tear side, if an end-to-end gap smaller than 5 mm is present (Burkhart, Diaz Pagàn, Wirth, & Athanasiou, 1997).

Tendon transplantation is required for the severely damaged tendon. Autograft in tendon treatment, which is patient's tendon obtained from another tendon site, is "gold standard" for tendon repair. The significance of the autograft comes from the absence of immunological rejection (Wu & Han, 2018). The "golden standard", however, is not always available because of the limited donor side. Furthermore, a secondary surgery is required to obtain tendon tissue from a patient and it can lead donor side morbidity. Therefore, alternative forms of tendon transplantation are developed to overcome autograft limitations with the use of allografts, tissue taken from cadavers, and xenograft, tissue taken from other species. Although autograft drawbacks are eliminated, allograft or xenograft implanted patients are at risk of disease transmission, immunological rejection, and high rerupture rate (Moshiri & Oryan, 2012). Eventually, sterilization and decellularization of allograft or xenograft are performed to prevent risks, with a drawback as a decrease in mechanical properties of the implants and increase in reinjury (Marrale, Morrissey, & Haddad, 2007).

Tendon prostheses- which are produced by using synthetic materials such as polyester, polypropylene, silicone, nylon, etc.- are commonly used from the early

1980s to 1990s. Mechanical properties of these implants were better than transplants. Nonetheless, these devices created trouble in terms if biocompatibility, prosthesis degradation, and failure. They could not meet all these requirements and pulled back from the market (Chen, Xu, Wang, & Zheng, 2009).

1.3.Tendon tissue engineering (TTE)

Since conventional treatments have the above-mentioned limitations, tissue engineering takes place as an alternative treatment strategy for tendon injuries. The aspect of tissue engineering (Figure 7) has a great potential paradigm for tendon healing. Engineered tissue scaffolds integrated with biochemical and physical cues enables to reconstruct native tissue (Thayer & Goldstein, 2016). In this point of view, the ultimate goal of the tissue engineering is mimicking both the structure and environment of the native tissue. Tissue engineering approach gives opportunity either *in vivo* treatments or *in vitro* tissue growth for later transplantation.

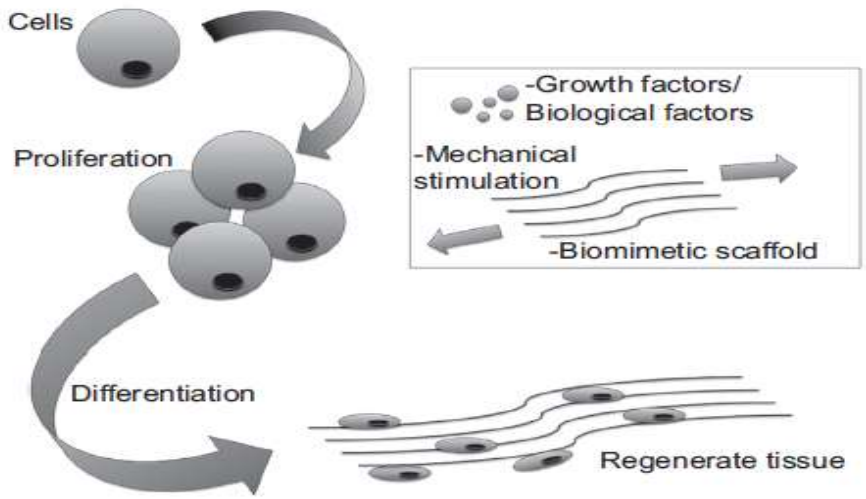

Figure 7. Tissue engineering approach (Ramos, Peach, Mazzocca, Yu, & Kumbar, 2015).

1.3.1. Materials

Materials in tendon tissue engineering field can be divided into two groups as natural materials (e.g. gelatin) and synthetic materials (e.g. PCL). Biodegradable and biocompatible synthetic materials such as poly-ε-caprolactone (PCL) (Peach et al., 2012) are highly studied in TTE. The importance of synthetic materials is that properties of the synthetic materials can be tailored in terms of pore size, degradation rates, mechanical strength, shape, biological properties, etc.

Natural materials can be obtained from animal or plant sources and draw attention in TTE applications mostly for resembling native tissue components (Ramos et al., 2015). In contrast to synthetic materials, natural materials have good biocompatibility and degradability to stimulate cell response (Wu & Han, 2018). Main drawbacks of natural materials, on the other hand, can be said as inconsistency of chemical, biological, and material properties between batches (Andrews, Scholes, & Wiederrecht, 2010), uncontrollable degradation rate, inappropriate mechanical properties for load bearing applications (Yamane et al., 2005), and poor processing ability (Laurencin & Nair, 2015). In order to overcome these drawbacks, natural materials can be combined with synthetic materials such as PCL-gelatin (Patel & Fisher, 2008).

Gelatin which is produced from collagen denaturation is widely used in pharmaceutical and medical fields because of its biological origin, biodegradability, biocompatibility, and commercial availability at relatively low cost (Y. Zhang, Ouyang, Chwee, Ramakrishna, & Huang, 2005). Gelatin can be classified by two types; type A and B. Type A is that collagens are subjected to the acidic pretreatment to obtain gelatin while gelatin is extracted by alkaline pretreatment from collagens. Carboxyl acid presence in Type B is greater than Type A since glutamic and aspartic

acid are increased by glutamine and asparagine residues due to alkaline pretreatment (Ward & Courts, 2013).

PCL (Figure 8) is a biodegradable polyester which is produced from e-caprolactone monomer. PCL and PCL including scaffolds are commonly used in TTE because of biocompatibility and nontoxic degradation products as well as long degradation time up to 2 years in vivo (Yildirimer & Seifalian, 2014). Moreover, a high degree of crystallinity and hydrophobicity are other worth to mentioned properties of PCL (Yildirimer & Seifalian, 2014).

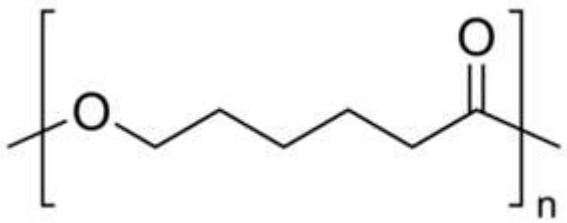

Figure 8. Chemical structure of PCL.

1.3.2. Fibers

Mechanical properties and biocompatibility are important criteria in material selection. Besides that, the surface chemistry is important for the initial and continuous interaction between biomaterial and cell. The microstructure of a material, on the other hand, has crucial role in tissue repair. For example, the material should ensure proper porosity for nutrient, waste exchange, and cell infiltration. Furthermore, high aspect ratio, surface area, and mechanical properties-also can be tailored by morphology- must meet requirements for soft tissue engineering (Kumbar, James, Nukavarapu, & Laurencin, 2008). Fibers, therefore, are suitable for tendon tissue engineering, since native tendon ECM mostly consist of collagen type I fibers that are aligned in tendon structure.

The interest of fiber networks lies in the phenomenon of contact guidance that cell morphology, the orientation of cells, and expression of phenotypic markers can be

modulated (Han, Zhu, Chen, Wicks, & Li, 2017). Studies state that cell morphology is guided by fiber diameter, as well as fiber orientation (Xie et al., 2010). In addition, Xie et al. (2010) shows that cells are elongated on aligned fibers similar to tenocytes at healthy tendon while random oriented fibers provide rounded shape cells. In this concept, nanofibers that are randomly oriented mimic wounded tendon that leads tendon fibroblast cell proliferation and ECM deposition on aligned microfibers mimic native tendon that cells preserve fibroblastic phenotypes (Erisken, Zhang, Moffat, Levine, & Lu, 2013).

1.3.3. Scaffold Production Techniques

The goal of the scaffold is mimicking tissue microenvironment and microarchitecture at the site of defect or implantation (Liu Tsang & Bhatia, 2004). Therefore, produced scaffold must meet the requirements of the mechanical and biological function of the tissue. Since tendon structure is made of collagen fibers (Kannus, 2000), designed tissue engineering platform also need to consist of fibers to mimic the architecture of tendon. In addition, produced fibers should be in aligned form for complete mimicking. Another design constraint of the scaffold is enabling cells to migrate to the site, proliferate, initiate remodeling and maturation (Moshiri & Oryan, 2012). In short, tissue construct must have optimal an environment for tissue regeneration.

Electrospinning (Figure 9A) method is one of the most commonly used fiber production processes in which high-voltage is applied to form electric field between a nozzle and collector. This electric filed provides a thin wet polymer filament to be expelled from syringe needle to mostly grounded collector (Huang, Zhang, Kotaki, & Ramakrishna, 2003). Electrospinning parameters that affect fiber characteristic are solution concentration, polymer and solvent used in solution, ejection flow rate, intensity of the electrical field, the needle diameter, and distance between the needle and the collector (Luo, Stoyanov, Stride, Pelan, & Edirisinghe, 2012). Main advantages of electrospinning are simple system setup, easy to produce lab-scale

pilot model and ability to control fiber dimensions from micron-to-nanometer sizes (S.-E. Kim, Jordan, Korley, & Pokorski, 2017). Conventional electrospinning method, nonetheless, cannot provide proper pore size for cellular activity due to 2D nature of final fiber matrix (Dalton et al., 2013). Furthermore, the final structure of the fiber matrix cannot be controlled because of electrostatic repulsion (Centola et al., 2010). In order to overcome these limitations, wet electrospinning (Figure 9B) method where fibers are collected in the non-solvent bath is used to produce 3D scaffold (Luo et al., 2012). Even so, there are other electrospinning related disadvantages such as the requirement of a high-voltage power source, solvents within a specific range of dielectric constant, unprecise control over fiber orientation, and low fiber yield. (McEachin & Lozano, 2012; Rogalski, Bastiaansen, & Peijs, 2017).

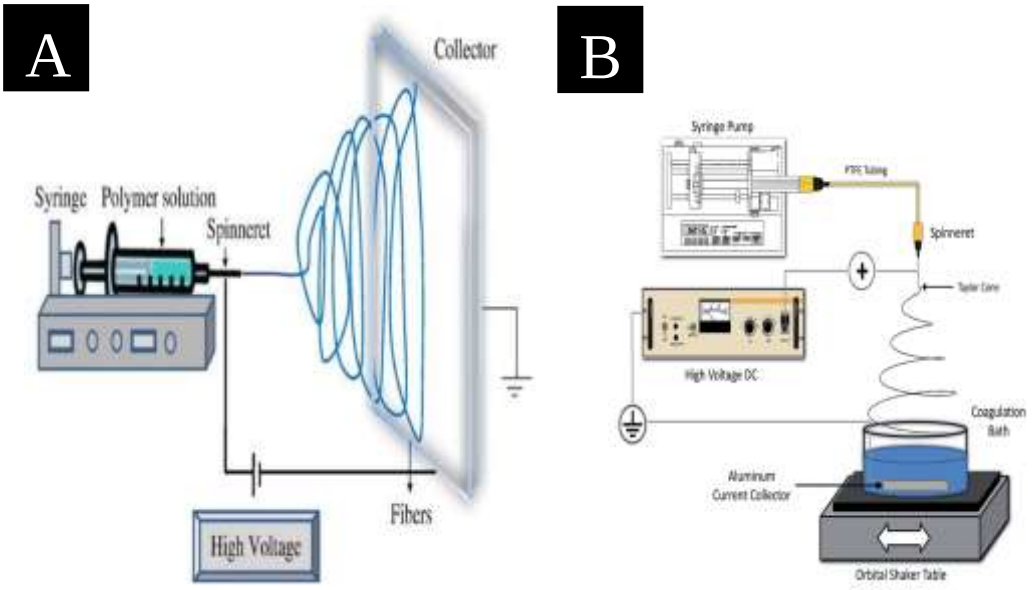

Figure 9. Schematic illustration of ES (N. Zhu & Che, 2013) and wet electrospinning (Zheng et al., 2014).

Rotary jet spinning (RJS or force spinning, Figure 10) was introduced in 2010 to fabricate fine aligned micro and nanofibers. Fiber production is driven by a

centrifugal force that needs to overcome surface tension forces for fibers formation (Mohammad Reza Badrossamay, McIlwee, Goss, & Parker, 2010). Fiber characteristics can be designed by device dependent parameters, such as orifice diameter, rotation speed, and collector and solution dependent parameters that are solvent volatility and viscosity of the solution (Mohammad Reza Badrossamay et al., 2010). Main advantages of RJS are high fiber yield, low power consumption, easy setup, its natural process provides aligned fiber (Golecki et al., 2014).

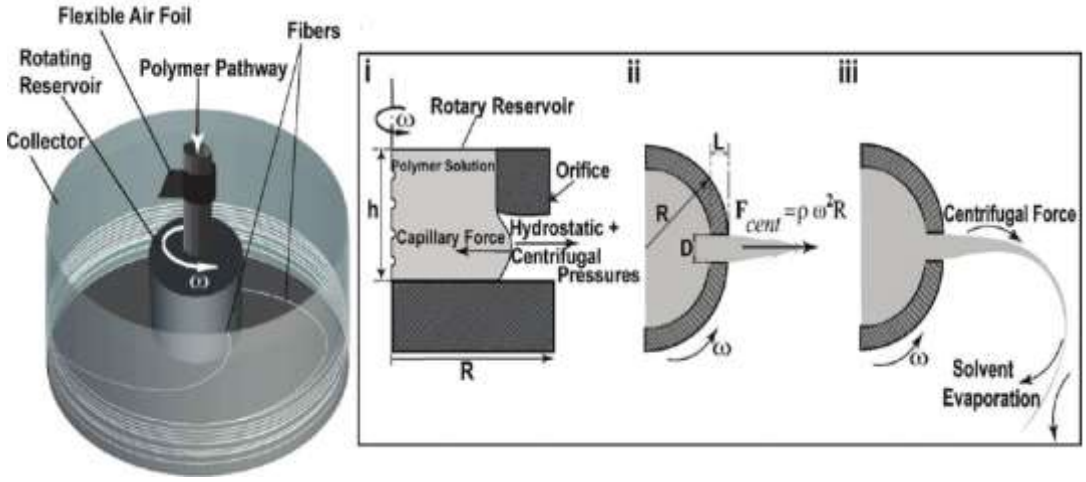

Figure 10. Schematic illustration of RJS (Mohammad Reza Badrossamay et al., 2010).

1.3.4. Cells

Seeding cell on the engineered scaffold is a well-known strategy in order to improve wounded tissue healing. Moreover, studies state that cell seeding promotes treatment of injured tissue (Y. S. Kim, Lee, Ok, Park, & Kim, 2013; Loeffler et al., 2013). There are different cell types used in tendon tissue engineering. For example, mesenchymal stem cells (MSCs) from different sources, tenocytes, and tendon stem cells, have been examined to develop cell loaded constructs for tendon tissue engineering application (Mazzocca et al., 2012).

Although tenocytes provide great opportunity due to being derived from tendon itself. However, being highly differentiated limits its proliferation. Moreover, enough number of tenocytes cannot be isolated from the tendon. A sufficient number of tendon stem cells is not available for cell isolation from tendon (Bieback, Kern, Kocaömer, Ferlik, & Bugert, 2008). Therefore, using a different cell source for tendon tissue engineering would be more efficient. For this purpose, MSCs could be a better candidate.

MSCs that are derived from different sources show almost the same property (Bieback et al., 2008). Especially, adipose-derived MSCs can be an efficient cell source for tendon tissue engineering in terms of the number of cells and ease of isolation (Merceron et al., 2008). One thing that should be considered when using MSCs in tendon tissue engineering is that ectopic bone growth will be an issue due to deficiency of oxygen since MSCs have capable of differentiating to other tissues like bone (Pietschmann et al., 2013).

1.3.5. Growth factors

Since the natural healing process of the tendon is not enough to generate fully restored tendon increasing research on tendon development mechanisms provides new ideas to improve regeneration. Towards this aim, growth factors like transforming growth factor-β (TGF-β), insulin-like growth factor-1 (IGF-1), fibroblast growth factor (FGF), and platelet derived growth factor (PDGF), which bind to cell surface receptor to promote specific cellular events (Nixon, Watts, & Schnabel, 2012), are investigated in tendon tissue engineering applications (Molloy, Wang, & Murrell, 2003).

While chemotaxis and fibroblasts proliferation are increased at first stage of tendon healing by PDGF presence, tenomodulin expression and biomechanical properties were not affected suggesting that PDGF fails to contribute complete tendon regeneration (Nourissat, Berenbaum, & Duprez, 2015).

IGF-1 is involved in first and second stages of tendon healing (Molloy et al., 2003) by stimulating migration and proliferation of fibroblasts and inflammatory cells. Moreover, collagen and ECM components' synthesis is increased at third stage of tendon healing by IGF-1 (Costa et al., 2006; Roshan James et al., 2008; Molloy et al., 2003).

FGF is related with angiogenesis and migration of cells that increase wound closure rate of patellar tendon by the proliferation of fibroblasts (Costa et al., 2006). Furthermore, it was shown in an in vivo study with a chick that FGF is involved in the first stage of tendon healing by stimulating scleraxis expression, resulting in enhanced biomechanical properties in the healed tendon (Thomopoulos et al., 2010). Nonetheless, FGF contributions are rejected by other observation in terms of mechanical and functional properties of the healed tendon (Ngo, Pham, Longaker, & Chang, 2001).

TGF-β is involved in early and mid-stages of tendon healing by stimulating cell migration and proliferation (Roshan James et al., 2008). In addition, collagen type I synthesis are improved by TGF-β at *in vitro* conditions, suggesting that tendon healing mechanisms can be enhanced by TGF-β (Manning et al., 2011). Scar tissue formation, on the other hand, is increased at late stage of tendon healing by a late expression of TGF- β (Roshan James et al., 2008).

Growth Differentiation Factor-5 is a part of Transforming growth factor-β (TGF- β) family and also can be classified as cartilage-derived morphogenetic protein-1 (CDMP-1) or bone morphogenetic protein-14 (BMP-14). TGF- β family members signaling mechanism, in general, is induced by a ligand that constitutes tetrameric complex with cell surface receptors type I and type II are known as serine/threonine receptors (Heldin, Miyazono, & Ten Dijke, 1997; Massagué, 1998). Briefly, members of TGF- β family signal transduction is beginning to from an attachment to type II receptor. Following, the ligand and type II receptor complex is identified by type I receptor to generate the heteromeric complex. Due to final complex, phosphorylation and activation of type I receptor is driven by type II receptor, revealing type I receptor activation has vital role to transduce TGF- β family

members signals. Finally, transduced signal through type I receptor phosphorylate receptor-regulated SMADs (R-SMADs), resulting in activation of R-SMADs to form trimers that are consisting of two R-SMADs and SMAD4 to translocate to nucleus and regulate gene expression (Hata & Chen, 2016). TGF- β family members demonstrate analogy to their general signal transduction, despite the fact that each member inducts specific signaling pathway (Macfarlane, Haupt, Dietz, & Shore, 2017). On the other hand, signaling mechanism of GDF-5 initiated tenogenic differentiation is mainly unidentified (Y. J. Zhang et al., 2018) even though certain studies were attempted to identify signaling pathways of GDF-5 lead to tenogenic differentiation . Statements of these researches can be summarized as GDF-5 ligand randomly binds to the activin type II and IIB receptors, and the BMP type II receptor (Nishitoh et al., 1996). Interestingly, in vivo and in vitro studies affirmed that GDF-5 ligand almost always binds to the ALK6 type I receptor due to single arginine438 residue in the sequence of GDF-5 (Nickel, Kotzsch, Sebald, & Mueller, 2005; Nishitoh et al., 1996). Additionally, the heteromeric complex consist of ALK6 type I receptor activates the SMAD 1/5/8 signaling pathways (Shen, Gelberman, Silva, Sakiyama-Elbert, & Thomopoulos, 2013) that both in vitro and in vivo studies informed SMAD8 activation triggers MSCs to tenogenic differentiation (Hoffmann et al., 2006; Shahab-Osterloh et al., 2010).

Researches in literature were also evaluated for GDF-5 effects of tendon formation and tenogenic differentiation. Wolfman et al reported that subcutaneous or intramuscular implantation of GDF-5 in rats provides development of ectopic neotendon for the first time. Furthermore, When GDF-5 was implanted with bone morphologic factor-2 rather than being implanted alone, regenerated tissue was composed of two distinct tissue: tendon tissue and bone tissue. It was stated that GDF-5 maintain its tenogenic effects (Wolfman et al., 1997). More interestingly, in another study, GDF-5 null mutation in branchypodism mice was examined as model to evaluate the Achilles tendon. Results revealed that GDF-5 deficiency in mice causes the compositional, mechanical, ultrastructural properties inferior to that of mice native Achilles tendon (Mikic, Schalet, Clark, Gaschen, & Hunziker, 2001). Following study shown that Achilles tendon healing was prolonged by deficiency of

GDF-5 in branchypodism mice (Chhabra et al., 2003). Additionally, tenogenic differentiation of adipose-derived mesenchymal stem cells has been shown that tendon ECM, such as COL I, and specific tendon markers, such as, tenomodulin and SMAD8 were promoted by GDF-5 presence in the cell culture media (Park et al., 2010).

1.4.Aim of the study

When tendon injuries are beyond the capacity of natural healing processes and do not respond to the conventional treatments, tendon tissue engineering (TTE) techniques may be required. In this way, tendon repair can be achieved by using a combination of scaffolds with growth factors and/or cells. TTE scaffolds with fibrous microstructure can be produced by different techniques. Manufacturing methods must provide reproducible, and industrially applicable scaffolds that were proved to be successful with in vitro and in vivo studies.

This thesis aims to produce fabrication of 3D scaffolds supplemented with stem cells and growth factor to mimic healthy and wounded extra cellular matrix of tendon to increase cell adhesion, proliferation, and orientation for TTE applications. Here, aligned 3D scaffolds of poly-ε-caprolactone (PCL) and gelatin fibers which were manufactured to mimic healthy and wounded ECM tendon structure. The scaffolds are supplemented with human adipose derived mesenchymal stem cells (HAMSCs) and growth differentiation factor 5 (GDF-5) in order to investigate potency as TTE

construct for complete tendon regeneration with initial in vitro studies. 3D scaffolds were produced with optimum properties for tissue engineering strategies. In order to do so, aligned 2D fiber sheet was produced considering different parameters for RJS and characterized in terms of degree of alignment and fiber diameters. Then, the optimized sheet was combined with wet electrospun PCL and PCL/Gelatin fibers to manufacture aligned 3D scaffolds. Morphology, degradation and water uptake, and mechanical properties of final scaffolds were characterized to evaluate tendon tissue regeneration related capacities. In addition, attachment and viability of the mouse fibroblast cells(L929) were investigated with *in vitro* cell culture experiments. The optimized scaffold in the first part was supplemented with HADMSCs and GDF-5 at different concentrations to investigate the stem cell response in engineered tendon tissue construct. The evaluation was done by the cell viability, quantitative measurement of collagen production, and immunocytochemistry (ICC) analyses.

CHAPTER 2

MATERIALS AND METHODS

2.1. Materials

For scaffolds production, Poly(ε-caprolactone) (PCL; Mn, 80000), chloroform, gelatin from porcine skin, and absolute ethanol were the products of Sigma-Aldrich (Germany). Electrospinning solvent, 1,1,1,3,3,3-Hexafluoro-2-propanol (HFIP) was purchased from Merck (Merck, Germany).

For in vitro cell culture studies, low glucose Dulbecco's Modified Eagle Medium (DMEM) from Biowest (France), high glucose DMEM from Biowest (France), DMEM medium without phenol red (Biochrom, Germany), fetal bovine serum (FBS) from Biowest (France), penicillin/streptomycin from Biowest (France), Alamar Blue® from Invitrogen (U.S.), trypsin/ EDTA from Biowest (France), growth differentiation factor-5 from R&D Systems (U.S.A) were used. Mouse fibroblast cell line L929 were obtained from ATCC (USA).

Human lipoaspirates were obtained from Liv Hospital (Ankara, Turkey, Ethical committee 2018/005). For the isolation, collagenase from clostridium histolyticum, type I A purchased from Sigma-Aldrich (Germany). Characterization of isolated cells was performed by using CD 90 and CD11b/c from Biolegend, CD 105 from Abcam (U.K.), CD 44, CD 45 and CD 31 from Cell Signaling Technology (U.S.A).

For quantitative total collagen measurement, Chloramine-T, L-hydroxyproline, sodium acetate, 4-(Dimethylamino)benzaldehyde, citric acid, perchloric acid, 1-propanol, and sodium hydroxide were purchased from Sigma-Aldrich (Germany). Acetic acid was obtained from Merck (Germany).

Immunofluorescence staining was performed by using collagen α1 type III antibody (Santa Cruz Biotechnology, U.S.A), collagen type I antibody (Abcam, U.K), TNMD antibody (Biorbyt, U.K), Alexa Fluor® 488 and 532 phalloidin Cell Signaling Technology, U.S.A, Alexa Fluor® 488, 647 (Cell Signaling Technology, U.S.A), DRAQ5 (Cell Signaling Technology, U.S.A), and DAPI (Invitrogen, U.S.A).

2.2.Methods

2.2.1. Production of 3D Constructs

Outer Part: Fiber Production by Rotary Jet Spinning (RJS)

Aligned PCL micro fibrous sheets were produced by custom made RJS device (Mekoptronik, Turkey). Custom made collector which was made of a flat aluminum sheet was placed horizontally under the spinning container. PCL solutions were prepared in chloroform at 5%, %10, and %15 concentrations (w/v) and rotated at different rotation per minutes (rpm), while feeding the reservoir with polymer solution at various flow rates;1.5, 2.0, 2.5, and 3.0 mL/min. Final products of the spinning process were collected from the collector and cut into rectangles (5x4 cm x cm) for characterizations. RSJ products were designed to be the outer part of the final 3D construct.

Inner Part: Fiber Production by Wet Electrospinning (WES)

PCL and PCL/Gelatin fibers which were aimed to be the inner part of the 3D construct were electrospun by wet electrospinning system using ethanol bath onto a rotating stand collector (Gozeler Electronic Corporation, Turkey). PCL or PCL/Gelatin (3:1) (w/w) solutions were prepared in HFIP at a concentration of 10% (w/v) and were pumped through NE-1000 syringe pump (New Era Pump Systems, USA). The distance between syringe tip and collector was arranged as 12 cm. The polymer solution was pumped at 3.5 ml/h flow rate and a voltage of 6.9 kV was applied to syringe using Gamma High Voltage Source ES30 (Gamma High Voltage Research, Inc., USA).

Preparation of Combination of The Two Parts: 3D Construct

Final form of the scaffolds (Figure 11) as 3D constructs of inner and outer fibrous parts were obtained by combining RJS and WES products after separate production. Aligned fibrous sheets which have alignment along the long axis of the RJS. Then, a long, WET electrospun PCL 3D cylinder which has the same length with the long edge of rectangular sheets was placed on of the two long edges. Then a tube shape was obtained by rolling aligned PCL fiber sheet around the electrospun PCL fibers. In order to create the final shape of the 3 D construct, the two ends of the tube were clamped and were horizontally rotated three times for 360°. The tightened bundle formed a solid and stable structure that has formed the hybrid scaffold. Then produced scaffolds were freeze at -80 °C, lyophilized (Labconco Corporation, USA) in order to remove ethanol and form the final structure of the scaffolds.

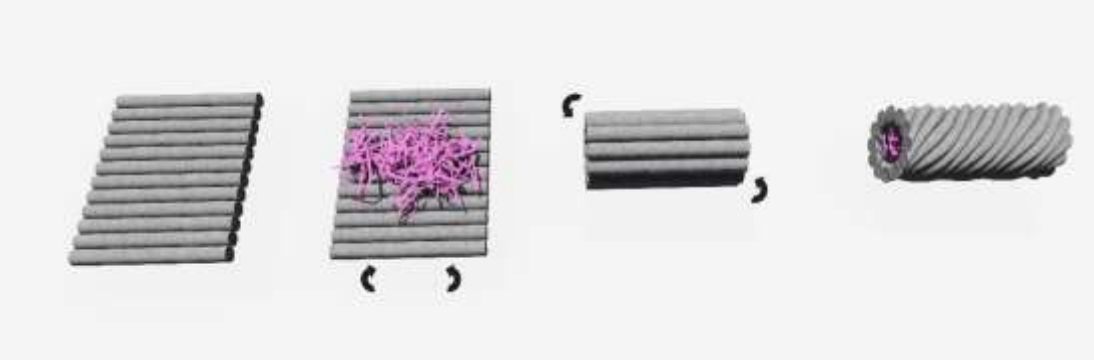

Figure 11. Schematic illustration of scaffolds preparation.

2.2.2. Characterization of The Scaffold

2.2.2.1. Scanning Electron Microscopy

Scanning electron microscopy (SEM) was used to evaluate fiber morphology and alignment. After 7 days of proliferation on scaffolds, moreover, cell attachment and morphology on overall scaffolds were characterized. Scaffold specimens were coated with gold and palladium with sputter coating device (Anatech Hummle VII, Istanbul,

Turkey) to prepare for SEM analysis. After that, the specimens were observed by micro and nano SEM devices (Stereoscan S4-10, Cambridge, UK and JSM-6400 Electron Microscope, Jeol Ltd., UK), equipped with NORAN System 6 X-ray Microanalysis System & Semafore Digitizer (Thermo Fisher Scientific Inc., USA) and Quanta 400F Field Emission SEM device (FEI, USA).

Fiber alignment of scaffolds were described by using SEM images for orientation order parameter (OOP, equation 1) (Volfson, Cookson, Hasty, & Tsimring, 2008) to measure its alignment by pixel-based image analysis using the developed MATLAB® code.

$$OOP = \sqrt{[< \cos 2\emptyset >^2 + < \sin 2\emptyset >^2]} \quad (1)$$

Where;

OOP= Orientation order parameter.

Ø= The angle between fiber axis and the image axis.

Cell fixation was performed to assess cell attachment and morphology on scaffolds. Grown cells on scaffolds at seventh days of incubation were fixed for SEM visualization. Cells on scaffolds were washed twice with PBS and incubated in 4% paraformaldehyde solution for 15 minutes. Then, scaffolds were washed again and dehydrated by using increasing concentrations of ethanol (50, 70, 80, 90 and 100 %, respectively). In the end, scaffolds were subjected to hexamethyldisilazane for 10 minutes and after removal of excess hexamethyldisilazane by PBS, they were dried under hood.

2.2.2.2. Mechanical Properties

Mechanical properties of scaffolds were measured by Univert biomaterial mechanical testing device (Cell scale, Canada). Specimens were cut to same length and thickness (30×1, length x thickness in millimeter). Subsequently, the test was conducted using 200N load cell and specimens were stretched 5mm for 1min and

data was collected to a remote computer. Graphs of stress-strain curves were prepared from the data by the software to evaluate the mechanical properties of scaffolds.

2.2.2.3. In vitro Degradation and Water Uptake Study

In vitro degradation experiments for scaffolds were performed for 1, 4, and 7 days. Scaffolds were placed in 10 mL PBS solution and incubated in shaking water bath at 37°C. PBS solution was replaced every other day. Weight changes of scaffolds were measure at each time point and reported as percentages according to equation 2:

$$\%\, Weight\ Loss = \frac{W_i - W_f}{W_i}\ x\ 100 \qquad (2)$$

where;

W_i= Weight of scaffolds before the incubation

W_f= Weight of scaffolds after the incubation

water uptake studies of scaffolds were conducted in 10 mL PBS while incubating in shaking water bath at 37°C. At time points; 1, 3, 24, 48, 96, and 120 hours, wet weight of the samples were measured. Prior to weight measurements, excess water on scaffolds were soaked by filter paper. Percent water uptakes of the scaffolds were calculated using following equation (3):

$$\%\, Water\ Uptake = \frac{W_w - W_i}{W_i}\ x\ 100 \qquad (3)$$

where;

W_D= Initial dry weight of the scaffolds.

W_w= Wet weight of the scaffolds at different time point.

2.2.2.4. Cell Culture Studies

For in vitro cell culture studies, scaffolds were cut in cylindrical shape (20×1 mm, length × width). Before cell seeding, scaffolds were sterilized by 2 hours of ethanol (70%, v/v) treatment followed by 30 minutes of UV treatment.

L929 cells were incubated with high Glucose DMEM including 10% (v/v) fetal bovine serum (FBS) and 10 U/mL penicillin/streptomycin (Pen/Strep). HADMSCs were incubated with low Glucose DMEM including 10% (v/v) fetal bovine serum (FBS) and 10 U/mL penicillin/streptomycin (Pen/Strep). Both cells were cultivated in an incubator (Panasonic, MCO-18AC, Kadoma, Japan) at 37^{o}C with 5% CO_2 and 95% humidity. Cells were passaged when they reached at least 80% confluency, via 0.1% Trypsin/ethylenediaminetetraacetic acid (EDTA).

2.2.2.4.1. Adipose Derived Stem Cells (ADMSCs)

2.2.2.4.1.1.Isolation

Human adipose tissue was obtained from lipoaspirate surgical procedure with approval from Liv Hospital Ethical Committee. Adipose derived mesenchymal stem cells (ADMSCs) were isolated according to enzymatic digestion (M. Zhu, Heydarkhan-Hagvall, Hedrick, Benhaim, & Zuk, 2013). Collected lipoaspirates were washed by PBS until adipose tissue layer become yellow/gold color indicting removal of blood and other contaminants. Afterward, adipose tissue was digested in PBS with 0.1-0.075% collagenase Type I solution (Adipose tissue/enzyme solution 1:1 v/v) at 37 °C for 30 minutes. Digested sample was mixed with equal volume of DMEM-low glucose containing 10% FBS and 1% penicillin/streptomycin and incubated at room temperature for 5 minutes in order to inactivate the collagenase. After that, the sample was centrifuged for 10 min at 2100 g to collect singular vascular fraction (SVF). SVF pellet containing adipose mesenchymal stem cells (AMSCs) was resuspended in the media. Cells in media were seeded to 25 cm^2

flasks and incubated for 3-4 days at 37 °C, 5% CO_2 incubator without change of media. After 3-4 days, the flask was washed with PBS to discard non-adherent cells and other contaminants.

2.2.2.4.1.2.Flow Cytometry Analysis

After ASCs isolation, stemness of the cells was characterized for cell surface cluster of differentiation (CD) antigen profile by using flow cytometry. Anti-CD11, Anti-CD31, and Anti-CD44 for negative, and Anti-CD45, Anti-CD73, Anti-CD90, and Anti-CD105 for positive antibodies were used for the analysis. Trypsinized cells at passage 3 were centrifuged at 2000 rpm for 5 minutes. Cell pellets were washed with fluorescence-activated cell sorting (FACS) buffer containing PBS with 0.1% BSA and 0.001% sodium azide and cells in solution were collected by centrifugation. Cells were resuspended in 1 mL of 4% paraformaldehyde for fixation step during which the suspension was agitated every 10 minutes with a vortex. Fixed cells were washed by FACS and centrifuged at 2000 rpm for 5 minutes. Then, supernatant was removed, and pellet was resuspending in FACS buffer based on number of sample (100 µL/sample) and aliquots were transferred into eppendorf tubes as 100 µL/tube. First, antibodies were added into aliquots according to manufacturer's recommendations, and incubated overnight at 4 °C. Then, 1 mL of FACS buffer was added to samples to centrifuge step. Later that, secondary antibodies were added into aliquots according to manufacturer protocols, and the aliquots were incubated for 1 hour at 37 °C. Again, 1 mL of FACS buffer was added to samples and centrifuged. Pellets were resuspended in 100-200 µL of FACS and analyzed by flow cytometer in Center of Excellence in Biomaterials and Tissue Engineering (BD Accuri C6 Flow Cytometer, BD Biosciences, USA). Gating was done by the reference of unstained ASCs, and mouse and rabbit isotype IgG were used as control for the experimental antibodies.

2.2.2.4.2. Cell Viability

Alamar Blue® analyses were carried out to assess cells attachment and proliferation on scaffolds. For L929 cell line assessment, briefly, sterilized scaffolds were placed in 48-well plates and seeded inner side of the scaffolds with L929 cells from passage 10 at a concentration 10 000 cells/ scaffold. While tissue culture polystyrene (TCPS) was used as control and not seeded scaffolds were used as scaffolds negative. After cell seeding, scaffolds were incubated 7 days. L929 cell attachment was characterized at 6 hours post seeding. Moreover, proliferation of L929 cells was quantified at days 1, 3, 7. For Alamar Blue® assay, media of specimens were discarded, and they were washed with PBS. After aspiration of PBS, specimens were incubated with 500 μL of Alamar Blue® solution (10% v/v) prepared with DMEM without phenol red in carbon dioxide incubator (Panasonic, MCO-18AC, Kadoma, Japan) at 37°C for 6 hours in dark At the end of incubation period Alamar Blue® solution of each well was relocated into a new 48 well plate for optical density measurements at 570 and 600 nm wavelengths. By using spectrophotometer (Paradigm Fluorescence Plate Reader, Molecular Devices, ABD). Calculation were performed based on the manual.

To evaluate concentration effect of GDF-5 on the cell viability, HADMSCs were seeded inner side of the scaffolds at density of 20 000 cells/ scaffold. After that, samples were cultivated in culture media (DMEM-high glucose with 10% PBS and 1% penicillin/streptomycin), supplemented with different GDF-5 at concentration of 0, 10, 50, and 100 ng/mL. Tissue culture polystyrene (TCPS) was used as control whereas not seeded scaffolds served as scaffold negatives. The medium was replaced every two days. Alamar Blue® assay was performed and evaluated at day 4 as described above.

To asses time dependent effect of GDF-5, HADMSCs were seeded on scaffolds as mentioned above and incubated for 14 days in GDF-5 (100 ng/ mL and 0 ng/ ml) containing culture media. Tissue culture polystyrene (TCPS) was used as control whereas not seeded scaffolds served as scaffold negatives. The medium was replaced

every two days. Alamar Blue® assay was performed and evaluated at days 1, 4 , 7, 14 as described above.

2.2.2.4.3. Hydroxyproline Assay

Total collagen amount in cell seeded scaffolds were measured by hydroxyproline (HYP) assay (Reddy & Enwemeka, 1996). Briefly, scaffolds were digested in 1 mL of papain solution. Then, 2 N sodium hydroxide was added onto digested scaffolds for hydrolyzation by autoclaving. Chloramine-T reagent (0.056 M) containing 50 % n-propanol and acetate-citrate was mixed with the hydrolyzate. The hydrolyzate was oxidized at room temperature for 25 minutes. After the oxidation, Ehrlich's Reagent was added to sample which is followed by incubation at 65°C for 20 min. Finally, optical density measurement was carried out at 550 nm wavelength. Calibration curve was prepared by using 4-hydroxyproline standard.

2.2.2.4.4. Confocal Analysis

Cell fixation was performed before confocal analysis of cell seeded scaffolds. Firstly, cells on scaffolds were washed twice with PBS and incubated in 4% paraformaldehyde solution for 15 minutes. Then, 1% Triton X-100 in PBS treatment was applied at room temperature for 5 minutes. After that, samples were washed twice with PBS and subjected to 1% BSA in PBS at 37°C for 30 minutes. BSA solution (1%) was removed, and then, the samples were washed again. Then, Prepared scaffold were examined by immunofluorescent staining.

To evaluate L929 cell morphology, Scaffolds were incubated with Alexa Fluor 488 Phalloidin at 37°C for 1 hour in order to visualize the cytoskeleton, and then, with DRAQ5 at room temperature for 30 min to stain cell nuclei. A confocal laser scanning microscope (CLSM) (Leica DM 2500, Germany) was used to investigate the cell distribution and localization within scaffolds.

To evaluate Tenogenic differentiation of HADMSCs seeded scaffolds treated with GDF-5 at various concentration (0, 10, 50, and 100 ng/mL), tenomodulin presence in scaffolds were visualized. Briefly, cell seeded Scaffolds (Day 4) were incubated with mouse primary antibody against tenomodulin for 12 hours at 4 °C, Dyight 488-labeled donkey anti-mouse for 1 hour at 37 °C in dark, Alexafluor 532-labelled phalloidin for 1 hour at 37 °C in dark, and DRAQ5 at room temperature for 30 min in dark. Scaffolds were washed with PBS and evaluated by CLSM (ZEISS LSM800, Germany).

In order to visualize COL I and COL III production on HADMSCs seeded scaffolds treated with GDF-5 (100, 0 ng/ mL), fixed samples (Day 7) were incubated with mouse primary antibody against COL III for 12 hours at 4 °C, rabbit primary antibody against COL I for 12 hours at 4 °C, Alexafluor 488-labeled goat anti-mouse for 1 hour at 37 °C in dark, Alexafluor 647-labeled goat anti-rabbit for 1 hour at 37 °C in dark, Alexafluor 532-labelled phalloidin for 1 hour at 37 °C in dark, and DAPI at room temperature for 10 min in dark. Scaffolds were washed with PBS and evaluated by CLSM (ZEISS LSM800, Germany).

Tenomodulin, COL I, and COL III stained areas in the images were measured by image segmentation using MATLAB. Note that, All sample visualizations using CLSM were performed in Center of Excellence in Biomaterials and Tissue Engineering

2.2.3. Statistical Analysis

Results of experiments were statistically analyzed using one-way analysis variance (ANOVA) with Tukey's Post-hoc test for multiple comparisons by MATLAB®. $P < 0.05$ was considered statistically significant. The results are stated as mean ± standard deviation (SD).

CHAPTER 3

RESULTS AND DISCUSSION

3.1. Characterization of Dual Part Scaffolds Produced for Tendon Tissue Engineering

3.1.1. Characterizations for Optimization of RJS Parameters

First trials of fiber production with RJS started with 5% and 10% solutions showed that fiber formation was achieved under various conditions. However, the fibers were too delicate to collect from collector without harm. During trials, when 5% PCL solution was spun at 30 000 RPM collection at 15 cm distance was not repeatable. Then, the effect of feeding speed of polymer solution into RJS was investigated to understand the possible cause of batch to batch variation. This study showed that rapid feeding of the solution increased the distance traveled by fiber jet, nevertheless, slow poured solution decreased the distance traveled.

According to results of these initial experiments, fiber production parameters were decided to be fixed as; 15% PCL in chloroform 30 000 RPM. Similarly, high polymer concentration, high rotational speed, and volatile solvent are suggested in literature for avoiding bead formation during fiber production (Mohammad Reza Badrossamay et al., 2010; Golecki et al., 2014). In addition, effects of various feeding rates (1.5, 2.5, and 3.0 mL/min) on fiber morphology were examined. Results of these processes can be seen in Figure 12**,** demonstrating that bead free RJS fibers were effectively fabricated. Furthermore, it is also suggesting that bead formation was not triggered by feeding rates. Diameter and orientation order parameter (OOP) of fibers (Table 1**)**, however, were affected by the infusion rate.

Feeding rate of 2.5 mL/min showed statistically significant differences in OOP compared to other two feeding rates. The diameter results displayed increasing trend in fiber diameter with increasing feeding rate. Additionally, 3.0 mL/ min feeding rates generated less homogenous fibers in terms of diameter. This outcome can be explained by the fiber production process where jet initiation starts when centrifugal force with hydrostatic pressure overcomes capillary force (Mohammad Reza Badrossamay et al., 2010). In that respect, continuous infusion of the solution maintains or increases hydrostatic pressure depending on the flow rate, thus resulting in higher jet velocity. Consequently, higher jet velocity causes rapid solidification of the jet before getting thinner fibers (Golecki et al., 2014). In literature, there are three main collector types which are static vertical collector (Ren et al., 2013; Taghavi & Larson, 2014), round bottom collector (Loordhuswamy, Krishnaswamy, Korrapati, Thinakaran, & Rengaswami, 2014) and rotating (Gonzalez et al., 2016). In that devices in this thesis, horizontal collector was used and placed right under the rotating reservoir where jets cannot travel in air for enough time to complete solidification and reach at the vertical collector surface (Golecki et al., 2014; Padron, Fuentes, Caruntu, & Lozano, 2013), finally causing thick fibers collected at the horizontal collector. Similar RJS setup provided smaller fibers diameter (Mohammad R. Badrossamay et al., 2014) than those obtained in this thesis based on collector differences that their fibers were collected from rotating collector. Consequently, fibers, that were subjected to tension force during collection, became thinner

Table 1. Diameter and OOP results of infusion rates. (*$p<0.05$, n=4)

Flow Rate (mL/min)	**Diameter (µm)**	**OOP**
1.5	5.235± 1.917	0.647± 0.075
2.5	6.710± 0.944	0.8716± 0.054*
3.0	10.213± 4.092	0.709± 0.025

In general perspective, the RJS device was particularly selected in this study to mimic not only a general structure of healthy tendon, but, mimicking collagen type I thickness, and alignment for injured-healing tendon model. Considering these results, the infusion at the rate of 2.5 mL/min was a suitable candidate for outer part of engineered 3D scaffold.

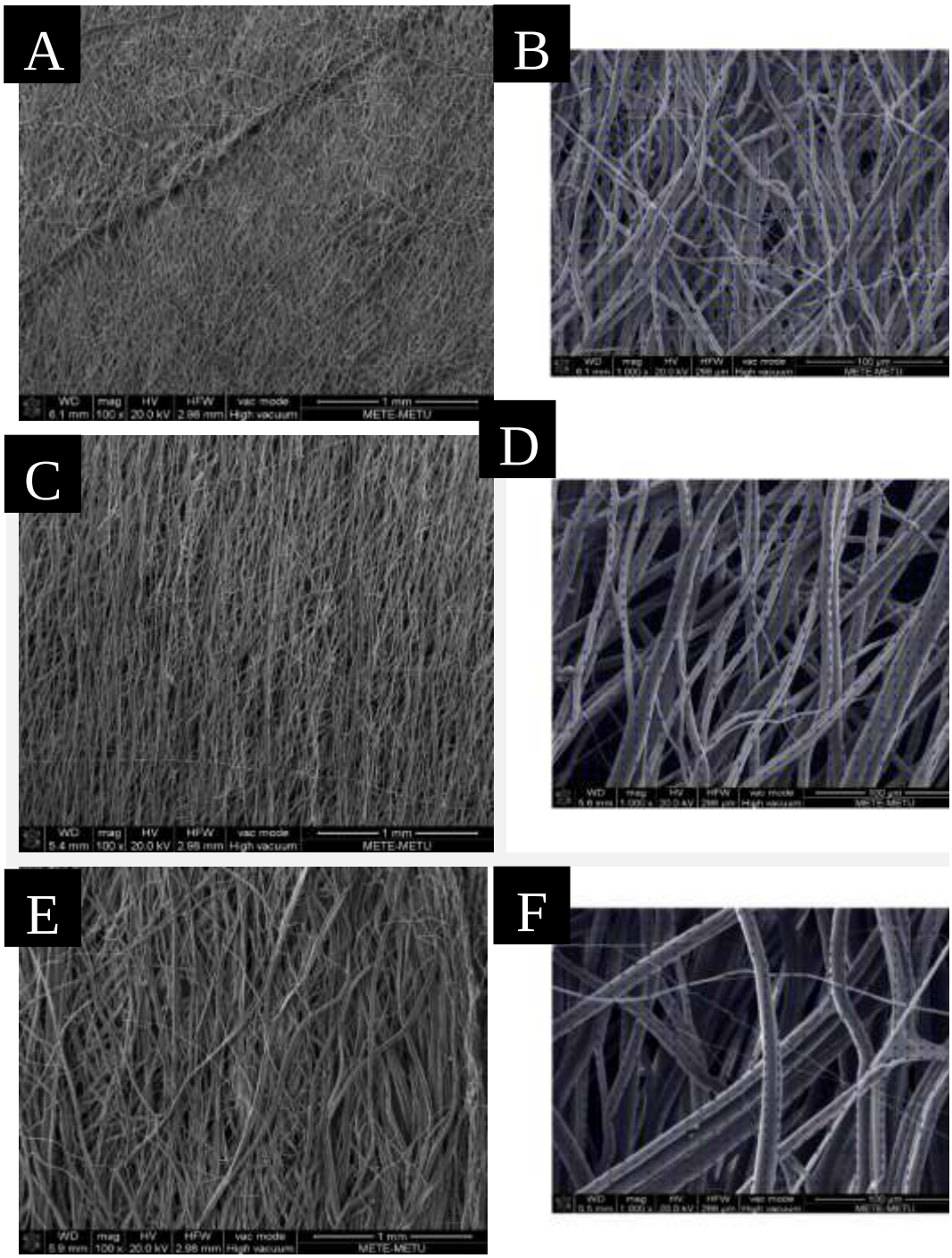

Figure 12. SEM image of RJS fibers flow rates at (A) 1.5 mL/min (C) 2.5 mL/min (E) 3.0 mL/min. Pixel-based alignment analysis of fibers flow rates at (B) 1.5 mL/min (D) 2.5 mL/min (F) 3.0 mL/min.

3.1.2. Characterizations of TTE Scaffold Morphology

RJS provided 2D densely packed aligned fibers were combined with ES randomly aligned fibers to constitute the proposed 3D scaffolds without altering initial fiber alignment of RJS and ES fibers (Figure 13).

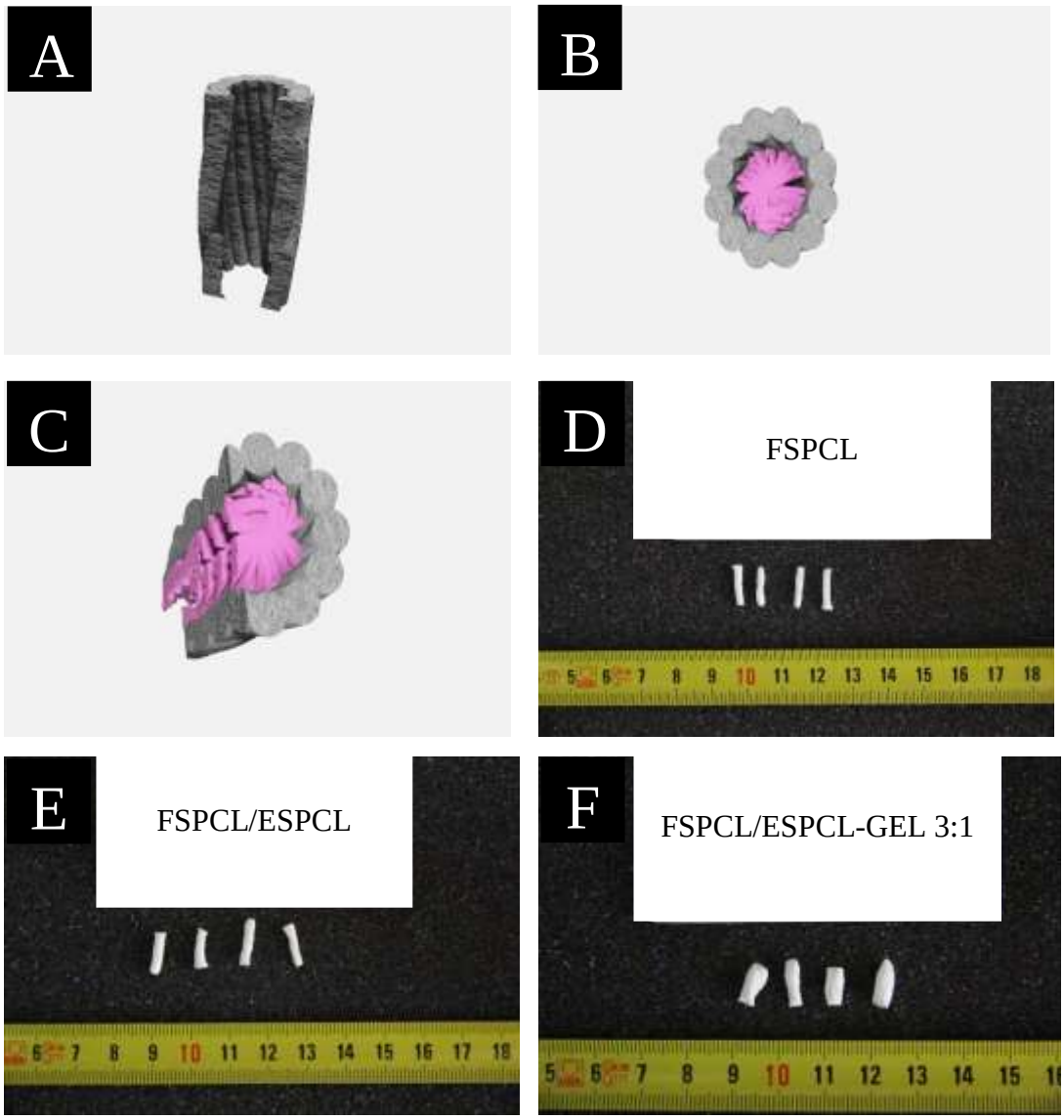

Figure 13. Photograph of final scaffolds and groups. (A, B, C) Schematic drawing of scaffolds and (D, E, F) images of scaffolds.

Mean diameter of RJS fibers in integrated 3D scaffolds was 6.73 ± 1.39 μm according to measurements from a total of 114 fibers of 4 different samples' SEM analyses (Figure 14). Average diameters of fibers in PCL and PCL/gelatin 3:1 scaffolds which were manufactured by the electrospinning system were 5.93±3.23 μm and 1.72±0.7 μm respectively. Hence, the two ES outcome were statistically different from each other in terms of fiber diameter. Presence of gelatin in PCL solution caused an increase in charge density of the solution in consequence of polyelectrolyte nature of gelatin. The solution conductivity, thus, increased because of existence of cationic - anionic polyelectrolyte (Son, Youk, Lee, & Park, 2004). As a result, the PCL/gelatin 3:1 solution provided thinner fibers than the PCL solution at same ES device and production parameters. Measurement of diameters of ES scaffolds' fibers suggested that only PCL fibers would better mimic that late stage of tendon wound, while PCL/gelatin 3:1 fibers were an appropriate candidate to mimic early stage of tendon wound.

Collagen arrangement has vital role in both healthy and wounded tendon. Therefore, the scaffolds must meet constraints of the state of arrangement to achieve planned goal. OOP results of the scaffolds were calculated as 0.96±0.022 for RJS fibers and 0.36±0.026 for ES fibers (Figure 14G-I). These results confirmed that RJS technique successfully yields aligned fibers and ES technique provides disorganized fibers, as expected. Note that, all characterizations were performed after designed scaffold was constructed. During final construction step as described, scaffolds were twisted horizontally for 360° three times, thus, that the scaffolds were subjected to tension force towards both ends which provide fibers to be more aligned.

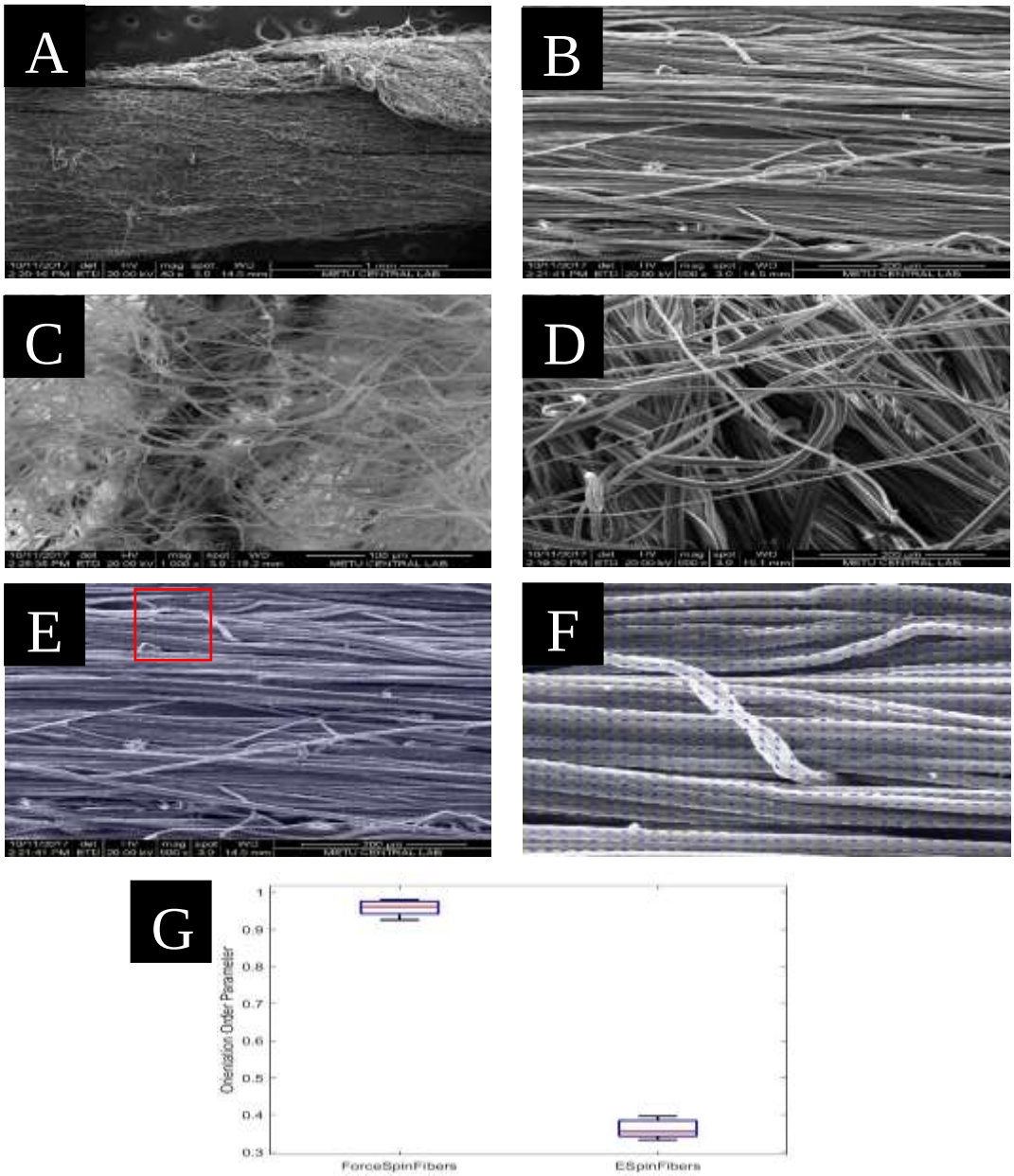

Figure 14. (A, B) Scanning electron micrograph of align part of scaffolds. (C, D) Electrospun part of the scaffolds. (C) SEM image of FSPCL/ESPCL-Gel electrospun part. (D) SEM image of FSPCL/ESPCL electrospun part. (E, F, G) Pixel-based alignment analysis (n=4) and its results.

3.1.3. Characterizations of Mechanical Properties

Representative stress-strain curves of scaffold groups (Figure 15A) and mechanical properties of proposed scaffolds (Figs 15B-D) were given in Figure 15. FSPCL/ESPCL and FSPCL/PCL-gelatin 3:1 scaffolds had significantly higher Young's modulus, yield strength, and ultimate stress compared to FSPCL scaffolds. Results showed that presence of ES PCL and PCL/gelatin fibers in RSJ PCL were caused much stiffer and stronger scaffolds. Tissue engineered scaffolds must meet mechanical requirements of tendon for proper replacement. Overall, ultimate stress of proposed scaffolds in this work provided better ultimate stress than native human tendons (Table 2). Nonetheless, Young's modulus of the scaffolds was drastically lower than the tendons (Table 2). In terms of TTE, implanted tendon scaffold should be able to sustain its shape under the load until neo tendon regenerates (Chan & Leong, 2008). Moreover, to calculate mechanical properties of material, an accurate measurement of specimen cross-sectional area is required, especially 3D scaffold consist fibers due to highly porous nature of fibers (Pauly et al., 2016). Therefore, the area of the material may be overestimated, then, the mechanical properties become less than as it should be. In this research, cross-sectional areas of scaffolds were measured as they are. For example, scaffolds can be compressed and then the area can be measured. This approach can be used to estimate true material cross sectional area without pore space leading increase of mechanical properties(Pauly et al., 2016). For this reason, our scaffolds mechanical properties may be underestimated.

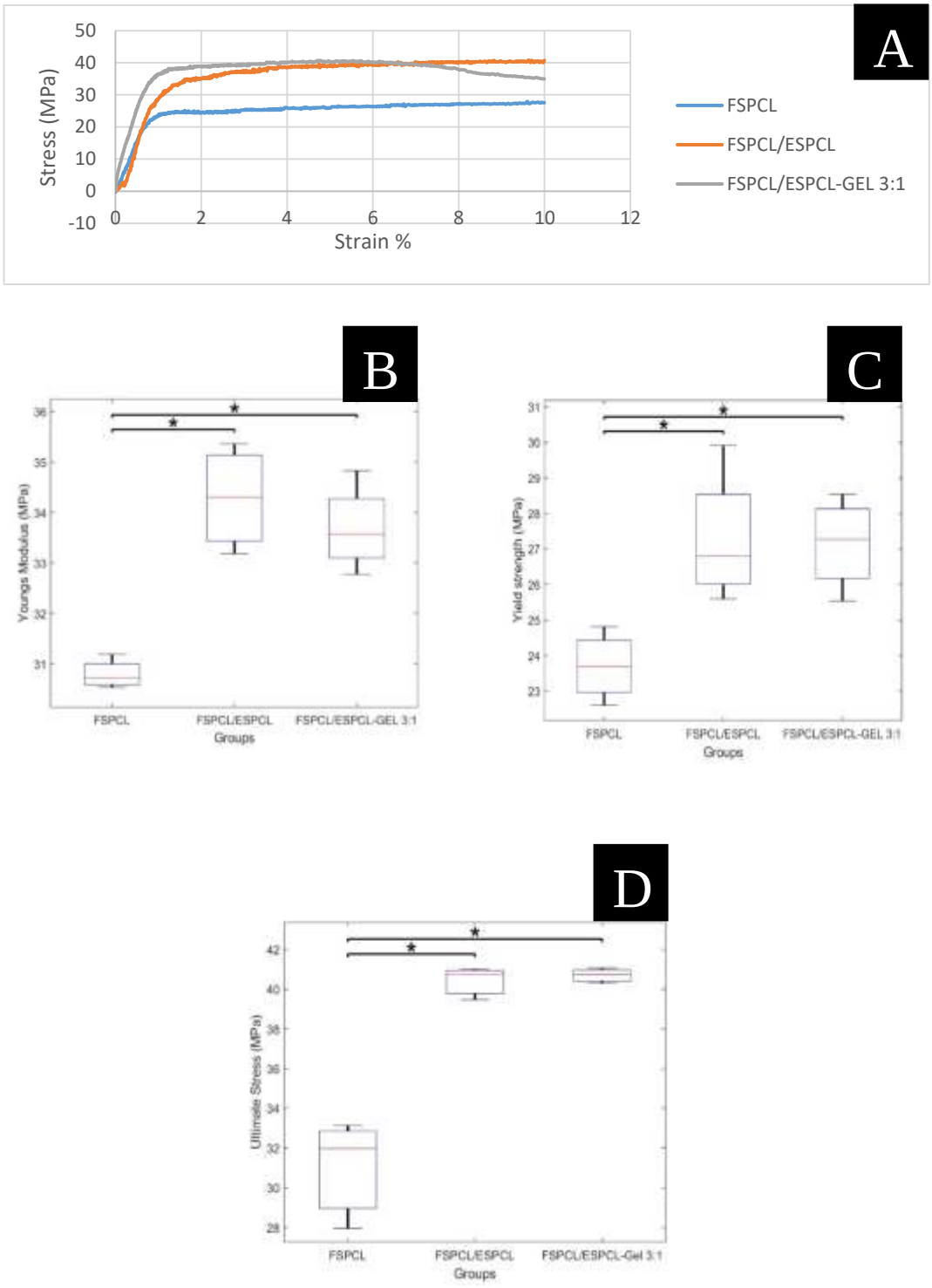

Figure 15. (A) Exemplary stress-strain curve of scaffolds. Calculated (B) Young's modulus, (C) Yield strength, and Ultimate stress. ($p<0.05$, $n=4$).

Table 2. Calculated material properties of tendons. (*p<0.05, n=4).

	Ultimate Stress (MPa)	Young's Modulus	
FSPCL	31.03±2*	30.8±0.35*	
FSPCL/ESPCL	40.4±0.82	34.1±1.13	
FSPCL/ESPCL-Gel 3:1	40.7±0.4	33.62±1	
Suprasinatus tendon anterior subregion	21.1± 5.4	592.4± 237.4	(Matsuhashi et al., 2014)
Suprasinatus tendon posterior subregion	11.6± 5.3	217.7±102.1	(Matsuhashi et al., 2014)
Medial triceps tendon	12.3± 5.6	103±74	(Baumfeld et al., 2010)
Central triceps tendon	16.5± 7.9	108±59	(Baumfeld et al., 2010)

3.1.4. Characterizations of TTE Scaffolds Degradation Properties

Degradation rate of scaffolds is another important property that should be investigated as native tendon tissue should substitute the scaffold in time. Furthermore, engineered tendon scaffold must maintain its mechanical properties and integrity during the substitution period. In massive tendon injuries, tendon healing requires approximately one year to generate its normal function (Denitsa Docheva, Müller, Majewski, & Evans, 2015b). Weight loss of engineered scaffolds after one-week degradation experiments can be seen in Figure 16; stating that almost no weight loss in only PCL containing scaffolds was observed, while around 5% of PCL/gelatin scaffold's mass was lost probably because of gelatin solubility in water. Since final mass of PCL/gelatin scaffold consisted of 15% gelatin, it can be presumed that 10% of gelatin was still remaining in the scaffold. Similar conclusion was attained by Dulnik et. al. with degradation profile of PCL/gelatin electrospun scaffold (9:1, 8:2, and 7:3) in PBS up to 90 days that overall mass of PCL/gelatin 9:1, 8:2, and 7:3 structures remained their gelatin with 8%, 12%, and 14% in a row (Dulnik, Denis, Sajkiewicz, Kołbuk, & Choińska, 2016)

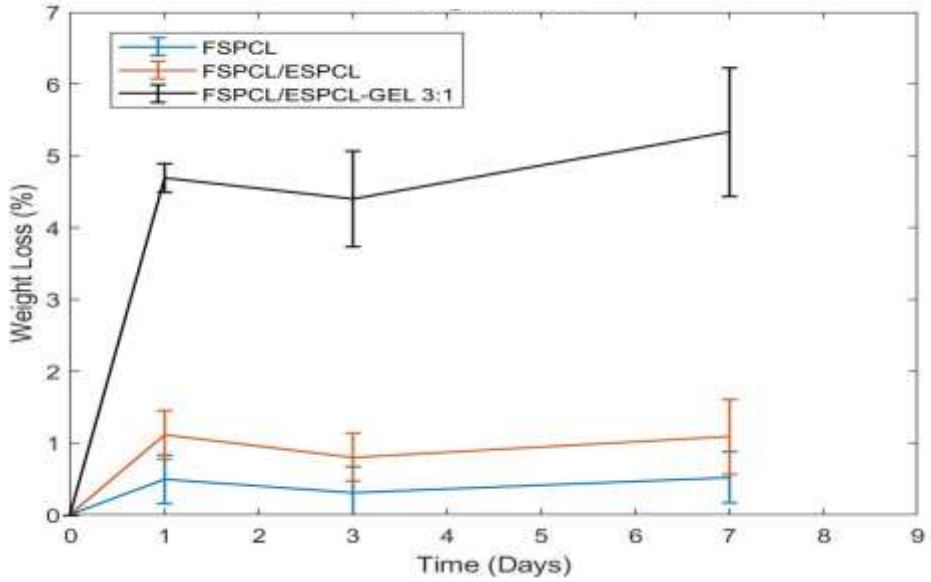

Figure 16. Weight loss after 7 days of degradation study in PBS (pH 7.4) at 37°C. (n=4)

It is suggested that complete degradation of PCL needs around two years depending on PCL fiber diameter. During degradation thinner fibers can degrade more easily than thicker fibers (Raghunath et al., 2009). In addition, another study claims that PCL scaffold immersion in PBS for 12 weeks did not show any marked changes in terms of molecular mass (Díaz, Sandonis, & Valle, 2014).

3.1.5. Water Uptake Analysis of TTE scaffolds

Water absorption behavior of scaffolds is important factor for tissue engineering not only to transport proteins and bodily solutes inside and outside of the scaffolds but also provide cellular invasion (Campos, Soares, & Anselme, 2013). Nevertheless, if scaffolds cannot preserve their dimensional stability in wet conditions or exhibit unrestrained water absorption capacity, consequences of the scaffold would be severe for tissue engineering. Calculated water uptake percentages can be seen in Figure 17. There was no significant difference was observed between the groups. 70% of total weight of tendon consists of water (Hess et al., 1989) that designed

scaffolds have similar water uptake capacity with tendon tissue. I was also observed that dimension changes of the specimens were between 5%-10% in humid conditions. It was noted that the groups had suitable dimensional persistence in wet conditions. Therefore, the scaffolds are appropriate certain environment where water content is limited.

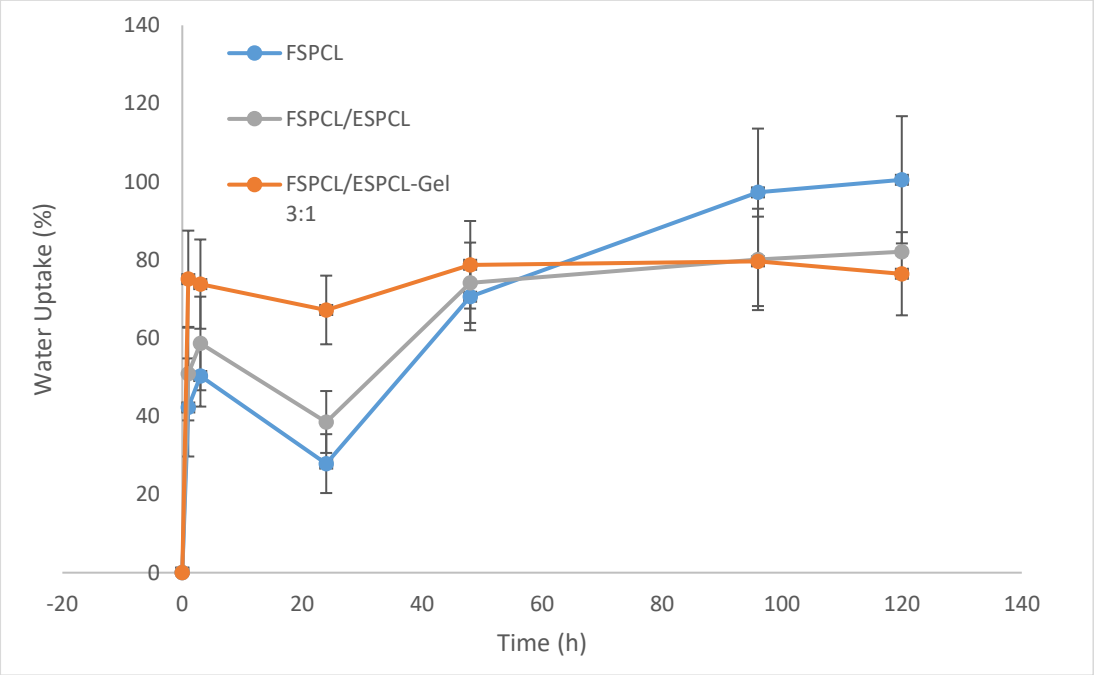

Figure 17. Water uptake properties of FSPCL, FSPCL/ESPCL, and FSPCL/ESPCL-Gel 3:1 scaffolds in PBS pH at 7.4. (n=4)

3.2. In Vitro Studies

3.2.1. L929 Cell Attachment and Viability

Proposed scaffolds for tendon tissue engineering are 3D cylindrical constructs which are designed to resemble native tendon healing steps from repair stage to remodeling stage in terms of collagen fibers deposition in the healing stages. In this point of view, inner core of the scaffolds, that consisted of ES unaligned nano and micro sized fibers, mimic randomly deposited collagen type III as in repair stage of tendon

healing to promote cell attachment and proliferation. In addition, aligned micron size fibers that form outer section of the scaffolds serves as reorganized collagen type I in the remodeling stage. By imitation of collagen type I and III structures, increasing cell attachment and proliferation is suggested, while guiding cell growth direction

Initial atachment of L929 cells on the scaffold groups is presented in Figure 18. FSPCL scaffold showed the lowest cell attachment compared to groups bearing an eletrospun core. The presence of randomly distributed electrospun fibers in the core of the scaffolds could have created a fiber net where seeded cells can be settled easily while some of the cells seeded on FSPCL scaffold would easily be washed away between aligned fibers. The highest cell attachment was achieved with FSPCL-ESPCL-GEL scaffold. The presence of the natural polymer, gelatin, within ESPCL-GEL fibers created a more suitable environment for cell atachment by introducing hydrophilicity to PCL fibers and providing gelatin which has similar biological properties with collagen in native ECM of tendon tissue (Zhang et al., 2005). The presence of gelatin provides amino acids like aarginine, glycine and aspartic acid in the fibers structures, thus, increases recognition of surface by the cells and could have increased adhesion strength of cells (Guarino et al., 2011).

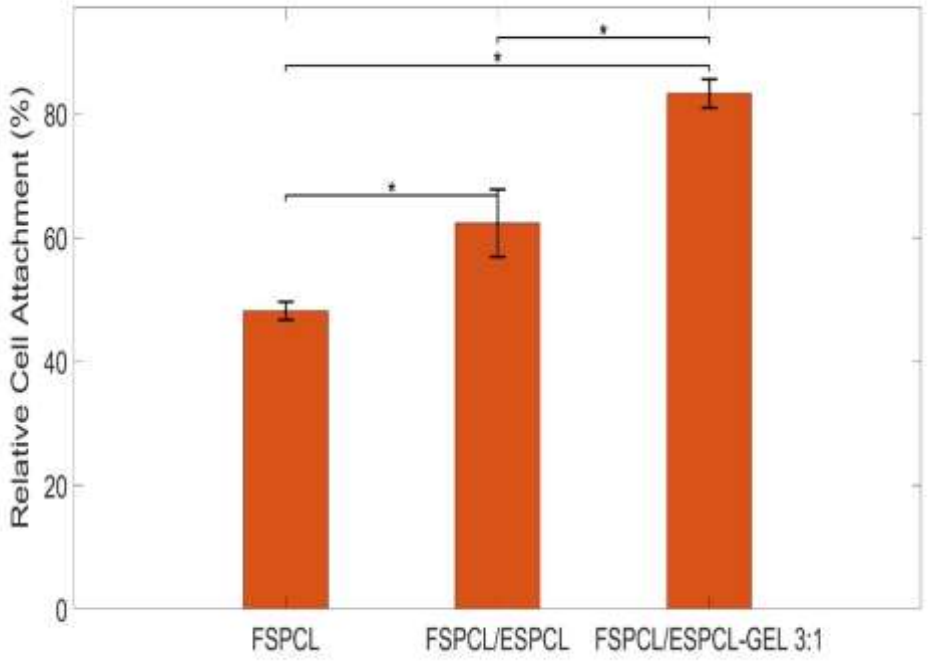

Figure 18. Alamar Blue® test for relative (TCPS was used as control) cell attachment of L929 cells after 6 hours (*$p<0.05$, n=4)

L929 cell viability on scaffold groups was studied through 7 days of incubation and results are presented in Figure 19. After first day of incubation, higher cell viability was observed on FSPCL/ESPCL-GEL 3:1 scaffold compared to other groups which was in parallel with higher initial cell attachment on this scaffold type. Higher cell viability was observed on FSPCL/ESPCL scaffolds compared to FSPCL after 7 days of incubation probably due to presence of nano fibers in FSPCL/ESPCL core which can provide more surface area for cell growth. This was enhanced with nano fibrous structure of electropsun PCL fibers which is known to support cell proliferation more, compared to micro sized fibers. Randomly oriented electrospun fibers lying on each other are more flexible compared to oriented thick micro fibers, and cells are able to migrate better through the pores of random electrospun fibers (W.-J. Li, Laurencin, Caterson, Tuan, & Ko, 2002). After 3 and 7 days of incubation, higher cell viability was observed on FSPCL/ESPCL-GEL 3:1 scaffolds than other groups. The gelatin phase in the core electropun matrix gradually dissolved during the incubation period, leaving micropores inbetween two electrospun meshes. Dissolution of gelatin phase could have created more space for cell infiltration and

proliferation. Also gelatin/PCL complex was reported to have high elongation and deformation potential that could decrease the resistance against cell penetration (Y. Zhang, Ouyang, Lim, Ramakrishna, & Huang, 2005). The presence of gelatin phase in scaffolds were also reported to enhance cell adhesion and proliferation (Gautam, Dinda, & Mishra, 2013; Meng et al., 2010; F. Zhang et al., 2011). In order to create mechanically strong scaffolds for tendon tissue engineeering, oriented fibrous scaffolds were prepared, aligned fibers which created a main drawback by decreasing cell viability compared to random fibers (Jahani et al., 2012). In this study, to overcome this effect by combining forcespinning and electrospinning techniques to form scaffold with mechanically strong, alligned PCL fiber shell and electrospun PCL core. Alligned fibers were also reported to improve collagen deposition compared to random fibers (C. H. Lee et al., 2005). Cell viability was further improved the incorporation of gelatin phase to electropun PCL core, which initially enhanced cell attachment by increasing hydrophilicity of the structure and later opened space for cell proliferation by sacrificially disolving. The developed duel phased FSPCL/ESPCL-GEL 3:1 scaffold was therefore found promising candidate to be used for tendon engineering.

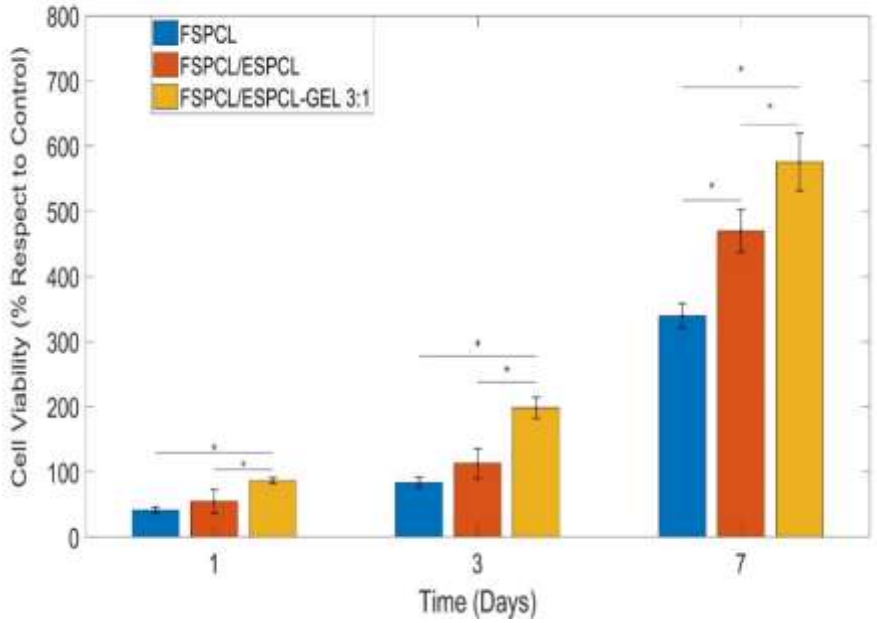

Figure 19. Alamar Blue® test for Relative (TCPS was used as control) cell viability of L929 cells (*p<0.05, n=4)

Morphology of L929 cells on scaffolds after 14 days of incubation (Figure. 20) was examined by SEM images. Cells adhered, spread, and proliferated on aligned fibers surface of each scaffold. It was noted that elongation of cell and cell-cell interaction on the surface can be clearly seen. One of the targeted aims of this work was achieved by aligned cells along the alignment of the fibers.

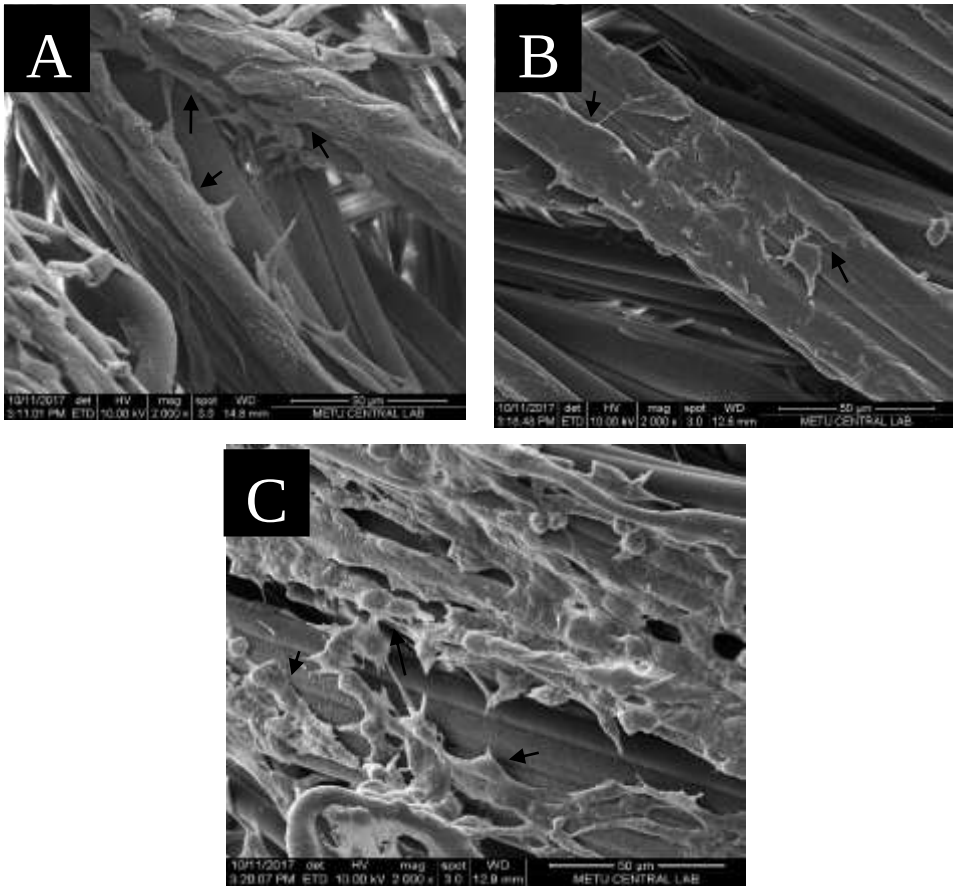

Figure 20. Morphology of L929 cell on (A) FSPCL, (B) FSPCL/ESPCL, and (C) FSPCL/ESPCL-GEL after 7 days of cell culture. Black arrows show the cells. (scale bar = 100 μm)

As visualized by cytoskeleton staining using Alexa Fluor 488-phalloidin, L929 on aligned scaffolds were almost uniformly oriented along the fiber direction and possessed spindle-shaped morphology (Figure 21). Their nuclei also appeared to be stretched. This is in agreement with previous studies, which have reported that aligned fibrous scaffolds induce cell orientation (F. Li, Li, Wang, & Wang, 2008;

Yin et al., 2010). These results indicated that aligned topographic cues are particularly directing cell in relation to the underlying molecular adhesion mechanisms that control cytoskeletal organization and nuclei shape.

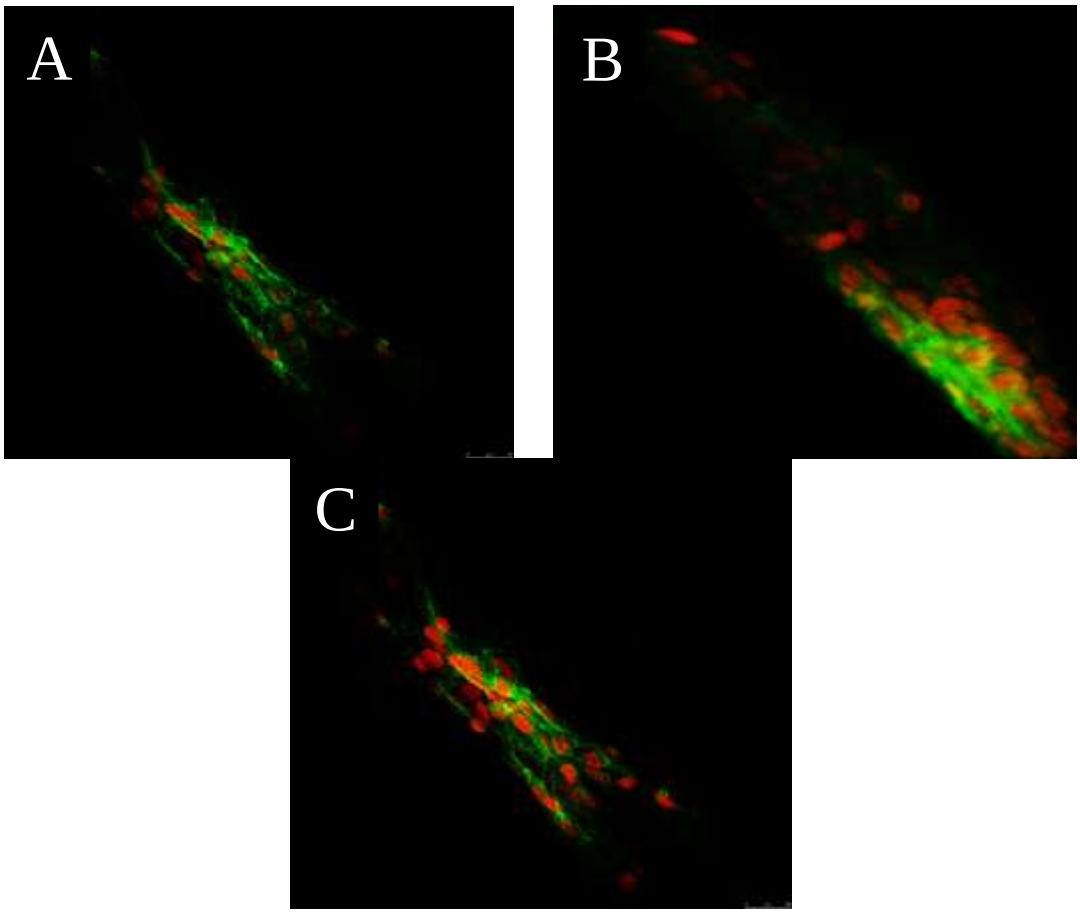

Figure 21. Confocal laser scanning microscopy (CLSM) images showing morphology of L929 cells on the scaffolds; (A) FSPCL, (B) FSPCL/ESPCL, and (C) FSPCL/ESPCL-Gel 3:1 after 7 days of incubation. Stains: DRAQ5 against nuclei (red), and Alexa Fluor 488-phalloidin against cytoskeletons (green).

3.2.2 Isolation of Human Adipose Derived Stem Cells (HASCs)

Obtained human adipose tissue from lipoaspirate surgical procedure was used to isolate ASCs. After isolation, cultivation flask surface was also occupied by blood

cells and some tissue fragments (Figure 22A). At the third day of the cultivation of ASCs, the flask was washed with PBS to remove the blood cells and the tissue were floating in cell medium that could not attach on the surface of the flask. At passage 0, there were 4 different cell morphologies; small and round cells, spindle-shaped - fibroblast like cells, large cells, and cuboidal cells as commonly observed in literature. There were small and round shaped ones as a result of rapid proliferation character of the cells (Zuk et al., 2001). Furthermore, small and round shaped cells showed greater expression of stem cell markers as well as greater multipotentiality (De Francesco et al., 2009; Haasters et al., 2009). Most of the flask surface was covered by spindle-shaped cells assuming more ASCs morphology that arise from these small and round shaped cells in time. Furthermore, increasing cell passages caused more spindle-shaped cells than passage 0 (Figure 22B). In terms of cell morphology, it can be said that ASCs were isolated for human adipose tissue. To investigate stemness of isolated cells, flow cytometry examinations were conducted.

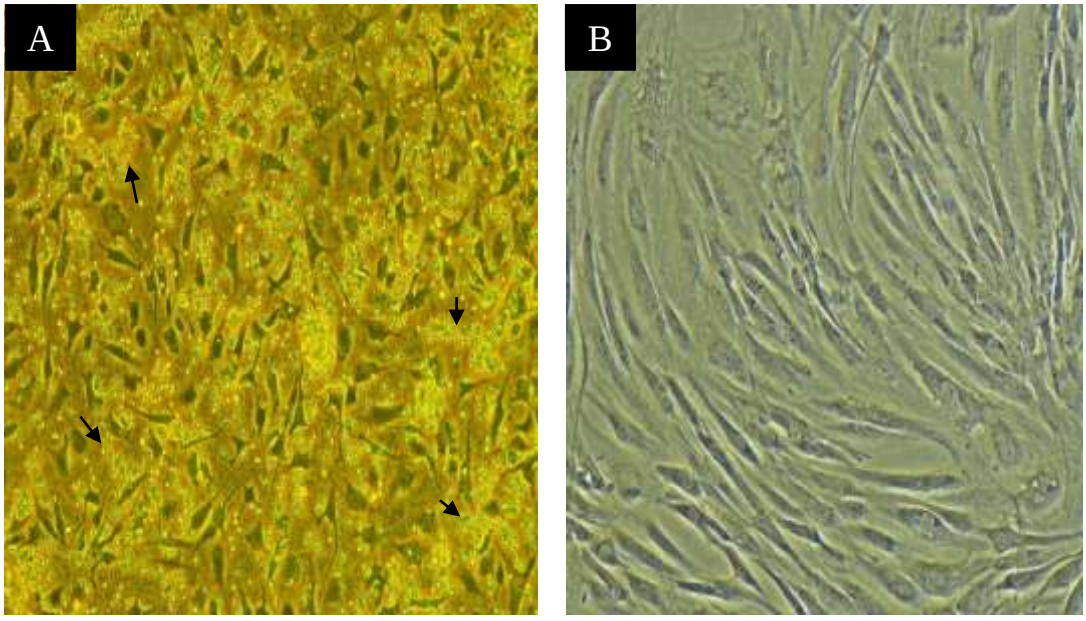

Figure 22. Phase contrast micrographs of (A) HADMSCs isolation after day 3. Spindle-shape cell with red blood cell contamination were observed. (B) Spindle-shaped cells at passage 4. Black arrows show red blood cells.

A lipoaspirate was used to isolate stromal vascular fraction (SVF) that has adipose mesenchymal stem, and hematopoietic origin cells (25-45% of total nucleated cells) and endothelial cells (10-20% of total nucleated cells) as well (Bourin et al., 2013). Thus, freshly isolated SVF are highly heterogeneous (Bourin et al., 2013). Therefore, homogeneity level of adipose mesenchymal stem cells in the culture should be increased (Baer, 2014). A study reported that, ADMSCs population in culture can be increased with increasing culturing time and passage number leading to less heterogeneous composition (Baer, 2014). Additionally, MSCs positive markers expression was enhanced with increasing passage number. CD11 and CD45 were selected to label hematopoietic origin cells and CD31 to identify endothelial cells (Dominici et al., 2006). Furthermore, CD105, CD90, and CD44, which are known main MSCs markers, were selected to detect MSCs in culture(Dominici et al., 2006). Isolated cells were subjected to flow cytometry analysis at passage 4 that were selected to generate HADMSCs rich culture and cell surface markers' expression profile was CD105 (98.4%), CD90 (93.5%), and CD44 (98.9%) indicating positive expression and CD11 (99.9%), CD31 (97.4%), CD45 (100%) showing negative expression (Figure 23). It is reasonable to conclude that isolated cells were homogeneous in culture since they were found as negative for hematopoietic origin cells and endothelial cells. Moreover, mesenchymal stem markers were highly expressed that they were maintained their stemness at passage 4. Overall, following experiments involving HADMSCs were performed at passage 4.

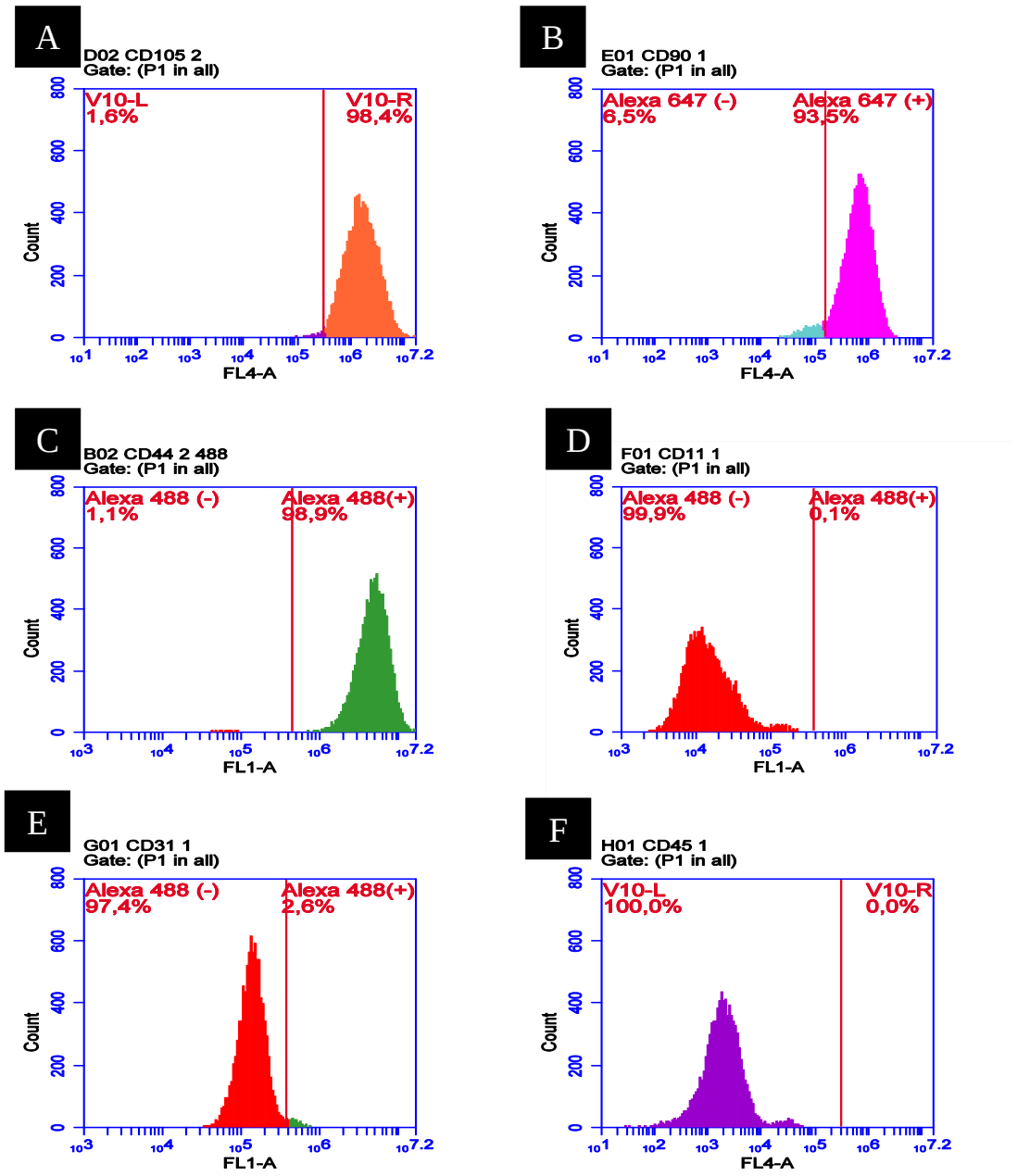

Figure 23. Flow cytometric analysis results of isolated HADMSCs; positive for (A) CD105, (B) CD90, and (C) CD44, - negative for (D) CD11, (E) CD31, and (F) CD45. CD, cluster of differentiation.

3.2.3 The Concentration Effect of GDF-5

Previous studies stated that deficiency of GDF-5 in mice not only affected biomechanics but also the structure of tendon (Mikic et al., 2001) in undesired way but also delayed tendon healing (Chhabra et al., 2003). In addition, media containing GDF-5 increased tenogenic differentiation of ADMSCs in terms of gene expression such as, COL I and scleraxis (R. James, Kumbar, Laurencin, Balian, & Chhabra, 2011a). Therefore, it was decided to improve tenogenic differentiation of ADMSCs on scaffolds using GDF-5 in this study. For this purpose, firstly, ADMSCs seeded to scaffolds or tissue culture plates (TCPS) were incubated in cell culture media containing GDF-5 at different concentrations in order to find the optimal concentration of GDF-5 for tendon tissue engineering, (Figure 24). GDF-5 significantly increased the viability at TCPS (Figure. 24A) compared to non-treated ADMSCs ($n=4$, $p<0.05$). Based on this result, a correlation between GDF-5 treatment and HADMSCs viability can be suggested. However, on 3D engineered scaffolds such improvement in viability with increased GDF-5 concentration was not observed (Figure. 24 A-B). The viability of cells on the scaffolds did not show a recognizable change with presence of GDF-5. This result was thought to be related with two possible explanation; (1) doubling times of the cells were stated as 55.12 h ± 4.48 (Gruber et al., 2012), or less availability of GDF-5 due to restricted penetration into scaffold structures in static cell culture conditions as compared with their free availability to cells in TCPS environment.

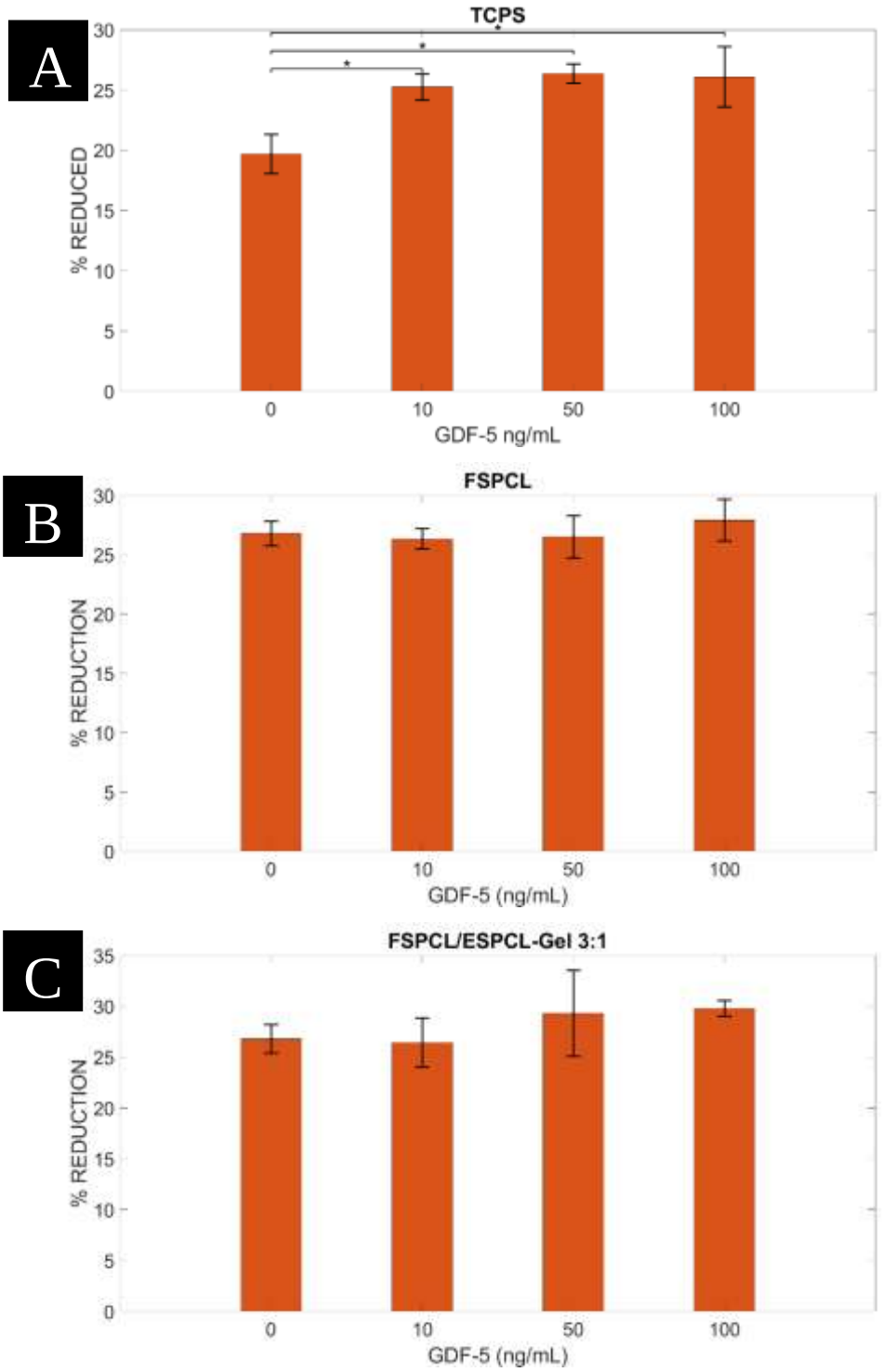

Figure 24. Concentration-dependent effect of GDF-5 on viability of HADMSCs on (A) TCPS, (B) FSPCL, and (C) FSPCL/ESPCL-Gel 3:1. (*$p<0.05$, n=4)

Further analysis was performed to assess which GDF-5 concentration would be suitable for HADMSCs in terms of tenogenic differentiation. Hence, HADSC carrying FSPCL/ESPCL-Gel 3:1 scaffold was examined under confocal microscopy after four days of incubation in GDF-5 containing media (Figure 25). Confocal images (Figure 25 A, C, E, and G) suggested that cells on this scaffold had more elongated shape, like tenocytes at healthy tendon, and as the concentrations of GDF-5 increased, the elongation also increased.

A major challenge in the field of tendon tissue engineering is the lack of unique biological markers to characterize differentiation to tendon (Kuo & Tuan, 2008). Tenomodulin (TNMD) is primarily expressed in tendons, ligaments and eyes (D. Docheva, Hunziker, Fassler, & Brandau, 2005), and serves an important role in tendon tissue growth (Aslan, Kimelman-Bleich, Pelled, & Gazit, 2008). An association between tendon formation and tenomodulin expression was previously reported (Shukunami, Takimoto, Miura, Nishizaki, & Hiraki, 2008; Shukunami, Takimoto, Oro, & Hiraki, 2006). All articles published on Pubmed covering tenomodulin, 94 articles using TNMD as a tendon marker (Dex, Lin, Shukunami, & Docheva, 2016). Therefore, in this study, to compare tenogenic differentiation of HADMSCs, confocal images were used to calculate TNMD area in images (n=4, results were normalized by total are of each image, FIGURE 23 B, D, F, and H). As given in Table 3, 100 ng/mL of GDF-5 treated FSPCL/ESPCL-Gel 3:1 scaffolds had significantly higher TNMD than 50 ng/mL of GDF-5 treated at fourth days of incubation.

Table 3. Area ratio of TNMD expressed regions to total area in confocal images (*$p<0.05$, n=4) in relation to GDF-5 concentrations. Semi-quantification of TNMD stained were normalized by total image area.

GDF-5 Concentration	**TNMD Area/Total Area (μm^2/ μm^2)**
0 ng/mL	not detected
10 ng/mL	not detected
50 ng/mL	0.01 ± 0.0007
100 ng/mL	$0.02 \pm 0.002^{*}$

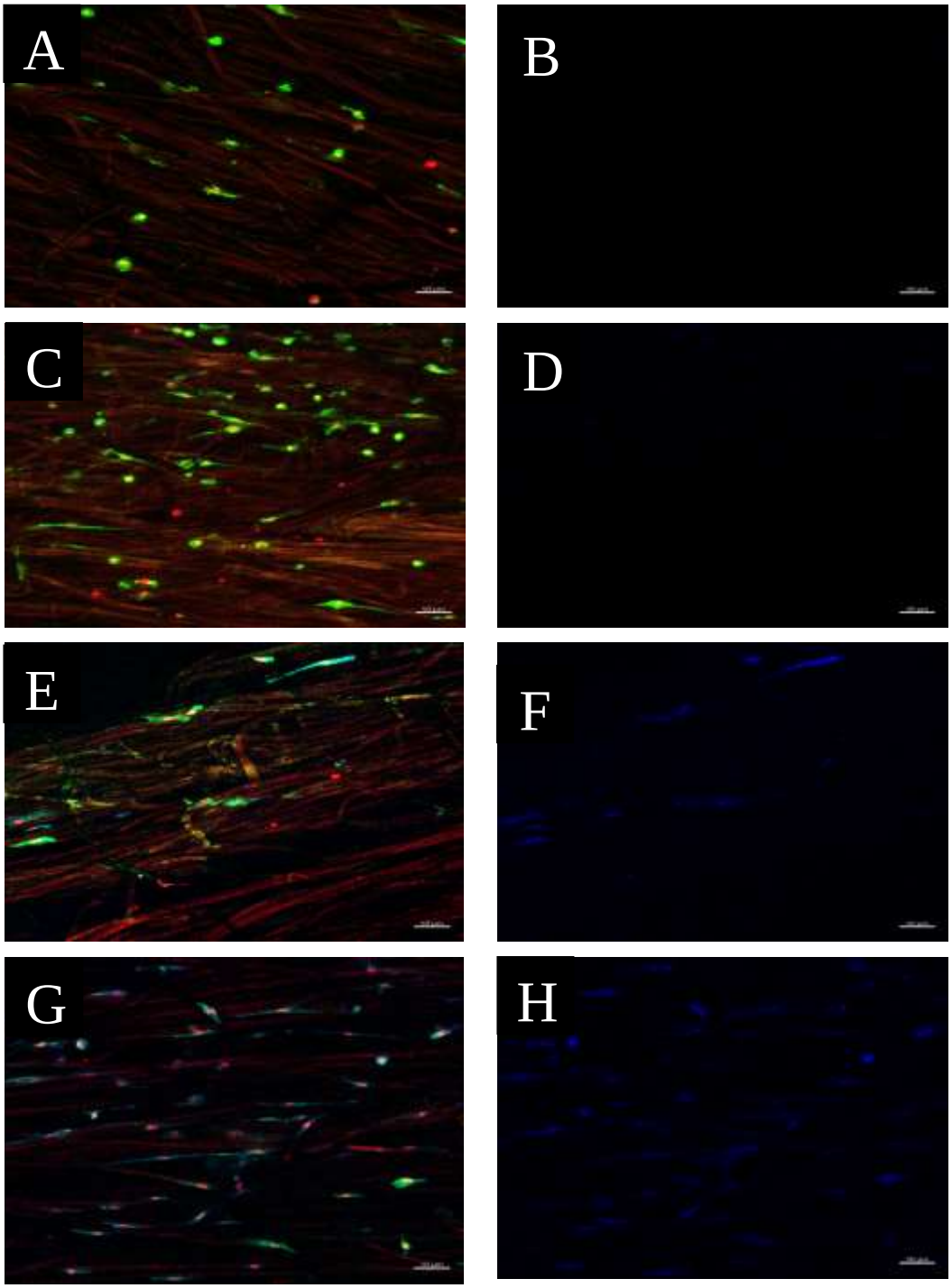

Figure 25. Cell morphology on the scaffolds. Confocal laser scanning microscopy (CLSM) images of HADMSCs cells on FSPCL/ESPCL-Gel 3:1 scaffolds supplemented with media containing GDF-5 (A, B) 0 ng/mL, (C, D) 10 ng/mL, (E, F) 50 ng/mL, and (G, H) 100 ng/mL after 4-day incubation. Stains: DRAQ5 against nuclei (red), Alexa Fluor 532-phalloidin against cytoskeletons (green), and Alexa Fluor 488 anti-rabbit against rabbit anti-TNMD (blue).

Collagen production of HADMSCs was investigated by measuring hydroxyproline in scaffolds for varying GDF-5 concentrations at day 4 (Figure. 26). Obtained results can be seen in Figure 26. 100 ng/ mL of GDF-5 treated HADMSCs on scaffolds produced hydroxyproline significantly higher than concentration level of 0 ng/ mL. Comparable results reported before. Tan et al. (2012) examined different GDF-5 concentration on human bone marrow mesenchymal stem cells to evaluate total collagen production. 100 ng/ mL of GDF-5 induced cells produced more collagen than 0, 5, and 25 ng/ mL. More importantly, total collagen production of GDF-5 (100 ng/ mL) treated cells was comparable human tenocyte collagen production (Tan et al., 2012). Another studies revealed that, GDF-5 (100 ng/ mL) induced HADMSCs enhanced COL III transcription (Park et al., 2010) and COL I transcription(Rodrigues, Reis, & Gomes, 2013). Furthermore, augmentation of COL III production was initiated at beginning of tendon healing to generate randomly organize fiber type matrix (Lin, Cardenas, & Soslowsky, 2004). In this way, while cell proliferation was increased, COL I synthesis was decreased (Voleti et al., 2012). Since inner core of FSPCL/ESPCL-GEL 3:1 scaffold was made of randomly organize fibers, GDF-5 treated cells might produce COL III more than COL I. Therefore, increase in total collagen was related with the COL III.

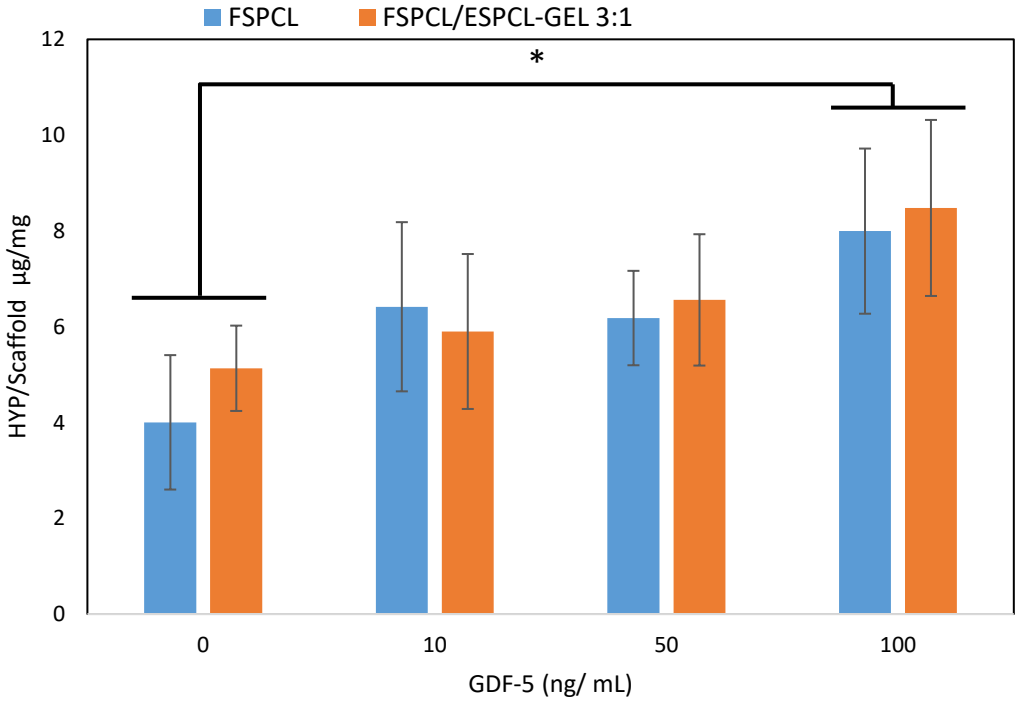

Figure 26. Hydroxyproline production of cells treated with GDF-5 (0,10,50, 100 ng/ mL) on FSPCL and FSPCL/ESPCL-GEL 3:1 scaffolds at day 4.

After examination of those experiments, 100 ng/mL was selected as the best concentration and proceeded to perform the time kinetics studies with the fixed concentration of GDF-5.

3.2.4. Time Effect of GDF-5

GDF-5 (100 ng/mL) supplemented HADMSCs viability on TCPS (TCPS with 0 ng/mL was used as control) and scaffolds were examined at time points: 1, 4, 7, 14 days of incubation (Figure 27). Cells that were not treated with GDF-5 was used as control. At incubation day 1, there was no differences between the groups for cell viabilities. After four-days incubation, GDF-5 treated FSPCL/ESPCL-Gel 3:1 showed significantly higher cell viability than TCPS. Through the incubation from 7 to 14 days, each GDF-5 treated group significantly increased cell viability compared to without GDF-5. At the last day of incubation, FSPCL/ESPCL-Gel 3:1 scaffold significantly greater viability than all other groups. Cell growth in FSPCL/ESPCL-Gel 3:1 scaffold was promoted by combination of nano sized ESPCL-Gel fibers which enhanced cell proliferation and GDF-5 supplementation. It is reasonable to assume that both GDF-5 (100 ng/mL and inner core of the scaffold (PCL-Gel 3:1 electrospun nano fibers) has effect in positive way on HADMSCs cell viability which was more recognizable after 4-day incubation. At day 7 and day 14, for example, there was no significant differences between GDF-5 treated FSPCL, which has no inner core, and GDF-5 non-treated FSPCL/ESPCL-gel 3:1 group. In literature, cell viability of HADMSCs tested on commercial 3D PCL scaffold (3D Biotek 3D Insert™) and TCP showed no significant difference (Su et al., 2018). Thus, the developed tendon tissue engineering scaffold with composition; FSPCL and FSPCL/ESPCL-Gel 3:1 in this study, can be suggested as suitable in terms of cell viability.

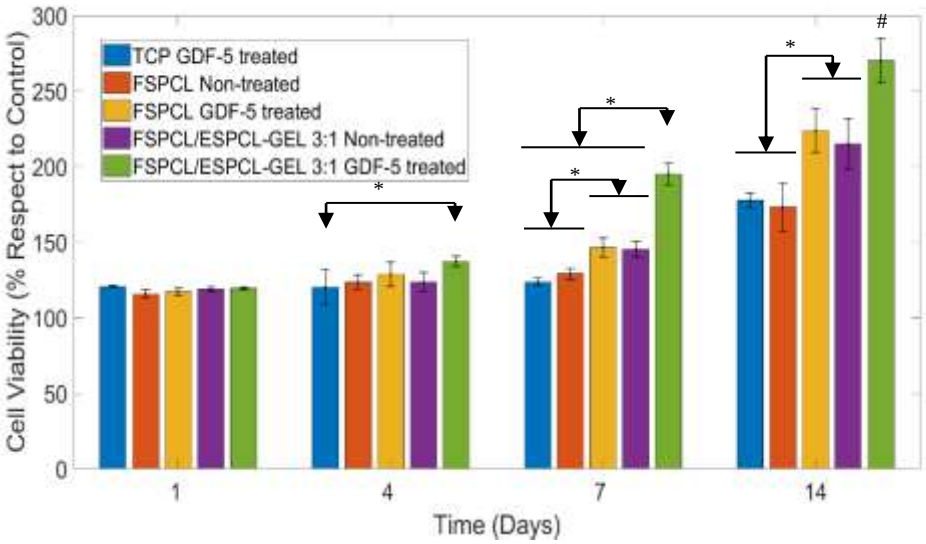

Figure 27. The time-dependent effect GDF-5 (100 ng/mL) on HADMSCs. (*p<0.05, significant differences between groups shown by bars and arrows, #: FSPCL/ESPCL-Gel 3:1 scaffold showed significantly higher cell viability than other groups at seventh and fourteenth day of incubation, n=4)

Hydroxyproline content of GDF (100, 0 ng/ mL) treated scaffolds is given in Figure 28. Through to incubation time, GDF-5 treated FSPCL/ESPCL-Gel :1 produced significantly higher than non-treated scaffolds. Moreover, GDF-5 treated FSPCL scaffolds had significantly more hydroxyproline than non-treated scaffolds at day 4. Then, significant hydroxyproline production seen at day 14 against non-treated FSPCL. These results revealed that GDF-5 treatment induced collagen synthesis on the scaffolds. As mentioned above, GDF-5 (100 ng/ mL) treatment induced cells to produce more collagen. Moreover, different studies demonstrated that GDF-5 treatment significantly increased COL I gene expression at day 12 (Park et al., 2010) and 14 (Su et al., 2018). Furthermore, HADMSCs treated with GDF-5 on 3D PLAGA scaffold increased not only COL I gene expression at day 7 but also compare to the 2D PLGA film (R. James, Kumbar, Laurencin, Balian, & Chhabra, 2011b). Therefore, total collagen increment during incubation time were related with COL I and COL III.

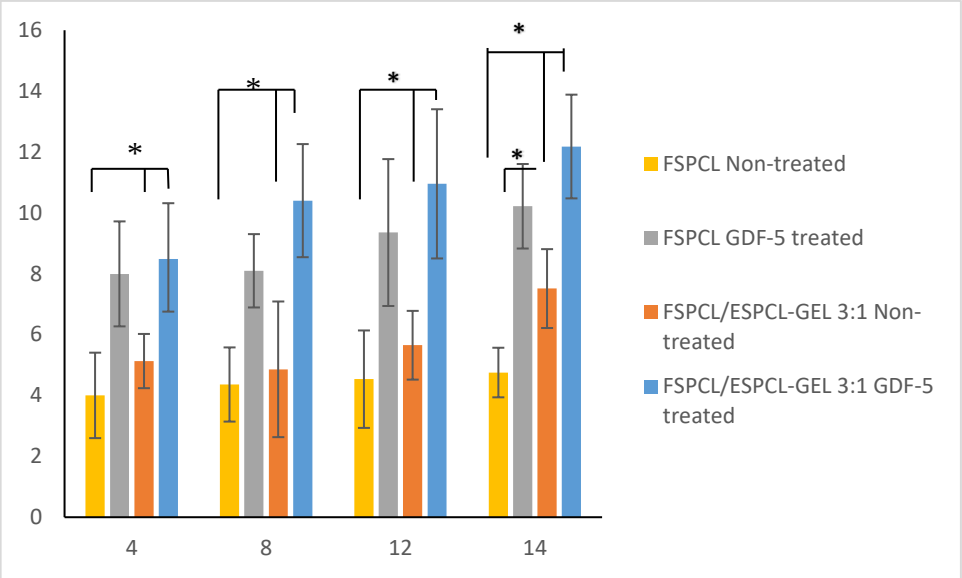

Figure 28. Hydroxyproline production of cells treated with or without GDF-5 (100 ng/ mL) on FSPCL and FSPCL/ESPCL-GEL 3:1 scaffolds.

During early stage of tendon healing, particularly the repair stage, COL III synthesis was increased to form endotenon and epitenon (Wang, Chen, & Piao, 2005). After that, COL III synthesis slowed and eventually replaced by COL I synthesis (Sharma & Maffulli, 2014). COL I fiber formation was regulated by COL III that provides its null structure to COL I (Liu, Wu, Byrne, Krane, & Jaenisch, 1997). In addition, Col III was used as indicator to evaluate differentiation of tendon (Kuo & Tuan, 2008). Consequently, semi-quantification of COL I and III from confocal images were evaluated for FSPCL/ESPCL-Gel 3:1. Table 4 showed that GDF-5 (100 ng/mL) treated FSPCL/ESPCL-Gel 3:1 showed significantly higher COL III presence than non-treated FSPCL/ESPCL-Gel 3:1 after 7-days of incubation. Similarly, COL I expression increased in GDF-5 supplied group. Based on these results, GDF-5 (100 ng/ mL) induced COL I and III production. Additionally, semi-quantification of COL I, COL III and TNMD (at day 4, Table 3) revealed that GDF-5 (100 ng/ mL) treated cells expressed tenogenic phenotype.

Table 4. Area ratio of COL I and III expressed regions to total area in confocal images (*and $p<0.05, n=4) in relation to GDF-5 (100 ng/mL). Semi-quantification COL I and III stained area were normalized by total image area.

GDF-5 Concentration	COL I Area/Total Area ($\mu m^2/ \mu m^2$)	COL III Area/Total Area ($\mu m^2/ \mu m^2$)
0 ng/mL	0.005 ± 0.0003	0.02 ± 0.005
100 ng/mL	0.07 ± 0.001$^{\$}$	0.11 ± 0.013*

In Figure. 29 A-E GDF-5 (100 ng/ mL) treated cells cytoskeleton, COL I and COL II exhibited aligned and elongated shape in fiber direction. Moreover, cells morpholog on FSPCL/ESPCL-GEL 3:1 with GDF-5 were similar to tenocytes. Since mesenchymal stem cell elongation strongly related with tenogenic differentiation, GDF-5 treated cells on the scaffold can be considered as tenocyte like cells. To evaluate role of GDF-5 in tenogenic differentiation, Tan et al. compared gene expression of bone marrow mesenchymal stem cells with GDF-5 (100 ng/ mL) and tenocytes. Results revealed that actin cytoskeleton reorganization, collagen fibrillogenesis, or GTPase activating protein related genes were similarly upregulated (Tan et al., 2015). Therefore, tenogenic differentiation MSCs can be also associated cytoskeleton reorganization (Maharam et al., 2015). In other study, bone marrow mesenchymal stem cell were subjected to cyclic strain which were promoted cytoskeleton reorganization and stress fiber formation during the tenogenic differentiation (Morita, Mukai, Ju, & Watanabe, 2013). Similar stress fiber formation was obtained GDF-5 treated ADMSCs on the scaffold can be seen in Figure. 29 B. In conclusion, obtained results were in concordance with other studies.

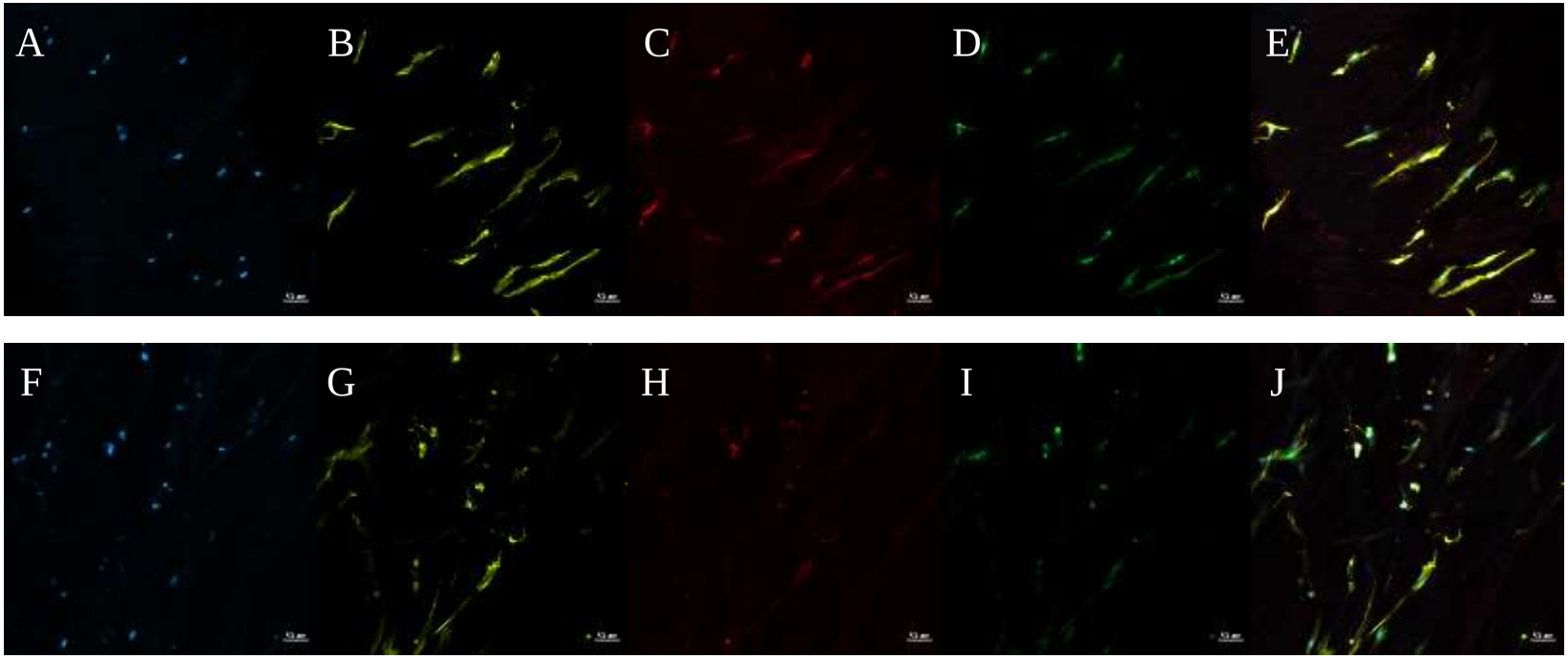

Figure 29. Immunofluorescence staining for cell morphology and ECM cell markers captured by Confocal laser scanning microscopy (CLSM). Sequential images of HADMSCs cells on FSPCL/ESPCL-Gel 3:1 scaffolds supplemented with media containing 100 ng/mL of GDF-5 A) cell nucleus, B) F-actin, C) COL I, D) COL III, and E) merged image, and 0 ng/mL of GDF-5 F) cell nucleus, G) F-actin, H) COL I, I) COL III, and J) merged image after 7 days of incubation. Stains: DAPI against nuclei (blue), Alexa Fluor 532-phalloidin against F-actin (yellow), Alexa Fluor 647 anti-rabbit against rabbit anti-COL I and Alexa Fluor 488 anti-mouse against mouse anti-COL III (green).

Cell migration on FSPCL/ESPCL-GEL 3:1 scaffold assessed by CLSM at day 7 (Figure. 30). Both GDF-5 treated and non-treated scaffolds were investigated. Since cells were seeded inner core of the scaffolds, flat surface of the scaffolds was examined to visualize radial and axial migration of cells by z stack analysis. Figure.30 A-D shows that GDF-5 treated and without GDF-5 cells migrated through radial direction. While GDF-5 treated cells uniformly distributed in the scaffold, cells without GDF-5 localized in inner core of the scaffold (Figure.30 F-I). Images revealed that GDF-5 (100 ng/ mL) treatment promoted cell migration. Limitation of this assessment was that distribution of the cells on scaffolds need to be calculated to provide more comparable results. Despite of the unfair observation, GDF-5 inducement on human bone marrow stem cell migration was reported before. Tan et al. (2015) combined 100 ng/ mL of GDF-5 in culture media in order to identify tenogenic differentiation pathway of bone marrow stem cell stimulated by GDF-5. Reorganization of Keratin filament in bone marrow stem cell cytoskeleton by GDF-5 was reported (Tan et al., 2015). While regulation of keratin filament playing major role in cell migration, relation between keratin filament signaling and tenogenic differentiation is still unknown (Tan et al., 2015). As seen in Figure Figure.30 F-I, HADMSCs morphology form inner core to outer core of scaffold gradually changed. Namely, the cells showed elongated shape in center of scaffold, while they were less elongated at the outer core. Suggesting that cells without GDF-5 kept their viability, and they were still in spreading in the scaffold. Overall, FSPCL/ESPCL-GEL 3:1 scaffolds allow cell spreading.

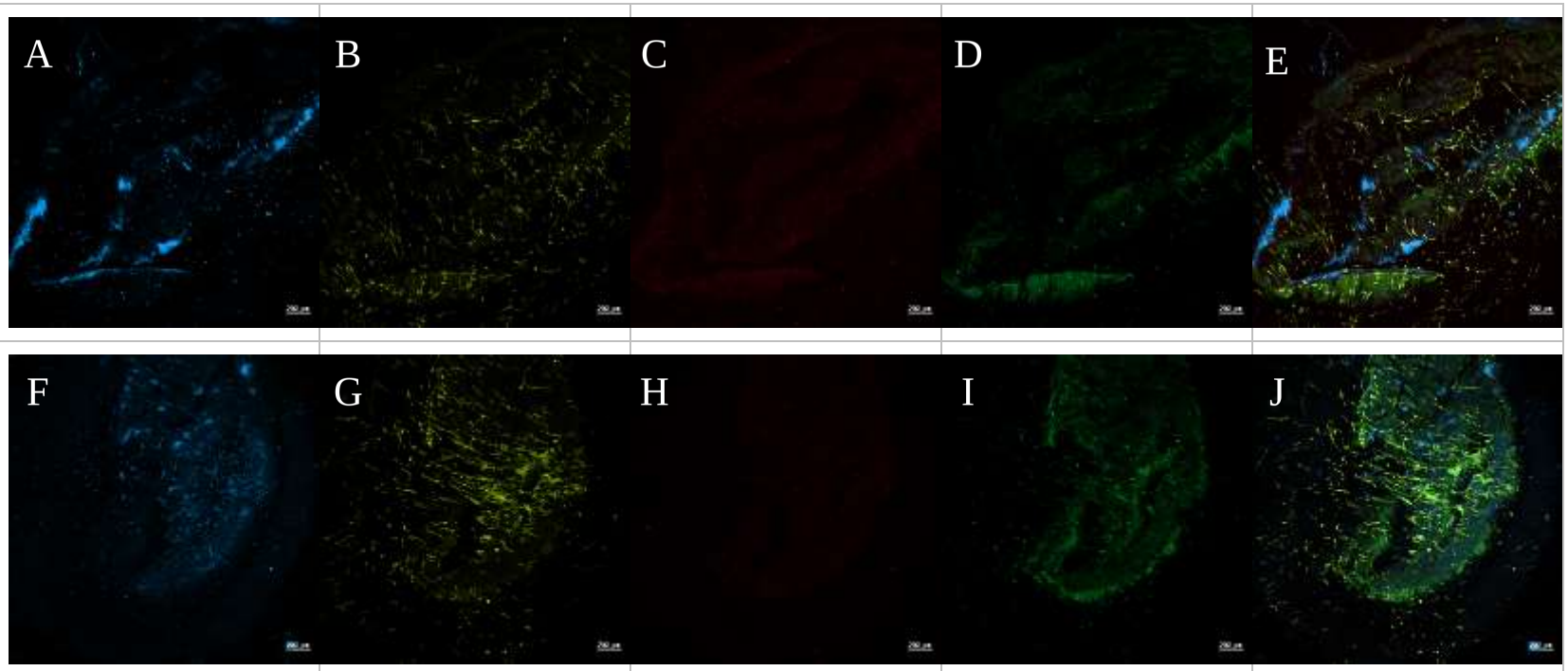

Figure 30. Immunofluorescence staining for cell migration and ECM cell markers captured by Confocal laser scanning microscopy (CLSM). Sequential images of HADMSCs cells on FSPCL/ESPCL-Gel 3:1 scaffolds supplemented with media containing 100 ng/mL of GDF-5 A) cell nucleus, B) F-actin, C) COL I, D) COL III, and E) merged image, and 0 ng/mL of GDF-5 F) cell nucleus, G) F-actin, H) COL I, I) COL III, and J) merged image after 7 days of incubation. Stains: DAPI against nuclei (blue), Alexa Fluor 532-phalloidin against F-actin (yellow), Alexa Fluor 647 anti-rabbit against rabbit anti-COL I and Alexa Fluor 488 anti-mouse against mouse anti-COL III (green).

CHAPTER 4

CONCLUSION

This study proposed fabrication of 3D scaffolds supplemented with stem cells and growth factor to mimic healthy and wounded extra cellular matrix of tendon to increase cell adhesion, proliferation, and orientation for TTE applications. 3D scaffolds composed of unaligned wet electrospun (ES) nanofibers in aligned rotary jet spinning (RJS) fibers were produced for the first time. Combination of these two fiber production techniques provide highly interconnective, mechanically strong 3D scaffolds. Mechanical properties were enhanced by presence of unaligned PCL fibers or PCL/GEL ES fibers. While all groups guided fibroblasts orientation, only FSPCL/ESPCL-GEL 3:1 scaffold showed higher fibroblast attachment and viability. Therefore, FSPCL/ESPCL-GEL 3:1 scaffold was selected to be most suitable for TTE applications. 100 ng/ mL of GDF-5 induced HADMSCs provided better cell viability, tenogenic differentiation, hydroxyproline production.

As conclusion, using RJS provides fast, reproducible, cost efficient, and above all suitable for industrial scale production. Proposed design and materials can be manipulated or replaced to address specific need. The results need to be supported with gene expression of GDF-5 induced HADMSCs and in vivo tests

REFERRENCES

Andrews, D. L., Scholes, G. D., & Wiederrecht, G. P. (2010). *Comprehensive Nanoscience and Nanotechnology*. Boston. Retrieved from https://www.sciencedirect.com/science/referenceworks/9780123743961

Aslan, H., Kimelman-Bleich, N., Pelled, G., & Gazit, D. (2008, February). Molecular targets for tendon neoformation. *Journal of Clinical Investigation*. American Society for Clinical Investigation. https://doi.org/10.1172/JCI33944

Badrossamay, M. R., Balachandran, K., Capulli, A. K., Golecki, H. M., Agarwal, A., Goss, J. A., … Parker, K. K. (2014). Engineering hybrid polymer-protein super-aligned nanofibers via rotary jet spinning. *Biomaterials*, *35*(10), 3188–3197. https://doi.org/10.1016/j.biomaterials.2013.12.072

Badrossamay, M. R., McIlwee, H. A., Goss, J. A., & Parker, K. K. (2010). Nanofiber assembly by rotary jet-spinning. *Nano Letters*, *10*(6), 2257–2261. https://doi.org/10.1021/nl101355x

Baer, P. C. (2014). Adipose-derived mesenchymal stromal/stem cells: An update on their phenotype in vivo and in vitro. *World Journal of Stem Cells*, *6*(3), 256. https://doi.org/10.4252/wjsc.v6.i3.256

Baumfeld, J. A., van Riet, R. P., Zobitz, M. E., Eygendaal, D., An, K. N., & Steinmann, S. P. (2010). Triceps tendon properties and its potential as an autograft. *Journal of Shoulder and Elbow Surgery*, *19*(5), 697–699. https://doi.org/10.1016/j.jse.2009.12.001

Benjamin, M., Kaiser, E., & Milz, S. (2008, March). Structure-function relationships in tendons: A review. *Journal of Anatomy*. https://doi.org/10.1111/j.1469-7580.2008.00864.x

Bieback, K., Kern, S., Kocaömer, A., Ferlik, K., & Bugert, P. (2008). Comparing mesenchymal stromal cells from different human tissues: bone marrow, adipose tissue and umbilical cord blood. *Bio-Medical Materials and Engineering*, *18*(1 Suppl), S71–S76. Retrieved from http://www.ncbi.nlm.nih.gov/pubmed/18334717

Bourin, P., Bunnell, B. A., Casteilla, L., Dominici, M., Katz, A. J., March, K. L., … Gimble, J. M. (2013). Stromal cells from the adipose tissue-derived stromal vascular fraction and culture expanded adipose tissue-derived stromal/stem cells: A joint statement of the International Federation for Adipose Therapeutics and Science (IFATS) and the International So. *Cytotherapy*, *15*(6), 641–648. https://doi.org/10.1016/j.jcyt.2013.02.006

Burkhart, S. S., Diaz Pagàn, J. L., Wirth, M. A., & Athanasiou, K. A. (1997). Cyclic loading of anchor-based rotator cuff repairs: Confirmation of the tension overload phenomenon and comparison of suture anchor fixation with transosseous fixation. *Arthroscopy*, *13*(6), 720–724. https://doi.org/10.1016/S0749-8063(97)90006-2

Campos, D. M., Soares, G. A., & Anselme, K. (2013). Role of culture conditions on in vitro transformation and cellular colonization of biomimetic HA-Col scaffolds. *Biomatter*, *3*(2). https://doi.org/10.4161/biom.24922

Carmeli, E., Patish, H., & Coleman, R. (2003). The aging hand. *The Journals of Gerontology. Series A, Biological Sciences and Medical Sciences*, *58*(2), 146–52. Retrieved from http://www.ncbi.nlm.nih.gov/pubmed/12586852

Centola, M., Rainer, A., Spadaccio, C., De Porcellinis, S., Genovese, J. A., & Trombetta, M. (2010). Combining electrospinning and fused deposition modeling for the fabrication of a hybrid vascular graft. *Biofabrication*, *2*(1), 014102. https://doi.org/10.1088/1758-5082/2/1/014102

Chan, B. P., & Leong, K. W. (2008). Scaffolding in tissue engineering: General approaches and tissue-specific considerations. In *European Spine Journal* (Vol. 17, pp. 467–479). Springer-Verlag. https://doi.org/10.1007/s00586-008-0745-3

Chen, J., Xu, J., Wang, A., & Zheng, M. (2009, January 9). Scaffolds for tendon and ligament repair: Review of the efficacy of commercial products. *Expert Review of Medical Devices*. https://doi.org/10.1586/17434440.6.1.61

Chhabra, A., Tsou, D., Clark, R. T., Gaschen, V., Hunziker, E. B., & Mikic, B. (2003). GDF-5 deficiency in mice delays Achilles tendon healing. *Journal of Orthopaedic Research*, *21*(5), 826–835. https://doi.org/10.1016/S0736-0266(03)00049-4

Chuen, F. S., Chuk, C. Y., Ping, W. Y., Nar, W. W., Kim, H. L., & Ming, C. K. (2004). Immunohistochemical characterization of cells in adult human patellar tendons. *Journal of Histochemistry and Cytochemistry*, *52*(9), 1151–1157. https://doi.org/10.1369/jhc.3A6232.2004

Costa, M. A., Wu, C., Pham, B. V., Chong, A. K. S., Pham, H. M., & Chang, J. (2006). Tissue engineering of flexor tendons: optimization of tenocyte proliferation using growth factor supplementation. *Tissue Engineering*, *12*(7), 1937–43. https://doi.org/10.1089/ten.2006.12.1937

Dalton, P. D., Vaquette, C., Farrugia, B. L., Dargaville, T. R., Brown, T. D., & Hutmacher, D. W. (2013, January 3). Electrospinning and additive manufacturing: Converging technologies. *Biomaterials Science*. The Royal Society of Chemistry. https://doi.org/10.1039/c2bm00039c

De Francesco, F., Tirino, V., Desiderio, V., Ferraro, G., D'Andrea, F., Giuliano, M., … Papaccio, G. (2009). Human CD34+/CD90+ASCs are capable of growing as sphere clusters, producing high levels of VEGF and forming capillaries. *PLoS ONE*, *4*(8), e6537. https://doi.org/10.1371/journal.pone.0006537

Derwin, K. A., Soslowsky, L. J., Kimura, J. H., & Plaas, A. H. (2001). Proteoglycans and glycosaminoglycan fine structure in the mouse tail tendon fascicle. *Journal of Orthopaedic Research*, *19*(2), 269–277. https://doi.org/10.1016/S0736-0266(00)00032-2

Dex, S., Lin, D., Shukunami, C., & Docheva, D. (2016). Tenogenic modulating insider factor: Systematic assessment on the functions of tenomodulin gene. *Gene*, *587*(1), 1–17. https://doi.org/10.1016/j.gene.2016.04.051

Diamant, J., Keller, A., Baer, E., Litt, M., & Arridge, R. G. (1972). Collagen; ultrastructure and its relation to mechanical properties as a function of ageing. *Proceedings of the Royal Society of London. Series B, Biological Sciences*, *180*(1060), 293–315. https://doi.org/10.1098/RSPB.1972.0019

Díaz, E., Sandonis, I., & Valle, M. B. (2014). In vitro degradation of poly(caprolactone)/nHA composites. *Journal of Nanomaterials*, *2014*, 1–8. https://doi.org/10.1155/2014/802435

Docheva, D., Hunziker, E. B., Fassler, R., & Brandau, O. (2005). Tenomodulin Is Necessary for Tenocyte Proliferation and Tendon Maturation. *Molecular and Cellular Biology*, *25*(2), 699–705. https://doi.org/10.1128/MCB.25.2.699-705.2005

Docheva, D., Müller, S. A., Majewski, M., & Evans, C. H. (2015a, April). Biologics for tendon repair. *Advanced Drug Delivery Reviews*. https://doi.org/10.1016/j.addr.2014.11.015

Docheva, D., Müller, S. A., Majewski, M., & Evans, C. H. (2015b, April 1). Biologics for tendon repair. *Advanced Drug Delivery Reviews*. Elsevier. https://doi.org/10.1016/j.addr.2014.11.015

Dominici, M., Le Blanc, K., Mueller, I., Slaper-Cortenbach, I., Marini, F. C., Krause, D. S., … Horwitz, E. M. (2006). Minimal criteria for defining multipotent mesenchymal stromal cells. The International Society for Cellular Therapy position statement. *Cytotherapy*, *8*(4), 315–317. https://doi.org/10.1080/14653240600855905

Doroski, D. M., Brink, K. S., & Temenoff, J. S. (2007, January 1). Techniques for biological characterization of tissue-engineered tendon and ligament. *Biomaterials*. Elsevier. https://doi.org/10.1016/j.biomaterials.2006.08.040

Dulnik, J., Denis, P., Sajkiewicz, P., Kołbuk, D., & Choińska, E. (2016). Biodegradation of bicomponent PCL/gelatin and PCL/collagen nanofibers electrospun from alternative solvent system. *Polymer Degradation and Stability*, *130*, 10–21. https://doi.org/10.1016/j.polymdegradstab.2016.05.022

Erisken, C., Zhang, X., Moffat, K. L., Levine, W. N., & Lu, H. H. (2013). Scaffold Fiber Diameter Regulates Human Tendon Fibroblast Growth and Differentiation. *Tissue Engineering Part A*, *19*(3–4), 519–528. https://doi.org/10.1089/ten.tea.2012.0072

Gathercole, L. J., & Keller, A. (1978). Early development of crimping in rat tail tendon collagen: A polarizing optical and SEM study. *Micron (1969)*, *9*(2), 83–89. https://doi.org/10.1016/0047-7206(78)90011-0

Gautam, S., Dinda, A. K., & Mishra, N. C. (2013). Fabrication and characterization of PCL/gelatin composite nanofibrous scaffold for tissue engineering applications by electrospinning method. *Materials Science and Engineering C*, *33*(3), 1228–1235. https://doi.org/10.1016/j.msec.2012.12.015

Gautieri, A., Vesentini, S., Redaelli, A., & Buehler, M. J. (2012). Viscoelastic properties of model segments of collagen molecules. *Matrix Biology*, *31*(2), 141–149. https://doi.org/10.1016/j.matbio.2011.11.005

Gelberman, R. H., Vandeberg, J. S., Manske, P. R., & Akeson, W. H. (1985). The early stages of flexor tendon healing: a morphologic study of the first fourteen days. *The Journal of Hand Surgery*, *10*(6 Pt 1), 776–84. Retrieved from http://www.ncbi.nlm.nih.gov/pubmed/2416800

Golecki, H. M., Yuan, H., Glavin, C., Potter, B., Badrossamay, M. R., Goss, J. A., … Parker, K. K. (2014). Effect of solvent evaporation on fiber morphology in rotary jet spinning. *Langmuir*, *30*(44), 13369–13374. https://doi.org/10.1021/la5023104

Gonzalez, G. M., Macqueen, L. A., Lind, J. U., Fitzgibbons, S. A., Chantre, C. O., Huggler, I., … Parker, K. K. (2016). Production of Synthetic, Para-Aramid and Biopolymer Nanofibers by Immersion Rotary Jet-Spinning. *Macromolecular Materials and Engineering*, *1600365*, 1–11. https://doi.org/10.1002/mame.201600365

Grinstein, M., & Galloway, J. L. (2018). Developmental Biology in Tendon Tissue Engineering. *Developmental Biology and Musculoskeletal Tissue Engineering*, 181–206. https://doi.org/10.1016/B978-0-12-811467-4.00008-5

Gruber, H., Somayaji, S., Riley, F., Hoelscher, G., Norton, H., Ingram, J., & Hanley, E. (2012). Human adipose-derived mesenchymal stem cells: serial passaging, doubling time and cell senescence. *Biotechnic & Histochemistry*, *87*(4), 303–311. https://doi.org/10.3109/10520295.2011.649785

Haasters, F., Prall, W. C., Anz, D., Bourquin, C., Pautke, C., Endres, S., … Schieker, M. (2009). Morphological and immunocytochemical characteristics indicate the yield of early progenitors and represent a quality control for human mesenchymal stem cell culturing. *Journal of Anatomy*, *214*(5), 759–767. https://doi.org/10.1111/j.1469-7580.2009.01065.x

Hampson, K., Forsynth, N. ., El Haj, A., & Mafulli, N. (2008). Tendon Tissue Engineering. In *Topics in Tissue Engineering* (Vol. 4). Retrieved from http://www.oulu.fi/spareparts/ebook_topics_in_t_e_vol4/abstracts/hampson.pdf

Han, F., Zhu, C., Chen, L., Wicks, J., & Li, B. (2017). *Bio-Instructive Scaffolds for Bone Regeneration*. *Bio-Instructive Scaffolds for Musculoskeletal Tissue Engineering and Regenerative Medicine*. Elsevier Inc. https://doi.org/10.1016/B978-0-12-803394-4.00003-3

Hata, A., & Chen, Y. G. (2016). TGF-β signaling from receptors to smads. *Cold Spring Harbor Perspectives in Biology*, *8*(9). https://doi.org/10.1101/cshperspect.a022061

Haut, R. C. (1986). The influence of specimen length on the tensile failure properties of tendon collagen. *Journal of Biomechanics*, *19*(11), 951–955. https://doi.org/10.1016/0021-9290(86)90190-9

Heldin, C. H., Miyazono, K., & Ten Dijke, P. (1997, December 4). TGF-β signalling from cell membrane to nucleus through SMAD proteins. *Nature*. Nature Publishing Group. https://doi.org/10.1038/37284

Hess, G. P., Cappiello, W. L., Poole, R. M., & Hunter, S. C. (1989). Prevention and Treatment of Overuse Tendon Injuries. *Sports Medicine*, *8*(6), 371–384. https://doi.org/10.2165/00007256-198908060-00005

Hoffmann, A., Pelled, G., Turgeman, G., Eberle, P., Zilberman, Y., Shinar, H., … Gazit, D. (2006). Neotendon formation induced by manipulation of the Smad8 signalling pathway in mesenchymal stem cells. *Journal of Clinical Investigation*, *116*(4), 940–952. https://doi.org/10.1172/JCI22689

Huang, Z. M., Zhang, Y. Z., Kotaki, M., & Ramakrishna, S. (2003). A review on polymer nanofibers by electrospinning and their applications in nanocomposites. *Composites Science and Technology*, *63*(15), 2223–2253. https://doi.org/10.1016/S0266-3538(03)00178-7

Ippolito, E., Natali, P. G., Postacchini, F., Accinni, L., & De Martino, C. (1980). Morphological, immunochemical, and biochemical study of rabbit Achilles tendon at various ages. *Journal of Bone and Joint Surgery - Series A*, *62*(4), 583–598. https://doi.org/10.2106/00004623-198062040-00014

Jahani, H., Kaviani, S., Hassanpour-Ezatti, M., Soleimani, M., Kaviani, Z., & Zonoubi, Z. (2012). The effect of aligned and random electrospun fibrous scaffolds on rat mesenchymal stem cell proliferation. *Cell Journal*, *14*(1), 31–38. Retrieved from http://www.ncbi.nlm.nih.gov/pubmed/23626935

James, R., Kesturu, G., Balian, G., & Chhabra, A. B. (2008, January). Tendon: Biology, Biomechanics, Repair, Growth Factors, and Evolving Treatment Options. *Journal of Hand Surgery*. https://doi.org/10.1016/j.jhsa.2007.09.007

James, R., Kumbar, S. G., Laurencin, C. T., Balian, G., & Chhabra, A. B. (2011a). Tendon tissue engineering: Adipose-derived stem cell and GDF-5 mediated regeneration using electrospun matrix systems. *Biomedical Materials*, *6*(2), 025011. https://doi.org/10.1088/1748-6041/6/2/025011

James, R., Kumbar, S. G., Laurencin, C. T., Balian, G., & Chhabra, A. B. (2011b). Tendon tissue engineering: Adipose-derived stem cell and GDF-5 mediated regeneration using electrospun matrix systems. *Biomedical Materials*, *6*(2). https://doi.org/10.1088/1748-6041/6/2/025011

Järvinen, T. A. H., Järvinen, T. L. N., Kannus, P., Józsa, L., & Järvinen, M. (2004). Collagen fibres of the spontaneously ruptured human tendons display decreased thickness and crimp angle. *Journal of Orthopaedic Research*, *22*(6), 1303–1309. https://doi.org/10.1016/J.ORTHRES.2004.04.003

Jørgensen, U., Bak, K., Ekstrand, J., & Scavenius, M. (2001). Reconstruction of the anterior cruciate ligament with the iliotibial band autograft in patients with chronic knee instability. *Knee Surgery, Sports Traumatology, Arthroscopy*, *9*(3), 137–145. https://doi.org/10.1007/s001670000163

Jozsa, L., Kannus, P., Balint, J. B., & Reffy, A. (1991). Three-dimensional ultrastructure of human tendons. *Cells Tissues Organs*, *142*(4), 306–312. https://doi.org/10.1159/000147207

Kannus, P. (2000). Structure of the tendon connective tissue. *Scandinavian Journal of Medicine and Science in Sports*, *10*(6), 312–320. https://doi.org/10.1034/j.1600-0838.2000.010006312.x

Kim, S.-E., Jordan, A. M., Korley, L. T. J., & Pokorski, J. K. (2017). Drawing in poly(e-caprolactone) fibers: tuning mechanics, fiber dimensions and surface-modification density. *J. Mater. Chem. B*, *5*(5), 4499–4506. https://doi.org/10.1039/c7tb00096k

Kim, Y. S., Lee, H. J., Ok, J. H., Park, J. S., & Kim, D. W. (2013). Survivorship of implanted bone marrow-derived mesenchymal stem cells in acute rotator cuff tear. *Journal of Shoulder and Elbow Surgery*, *22*(8), 1037–1045. https://doi.org/10.1016/j.jse.2012.11.005

Kumbar, S. G., James, R., Nukavarapu, S. P., & Laurencin, C. T. (2008). Electrospun nanofiber scaffolds: Engineering soft tissues. *Biomedical Materials*, *3*(3), 034002. https://doi.org/10.1088/1748-6041/3/3/034002

Kuo, C. K., & Tuan, R. S. (2008). Mechanoactive Tenogenic Differentiation of Human Mesenchymal Stem Cells. *Tissue Engineering Part A*, *14*(10), 1615–1627. https://doi.org/10.1089/ten.tea.2006.0415

Laurencin, C. T., & Nair, L. S. (2015). *Nanotechnology and Regenerative Engineering: The Scaffold*. https://doi.org/10.1017/CBO9781107415324.004

Lee, C. H., Shin, H. J., Cho, I. H., Kang, Y.-M., Kim, I. A., Park, K.-D., & Shin, J.-W. (2005). Nanofiber alignment and direction of mechanical strain affect the ECM production of human ACL fibroblast. *Biomaterials*, *26*(11), 1261–1270. https://doi.org/10.1016/j.biomaterials.2004.04.037

Lee, N. M., Erisken, C., Iskratsch, T., Sheetz, M., Levine, W. N., & Lu, H. H. (2017). Polymer fiber-based models of connective tissue repair and healing. *Biomaterials*, *112*, 303–312. https://doi.org/10.1016/j.biomaterials.2016.10.013

Li, F., Li, B., Wang, Q. M., & Wang, J. H.-C. (2008). Cell shape regulates collagen type I expression in human tendon fibroblasts. *Cell Motility and the Cytoskeleton*, *65*(4), 332–341. https://doi.org/10.1002/cm.20263

Li, W.-J., Laurencin, C. T., Caterson, E. J., Tuan, R. S., & Ko, F. K. (2002). Electrospun nanofibrous structure: A novel scaffold for tissue engineering. *Journal of Biomedical Materials Research*, *60*(4), 613–621. https://doi.org/10.1002/jbm.10167

Lin, T. W., Cardenas, L., & Soslowsky, L. J. (2004, June 1). Biomechanics of tendon injury and repair. *Journal of Biomechanics*. Elsevier. https://doi.org/10.1016/j.jbiomech.2003.11.005

Liu Tsang, V., & Bhatia, S. N. (2004, September 22). Three-dimensional tissue fabrication. *Advanced Drug Delivery Reviews*. https://doi.org/10.1016/j.addr.2004.05.001

Liu, X., Wu, H., Byrne, M., Krane, S., & Jaenisch, R. (1997). Type III collagen is crucial for collagen I fibrillogenesis and for normal cardiovascular development. *Proceedings of the National Academy of Sciences*, *94*(5), 1852–1856. https://doi.org/10.1073/pnas.94.5.1852

Loeffler, B. J., Scannell, B. P., Peindl, R. D., Connor, P., Davis, D. E., Hoelscher, G. L., … Gruber, H. E. (2013). Cell-based tissue engineering augments tendon-to-bone healing in a rat supraspinatus model. *Journal of Orthopaedic Research*, *31*(3), 407–412. https://doi.org/10.1002/jor.22234

Lomas, A. J., Ryan, C. N. M., Sorushanova, A., Shologu, N., Sideri, A. I., Tsioli, V., … Zeugolis, D. I. (2015, April 1). The past, present and future in scaffold-based tendon treatments. *Advanced Drug Delivery Reviews*. Elsevier. https://doi.org/10.1016/j.addr.2014.11.022

Loordhuswamy, A. M., Krishnaswamy, V. R., Korrapati, P. S., Thinakaran, S., & Rengaswami, G. D. V. (2014). Fabrication of highly aligned fibrous scaffolds for tissue regeneration by centrifugal spinning technology. *Materials Science and Engineering C*, *42*, 799–807. https://doi.org/10.1016/j.msec.2014.06.011

Lui, P. P. Y., Rui, Y. F., Ni, M., & Chan, K. M. (2011). Tenogenic differentiation of stem cells for tendon repair-what is the current evidence? *Journal of Tissue Engineering and Regenerative Medicine*, *5*(8), e144–e163. https://doi.org/10.1002/term.424

Luo, C. J., Stoyanov, S. D., Stride, E., Pelan, E., & Edirisinghe, M. (2012). Electrospinning versus fibre production methods: from specifics to technological convergence. *Chemical Society Reviews*, *41*(13), 4708–35. https://doi.org/10.1039/c2cs35083a

Macfarlane, E. G., Haupt, J., Dietz, H. C., & Shore, E. M. (2017, November 1). TGF-β family signaling in connective tissue and skeletal diseases. *Cold Spring Harbor Perspectives in Biology*. Cold Spring Harbor Laboratory Press. https://doi.org/10.1101/cshperspect.a022269

Maffulli, N., Longo, U. G., Loppini, M., & Denaro, V. (2010). Current treatment options for tendinopathy. *Expert Opinion on Pharmacotherapy*, *11*(13), 2177–2186. https://doi.org/10.1517/14656566.2010.495715

Maharam, E., Yaport, M., Villanueva, N. L., Akinyibi, T., Laudier, D., He, Z., … Sun, H. B. (2015). Rho/Rock signal transduction pathway is required for MSC tenogenic differentiation. *Bone Research*, *3*(1), 15015. https://doi.org/10.1038/boneres.2015.15

Manning, C. N., Kim, H. M., Sakiyama-Elbert, S., Galatz, L. M., Havlioglu, N., & Thomopoulos, S. (2011). Sustained delivery of transforming growth factor beta three enhances tendon-to-bone healing in a rat model. *Journal of Orthopaedic Research*, *29*(7), 1099–1105. https://doi.org/10.1002/jor.21301

Marrale, J., Morrissey, M. C., & Haddad, F. S. (2007). A literature review of autograft and allograft anterior cruciate ligament reconstruction. *Knee Surgery, Sports Traumatology, Arthroscopy*, *15*(6), 690–704. https://doi.org/10.1007/s00167-006-0236-1

Massagué, J. (1998). TGF-β SIGNAL TRANSDUCTION. *Annu. Rev. Biochem*, *67*(1), 753–91. https://doi.org/10.1146/annurev.biochem.67.1.753

Matsuhashi, T., Hooke, A. W., Zhao, K. D., Goto, A., Sperling, J. W., Steinmann, S. P., & An, K. N. (2014). Tensile properties of a morphologically split supraspinatus tendon. *Clinical Anatomy*, *27*(5), 702–706. https://doi.org/10.1002/ca.22322

Mazzocca, A. D., Chowaniec, D., McCarthy, M. B., Beitzel, K., Cote, M. P., McKinnon, W., & Arciero, R. (2012). In vitro changes in human tenocyte cultures obtained from proximal biceps tendon: Multiple passages result in changes in routine cell markers. *Knee Surgery, Sports Traumatology, Arthroscopy*, *20*(9), 1666–1672. https://doi.org/10.1007/s00167-011-1711-x

Mazzocca, A. D., McCarthy, M. B. R., Chowaniec, D. M., Cote, M. P., Arciero, R. A., & Drissi, H. (2010). Rapid Isolation of Human Stem Cells (Connective Tissue Progenitor Cells) From the Proximal Humerus During Arthroscopic Rotator Cuff Surgery. *The American Journal of Sports Medicine*, *38*(7), 1438–1447. https://doi.org/10.1177/0363546509360924

McEachin, Z., & Lozano, K. (2012). Production and characterization of polycaprolactone nanofibers via forcespinning™ technology. *Journal of Applied Polymer Science*, *126*(2), 473–479. https://doi.org/10.1002/app.36843

Meng, Z. X., Wang, Y. S., Ma, C., Zheng, W., Li, L., & Zheng, Y. F. (2010). Electrospinning of PLGA/gelatin randomly-oriented and aligned nanofibers as potential scaffold in tissue engineering. *Materials Science and Engineering: C*, *30*(8), 1204–1210. https://doi.org/10.1016/J.MSEC.2010.06.018

Merceron, C., Vinatier, C., Clouet, J., Colliec-Jouault, S., Weiss, P., & Guicheux, J. (2008, December). Adipose-derived mesenchymal stem cells and biomaterials for cartilage tissue engineering. *Joint Bone Spine*. https://doi.org/10.1016/j.jbspin.2008.07.007

Mikic, B., Schalet, B. J., Clark, R. T., Gaschen, V., & Hunziker, E. B. (2001). GDF-5 deficiency in mice alters the ultrastructure, mechanical properties and composition of the Achilles tendon. *Journal of Orthopaedic Research*, *19*(3), 365–371. https://doi.org/10.1016/S0736-0266(00)90018-4

Molloy, T., Wang, Y., & Murrell, G. A. C. (2003). The roles of growth factors in tendon and ligament healing. *Sports Medicine*. https://doi.org/10.2165/00007256-200333050-00004

Morita, Y., Mukai, T., Ju, Y., & Watanabe, S. (2013). Evaluation of Stem Cell-to-Tenocyte Differentiation By Atomic Force Microscopy to Measure Cellular Elastic Moduli. *Cell Biochemistry and Biophysics*, *66*(1), 73–80. https://doi.org/10.1007/s12013-012-9455-x

Moshiri, A., & Oryan, A. (2012). Role of tissue engineering in tendon reconstructive surgery and regenerative medicine: Current concepts, approaches and concerns. *Hard Tissue*, *1*(2). https://doi.org/10.13172/2050-2303-1-2-291

Ngo, M., Pham, H., Longaker, M. T., & Chang, J. (2001). Differential expression of transforming growth factor-beta receptors in a rabbit zone II flexor tendon wound healing model. *Plastic and Reconstructive Surgery*, *108*(5), 1260–7. Retrieved from http://www.ncbi.nlm.nih.gov/pubmed/11604629

Nickel, J., Kotzsch, A., Sebald, W., & Mueller, T. D. (2005). A single residue of GDF-5 defines binding specificity to BMP receptor IB. *Journal of Molecular Biology*, *349*(5), 933–947. https://doi.org/10.1016/j.jmb.2005.04.015

Nishitoh, H., Ichijo, H., Kimura, M., Matsumoto, T., Makishima, F., Yamaguchi, A., … Miyazono, K. (1996). Identification of type I and type II serine/threonine kinase receptors for growth/differentiation factor-5. *Journal of Biological Chemistry*, *271*(35), 21345–21352. https://doi.org/10.1074/jbc.271.35.21345

Nixon, A. J., Watts, A. E., & Schnabel, L. V. (2012). Cell- and gene-based approaches to tendon regeneration. *Journal of Shoulder and Elbow Surgery*, *21*(2), 278–294. https://doi.org/10.1016/j.jse.2011.11.015

Nourissat, G., Berenbaum, F., & Duprez, D. (2015, April 3). Tendon injury: From biology to tendon repair. *Nature Reviews Rheumatology*. https://doi.org/10.1038/nrrheum.2015.26

Padron, S., Fuentes, A., Caruntu, D., & Lozano, K. (2013). Experimental study of nanofiber production through forcespinning. *Journal of Applied Physics*, *113*(2). https://doi.org/10.1063/1.4769886

Park, A., Hogan, M. V., Kesturu, G. S., James, R., Balian, G., & Chhabra, A. B. (2010). Adipose-Derived Mesenchymal Stem Cells Treated with Growth Differentiation Factor-5 Express Tendon-Specific Markers. *Tissue Engineering Part A*, *16*(9), 2941–2951. https://doi.org/10.1089/ten.tea.2009.0710

Patel, M., & Fisher, J. P. (2008). Biomaterial scaffolds in pediatric tissue engineering. *Pediatric Research*, *63*(5), 497–501. https://doi.org/10.1203/01.PDR.0b013e318165eb3e

Pauly, H. M., Kelly, D. J., Popat, K. C., Trujillo, N. A., Dunne, N. J., McCarthy, H. O., & Haut Donahue, T. L. (2016). Mechanical properties and cellular response of novel electrospun nanofibers for ligament tissue engineering: Effects of orientation and geometry. *Journal of the Mechanical Behavior of Biomedical Materials*, *61*, 258–270. https://doi.org/10.1016/j.jmbbm.2016.03.022

Peach, M. S., James, R., Toti, U. S., Deng, M., Morozowich, N. L., Allcock, H. R., … Kumbar, S. G. (2012). Polyphosphazene functionalized polyester fiber matrices for tendon tissue engineering: in vitro evaluation with human mesenchymal stem cells. *Biomedical Materials (Bristol, England)*, *7*(4), 045016. https://doi.org/10.1088/1748-6041/7/4/045016

Pietschmann, M. F., Frankewycz, B., Schmitz, P., Docheva, D., Sievers, B., Jansson, V., … Müller, P. E. (2013). Comparison of tenocytes and mesenchymal stem cells seeded on biodegradable scaffolds in a full-size tendon defect model. *Journal of Materials Science: Materials in Medicine*, *24*(1), 211–220. https://doi.org/10.1007/s10856-012-4791-3

Raghunath, J., Georgiou, G., Armitage, D., Nazhat, S. N., Sales, K. M., Butler, P. E., & Seifalian, A. M. (2009). Degradation studies on biodegradable nanocomposite based on polycaprolactone/polycarbonate (80:20%) polyhedral oligomeric silsesquioxane. *Journal of Biomedical Materials Research - Part A*, *91*(3), 834–844. https://doi.org/10.1002/jbm.a.32335

Ramos, D., Peach, M. S., Mazzocca, A. D., Yu, X., & Kumbar, S. G. (2015). Tendon tissue engineering. *Regenerative Engineering of Musculoskeletal Tissues and Interfaces*, 195–217. https://doi.org/10.1016/B978-1-78242-301-0.00008-2

Reddy, G. K., & Enwemeka, C. S. (1996). A simplified method for the analysis of hydroxyproline in biological tissues. *Clinical Biochemistry*, *29*(3), 225–229. https://doi.org/10.1016/0009-9120(96)00003-6

Ren, L., Pandit, V., Elkin, J., Denman, T., Cooper, J. A., & Kotha, S. P. (2013). Large-scale and highly efficient synthesis of micro- and nano-fibers with controlled fiber morphology by centrifugal jet spinning for tissue regeneration. *Nanoscale*, *5*(6), 2337–45. https://doi.org/10.1039/c3nr33423f

Ricchetti, E. T., Aurora, A., Iannotti, J. P., & Derwin, K. A. (2012). Scaffold devices for rotator cuff repair. *Journal of Shoulder and Elbow Surgery*, *21*(2), 251–265. https://doi.org/10.1016/j.jse.2011.10.003

Rigby, B. J., Hirai, N., Spikes, J. D., & Eyring, H. (1959). The Mechanical Properties of Rat Tail Tendon. *The Journal of General Physiology*, *43*(2), 265–83. https://doi.org/10.1085/JGP.43.2.265

Robi, K., Jakob, N., Matevz, K., & Matjaz, V. (2013). The Physiology of Sports Injuries and Repair Processes. In *Current Issues in Sports and Exercise Medicine*. InTech. https://doi.org/10.5772/54234

Rodrigues, M. T., Reis, R. L., & Gomes, M. E. (2013, September 12). Engineering tendon and ligament tissues: Present developments towards successful clinical products. *Journal of Tissue Engineering and Regenerative Medicine*. Spandidos Publications. https://doi.org/10.1002/term.1459

Rogalski, J. J., Bastiaansen, C. W. M., & Peijs, T. (2017). Rotary jet spinning review – a potential high yield future for polymer nanofibers. *Nanocomposites*, *3*(4), 97–121. https://doi.org/10.1080/20550324.2017.1393919

Shahab-Osterloh, S., Witte, F., Hoffmann, A., Winkel, A., Laggies, S., Neumann, B., … Gross, G. (2010). Mesenchymal stem cell-dependent formation of heterotopic tendon-bone insertions (osteotendinous junctions). *Stem Cells*, *28*(9), 1590–1601. https://doi.org/10.1002/stem.487

Sharma, P., & Maffulli, N. (2014). Biology of tendon injury: healing, modeling and remodeling. *Journal of Musculoskeletal & Neuronal Interactions*, *6*(2), 181–90. https://doi.org/10.1016/j.math.2014.02.002

Shen, H., Gelberman, R. H., Silva, M. J., Sakiyama-Elbert, S. E., & Thomopoulos, S. (2013). BMP12 induces tenogenic differentiation of adipose-derived stromal cells. *PLoS ONE*, *8*(10), e77613. https://doi.org/10.1371/journal.pone.0077613

Shukunami, C., Takimoto, A., Miura, S., Nishizaki, Y., & Hiraki, Y. (2008). Chondromodulin-I and tenomodulin are differentially expressed in the avascular mesenchyme during mouse and chick development. *Cell and Tissue Research*, *332*(1), 111–122. https://doi.org/10.1007/s00441-007-0570-8

Shukunami, C., Takimoto, A., Oro, M., & Hiraki, Y. (2006). Scleraxis positively regulates the expression of tenomodulin, a differentiation marker of tenocytes. *Developmental Biology*, *298*(1), 234–247. https://doi.org/10.1016/j.ydbio.2006.06.036

Silver, F. H., Christiansen, D. L., Snowhill, P. B., & Chen, Y. (2001). Transition from viscous to elastic-based dependency of mechanical properties of self-assembled type I collagen fibers. *Journal of Applied Polymer Science*, *79*(1), 134–142. https://doi.org/10.1002/1097-4628(20010103)79:1<134::AID-APP160>3.0.CO;2-E

Son, W. K., Youk, J. H., Lee, T. S., & Park, W. H. (2004). The effects of solution properties and polyelectrolyte on electrospinning of ultrafine poly(ethylene oxide) fibers. *Polymer*, *45*(9), 2959–2966. https://doi.org/10.1016/j.polymer.2004.03.006

Spiesz, E. M., Thorpe, C. T., Chaudhry, S., Riley, G. P., Birch, H. L., Clegg, P. D., & Screen, H. R. C. (2015). Tendon extracellular matrix damage, degradation and inflammation in response to in vitro overload exercise. *Journal of Orthopaedic Research*, *33*(6), 889–897. https://doi.org/10.1002/jor.22879

Su, Y., Denbeigh, J. M., Camilleri, E. T., Riester, S. M., Parry, J. A., Wagner, E. R., … Kakar, S. (2018). Extracellular matrix protein production in human adipose-derived mesenchymal stem cells on three-dimensional polycaprolactone (PCL) scaffolds responds to GDF5 or FGF2. *Gene Reports*, *10*, 149–156. https://doi.org/10.1016/j.genrep.2017.12.004

Taghavi, S. M., & Larson, R. G. (2014). Regularized thin-fiber model for nanofiber formation by centrifugal spinning. *Physical Review E - Statistical, Nonlinear, and Soft Matter Physics*, *89*(2), 1–9. https://doi.org/10.1103/PhysRevE.89.023011

Tan, S.-L., Ahmad, R. E., Ahmad, T. S., Merican, A. M., Abbas, A. A., Ng, W. M., & Kamarul, T. (2012). Effect of Growth Differentiation Factor 5 on the Proliferation and Tenogenic Differentiation Potential of Human Mesenchymal Stem Cells in vitro. *Cells Tissues Organs*, *196*(4), 325–338. https://doi.org/10.1159/000335693

Tan, S.-L., Ahmad, T. S., Ng, W.-M., Azlina, A. A., Azhar, M. M., Selvaratnam, L., & Kamarul, T. (2015). Identification of Pathways Mediating Growth Differentiation Factor5-Induced Tenogenic Differentiation in Human Bone Marrow Stromal Cells. *Plos One*, *10*(11), e0140869. https://doi.org/10.1371/journal.pone.0140869

Thayer, P. S., & Goldstein, A. S. (2016). Bio-Instructive Scaffolds for Tendon/Ligament Regeneration. In *Bio-Instructive Scaffolds for Musculoskeletal Tissue Engineering and Regenerative Medicine* (pp. 87–112). Academic Press. https://doi.org/10.1016/B978-0-12-803394-4.00004-5

Thomopoulos, S., Kim, H. M., Das, R., Silva, M. J., Sakiyama-Elbert, S., Amiel, D., & Gelberman, R. H. (2010). The Effects of Exogenous Basic Fibroblast Growth Factor on Intrasynovial Flexor Tendon Healing in a Canine Model. *The Journal of Bone and Joint Surgery-American Volume*, *92*(13), 2285–2293. https://doi.org/10.2106/JBJS.I.01601

Voleti, P. B., Buckley, M. R., & Soslowsky, L. J. (2012). Tendon Healing: Repair and Regeneration. *Annual Review of Biomedical Engineering*, *14*(1), 47–71. https://doi.org/10.1146/annurev-bioeng-071811-150122

Volfson, D., Cookson, S., Hasty, J., & Tsimring, L. S. (2008). Biomechanical ordering of dense cell populations. *Proceedings of the National Academy of Sciences*, *105*(40), 15346–15351. https://doi.org/10.1073/pnas.0706805105

Wang, Q.-W., Chen, Z.-L., & Piao, Y.-J. (2005). Mesenchymal stem cells differentiate into tenocytes by bone morphogenetic protein (BMP) 12 gene transfer. *Journal of Bioscience and Bioengineering*, *100*(4), 418–422. https://doi.org/10.1263/jbb.100.418

Ward, A. G. (Alan G., & Courts, A. (Albert). (2013). The Science and Technology of Rubber. In *The Science and Technology of Rubber* (p. iii). Academic Press. https://doi.org/10.1016/B978-0-12-394584-6.00016-9

Wenstrup, R. J., Smith, S. M., Florer, J. B., Zhang, G., Beason, D. P., Seegmiller, R. E., … Birk, D. E. (2011). Regulation of collagen fibril nucleation and initial fibril assembly involves coordinate interactions with collagens V and XI in developing tendon. *Journal of Biological Chemistry*, *286*(23), 20455–20465. https://doi.org/10.1074/jbc.M111.223693

Wilson, J. J., & Best, T. M. (2005). Common overuse tendon problems: A review and recommendations for treatment. *American Family Physician*.

Wolfman, N. M., Hattersley, G., Cox, K., Celeste, A. J., Nelson, R., Yamaji, N., … Rosen, V. (1997). Ectopic induction of tendon and ligament in rats by growth and differentiation factors 5, 6, and 7, members of the TGF-β gene family. *Journal of Clinical Investigation*, *100*(2), 321–330. https://doi.org/10.1172/JCI119537

Wu, Y., & Han, Y. (2018). 3D functional scaffolds for tendon tissue engineering. In *Functional 3D Tissue Engineering Scaffolds* (pp. 367–390). Woodhead Publishing. https://doi.org/10.1016/B978-0-08-100979-6.00015-X

Xie, J., Li, X., Lipner, J., Manning, C. N., Schwartz, A. G., Thomopoulos, S., & Xia, Y. (2010). "Aligned-to-random" nanofiber scaffolds for mimicking the structure of the tendon-to-bone insertion site. *Nanoscale*, *2*(6), 923–6. https://doi.org/10.1039/c0nr00192a

Yamane, S., Iwasaki, N., Majima, T., Funakoshi, T., Masuko, T., Harada, K., … Nishimura, S. I. (2005). Feasibility of chitosan-based hyaluronic acid hybrid biomaterial for a novel scaffold in cartilage tissue engineering. *Biomaterials*, *26*(6), 611–619. https://doi.org/10.1016/j.biomaterials.2004.03.013

Yildirimer, L., & Seifalian, A. M. (2014). Three-dimensional biomaterial degradation - Material choice, design and extrinsic factor considerations. *Biotechnology Advances*, *32*(5), 984–999. https://doi.org/10.1016/j.biotechadv.2014.04.014

Yin, Z., Chen, X., Chen, J. L., Shen, W. L., Hieu Nguyen, T. M., Gao, L., & Ouyang, H. W. (2010). The regulation of tendon stem cell differentiation by the alignment of nanofibers. *Biomaterials*, *31*(8), 2163–2175. https://doi.org/10.1016/j.biomaterials.2009.11.083

Zhang, F., He, C., Cao, L., Feng, W., Wang, H., Mo, X., & Wang, J. (2011). Fabrication of gelatin–hyaluronic acid hybrid scaffolds with tunable porous structures for soft tissue engineering. *International Journal of Biological Macromolecules*, *48*(3), 474–481. https://doi.org/10.1016/j.ijbiomac.2011.01.012

Zhang, Y. J., Chen, X., Li, G., Chan, K. M., Heng, B. C., Yin, Z., & Ouyang, H. W. (2018). Concise Review: Stem Cell Fate Guided By Bioactive Molecules for Tendon Regeneration. *Stem Cells Translational Medicine*, *7*(5), 404–414. https://doi.org/10.1002/sctm.17-0206

Zhang, Y., Ouyang, H., Chwee, T. L., Ramakrishna, S., & Huang, Z. M. (2005). Electrospinning of gelatin fibers and gelatin/PCL composite fibrous scaffolds. *Journal of Biomedical Materials Research - Part B Applied Biomaterials*, *72*(1), 156–165. https://doi.org/10.1002/jbm.b.30128

Zhang, Y., Ouyang, H., Lim, C. T., Ramakrishna, S., & Huang, Z.-M. (2005). Electrospinning of gelatin fibers and gelatin/PCL composite fibrous scaffolds. *Journal of Biomedical Materials Research*, *72B*(1), 156–165. https://doi.org/10.1002/jbm.b.30128

Zheng, Y., Miao, J., Maeda, N., Frey, D., Linhardt, R. J., & Simmons, T. J. (2014). Uniform nanoparticle coating of cellulose fibers during wet electrospinning. *Journal of Materials Chemistry A*, *2*(36), 15029–15034. https://doi.org/10.1039/c4ta03221g

Zhu, M., Heydarkhan-Hagvall, S., Hedrick, M., Benhaim, P., & Zuk, P. (2013). Manual Isolation of Adipose-derived Stem Cells from Human Lipoaspirates. *Journal of Visualized Experiments*, *50585*(79). https://doi.org/10.3791/50585

Zhu, N., & Che, X. (2013). Biofabrication of Tissue Scaffolds. In *Advances in Biomaterials Science and Biomedical Applications*. InTech. https://doi.org/10.5772/54125

Zuk, P. A., Zhu, M., Mizuno, H., Huang, J., Futrell, J. W., Katz, A. J., … Hedrick, M. H. (2001). Multilineage Cells from Human Adipose Tissue: Implications for Cell-Based Therapies. *Tissue Engineering*, *7*(2), 211–228. https://doi.org/10.1089/107632701300062859

APPENDIX A

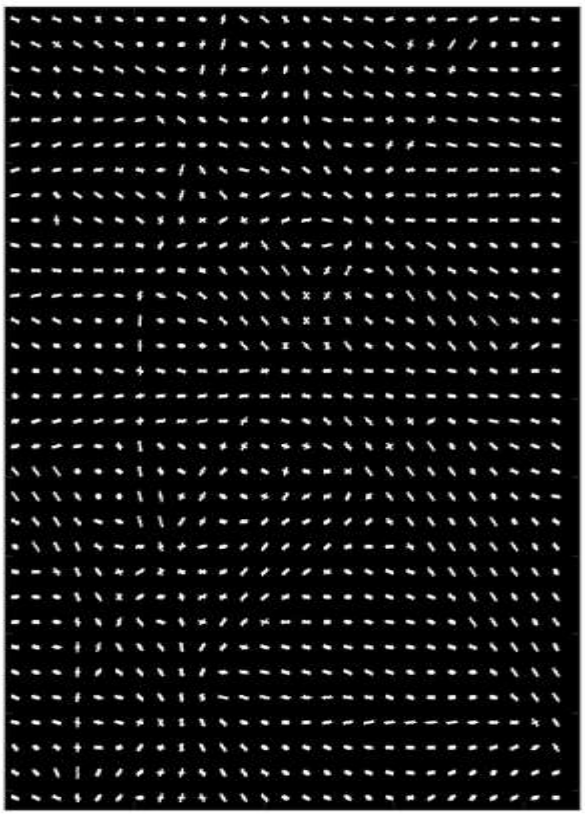

Figure A 1. Generated feature vector from pixel-based analysis. White color indicates the vectors.

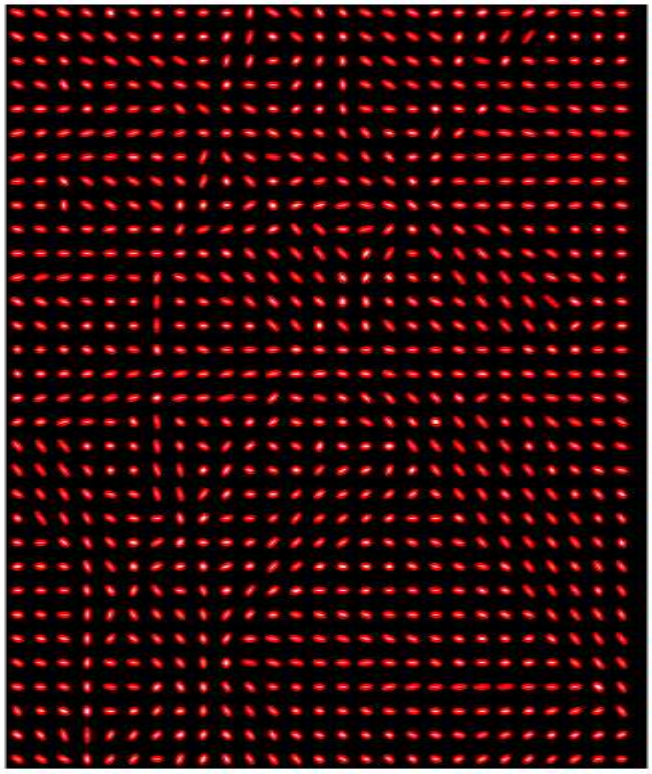

Figure A 2**.** Characterized angel between vector and x-axis.

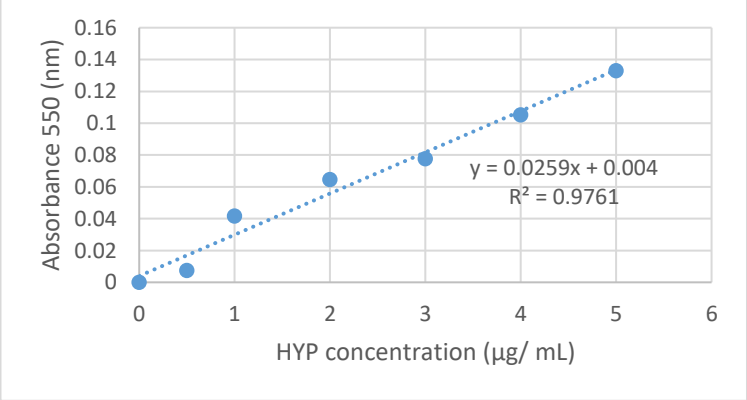

Figure A 3. Hydroxyproline calibration curve for hydroxyproline assay.